UNIVERSITY OF OKLAHOMA

GRADUATE COLLEGE

IMMUNOLOGICAL AND BIOCHEMICAL INVESTIGATION OF BRANCHED POLYETHYLENIMINES TO NEUTRALIZE PAMP-INDUCED INFLAMMATION, ERADICATE MULTIDRUG-RESISTANT BIOFILMS, AND BROADEN ANTIBIOTIC SPECTRUM IN ACUTE AND CHRONIC WOUNDS

A DISSERTATION

SUBMITTED TO THE GRADUATE FACULTY

in partial fulfillment of the requirements for the

Degree of

DOCTOR OF PHILOSOPHY

By

NEDA HEYDARIAN

NORMAN, OKLAHOMA

2023

IMMUNOLOGICAL AND BIOCHEMICAL INVESTIGATION OF BRANCHED POLYETHYLENIMINES TO NEUTRALIZE PAMP-INDUCED INFLAMMATION, ERADICATE MULTIDRUG-RESISTANT BIOFILMS, AND BROADEN ANTIBIOTIC SPECTRUM IN ACUTE AND CHRONIC WOUNDS

A DISSERTATION APPROVED FOR THE

DEPARTMENT OF CHEMISTRY AND BIOCHEMISTRY

BY THE COMMITTEE CONSISTING OF

DR. CHARLES V. RICE (CHAIR)

DR. CHRISTINA BOURNE

DR. KARA DE LEʹON

DR. SI WU

DR. SUSAN J. SCHROEDER

Acknowledgements

I am deeply grateful for the invaluable assistance and support I have received while pursuing this dissertation. Without the contributions and encouragement of numerous individuals, this achievement would not have been possible.

I extend my heartfelt gratitude to Dr. Charles Rice, my Ph.D. advisor, for his exceptional mentorship throughout this journey. His unwavering trust in me and willingness to let me develop my research methodology have been invaluable. I am truly appreciative of his openness to new ideas, which has been instrumental in shaping this work. Thank you for teaching me to think like a scientist! I would also like to extend my sincere appreciation to Toni Rice for her constant support and invaluable guidance. Toni and Dr. Rice have consistently been by my side, offering their help and support. I have felt like being around my family!

I would like to thank Dr. Christina Bourne for consistently being there to help me without any hesitation. She has always provided me with insightful guidance and a clear vision for the next steps in my research. I am so grateful for her. I also express my appreciation to my other committee members Dr. Kara De León, Dr. Susan Schroeder, and Dr. Si Wu for their invaluable guidance and feedback throughout this journey. Their expertise and constructive criticism have significantly enriched my research, and I am grateful for the time and effort they invested in evaluating my work.

I am extremely grateful to Dr. Karen Wozniak and her student Ayesha Nair from Oklahoma State University that the completion of this research would not have been possible without their scientific support and nurturing. Thank you from the bottom of my heart!

I would like to acknowledge the help and support of experts and colleagues throughout this PhD journey. Thank you to Dr. Tingting Gu and Dr. Preston Larson for all their help with light and electron microscopy. I would also like to acknowledge Dr. Phil Bourne in the Protein Production Core for his technical guidance throughout my experiments. Thank you to my great friends at the department of Chemistry and Biochemistry Zongkai Peng, Tra Nguyen, Yunpeng Lan for helping me with developing my cell culture skillset. Thank you to Savannah Morris for walking me though setting up my qPCR experiments. I would also like to acknowledge Marcee Olvera and Kriti Shukla for their unconditional friendship and support.

A specifical Thank you to Rice group for standing by my side through all the ups and downs of my Ph.D. research. Your unwavering support has meant the world to me. I would like to acknowledge Dr. Anh Lam, Dr. Hannah Lamb, Will Best, Chase Roedl, Tristan Haight and undergraduate students Maya Ferrell, Cassandra Wouters, Andrew Neel, and Andrew Boris for all the contributions they have made in this PhD research.

I am immensely grateful for my parents and sisters for always been super supportive and encouraging to me throughout my journey in grad school. Your presence has been invaluable, and I couldn't have navigated this experience without your help. Thank you for being my rock and helping me succeed. I want to extend my heartiest appreciation to my dear husband, Kianoosh Hassani, for his unconditional love, support, and constant presence throughout this process. His belief in my capabilities and potential has been instrumental in my personal and academic growth. I am incredibly grateful to have him by my side.

And lastly, I am deeply and sincerely grateful to God for making all this possible and making my dreams come true!

List of Tables

List of Figures

Abstract

Innate immunity has considerable specificity and can discriminate between individual species of microbes. In this regard, pathogens are “seen” as dangerous to the host and elicit an inflammatory response capable of destroying the microbes. This immune discrimination is achieved through the recognition of microbe-specific molecules (e.g., lipopolysaccharide, lipoteichoic acid, and peptidoglycan) by toll-like receptors on host cells. Lipopolysaccharide (LPS), lipoteichoic acid (LTA), and peptidoglycan (PGN) arising from dangerous bacteria are known as Pathogen-Associated Molecular Pattern (PAMP) molecules. PAMPs impede wound healing by lengthening the inflammatory phase of healing and contributing to the development of chronic wounds. Preventing PAMPs from triggering the release of inflammatory cytokines will restore the optimal inflammatory response. However, successful drugs are elusive because PAMPs originate from many different species of Gram-negative and Gram-positive bacteria. Therefore, the need exists for a universal broad-spectrum therapeutic against LPS, LTA, and PGN bacterial PAMPs. We envision our discoveries as topical agents applied to acute and chronic wounds because, in addition to the active moiety of the agent preventing TNF-α cytokine release, it also disables antibiotic resistance mechanisms and disrupts the biofilm matrix. This versatility of this agent suggests that it may be an ideal therapeutic agent for use in the hundreds of millions of non-chronic skin or soft-tissue infections (SSTIs), and the 4.5 million chronic wound infections, that occur each year. This work is innovative because we fill the technological gap with multi-purpose agents that disable PAMPs, dissolve biofilms, and overcome antibiotic resistance mechanisms, making them superior to existing technology.

Keywords: Chronic Wounds; Inflammatory Response; PAMPs; DAMPs; PRRs, TNF-α, Antibiotic Resistance; Biofilm; BPEI, PEG-BPEI

Chapter 1: Overview of PAMP- and DAMP-induced inflammation response and its link to wound healing.

Background and Significance

The innate immune system is an evolutionarily conserved pathogen recognition mechanism that serves as the first line of defense against tissue damage or pathogen invasion [1]. The response is not only involved in acute inflammation but also plays a crucial role in maintaining various homeostatic processes and characterized by a series of reactions, such as immune cell and plasma protein recruitment to the affected site, along with vasodilation, macrophages, dendritic cells (DCs), and neutrophils are key components of innate immunity and inflammation [2-4]. These innate immune cells have the ability to prevent sustained inflammatory responses by employing negative feedback mechanisms [5]. Unlike the adaptive immunity that recruits T-cells and specific antibodies against antigens, innate immune cells express pathogen recognition receptors (PRRs) that can detect various pathogen-associated molecular patterns (PAMPs) released by invading pathogens, as well as damage-associated molecular patterns (DAMPs) produced by necrotic cells and damaged tissues [2, 6]. Microbial molecular patterns include lipoteichoic acid (LTA) and peptidoglycan (PGN) from Gram-positive bacteria, lipopolysaccharide (LPS) from Gram-negative bacteria, bacterial proteins (e.g., flagellin), lipoarabinomannan (LAM), lipoglycans, lipomannans, and lipopeptides from mycobacteria, double-stranded (ds) RNA of viruses, zymosan from yeast, and DNA from both viruses and bacteria are all examples of pathogen-associated molecular patterns (PAMPs) [6-8]. Damage-associated molecular patterns (DAMPs) refer to endogenous intracellular molecules that are generated as a consequence of non-physiological cell death and injury [9]. DAMPs consist of extracellular matrix components such as hyaluronan and fibrinogen,

nuclear and cytosolic proteins including high-mobility group box protein 1 (HMGB1) and heat shock proteins (HSPs), plasma membrane constituents, as well as components of damaged or fragmented organelles such as mitochondrial DNA (mtDNA) [10]. There are five families of pathogen recognition receptors (PRRs) expressed by mammalian cells, namely Toll-like receptors (TLRs), C-type lectin receptors (CLRs), RIG-I-like receptors (RLRs), NOD-like receptors (NLRs), and cytosolic DNA sensors [2, 11-14]. These PRR families possess unique structural features and can detect different PAMPs and DAMPs [2, 4].

Table 1. PAMP Agonists that activate PRRs.

PAMPs Recognized by TLRs and NODs	PRR
lipopolysaccharide (LPS) from *P. aeruginosa*	TLR4
LPS from *E. coli* O111:B4	TLR4
LPS from *K. pneumoniae*	TLR4
peptidoglycan (PGN) from *E. coli* O111:B4	TLR2
PGN from *S. aureus* (PGN-SA)	TLR2
lipoteichoic acid from *S. aureus* (LTA-SA)	TLR2
L-Ala-γ-D-Glu-mDAP (tri-DAP)	NOD1
muramyl dipeptide (MDP)	NOD2

Stimulation of various PRRs triggers signaling cascades in the host, resulting in the production of pro-inflammatory cytokines including TNF-α, IL-1, IL-6, IL-8, IL-12, type 1 interferon (IFN-α and β), as well as immune modulators like chemokines and antimicrobial proteins [2, 6, 7, 15, 16]. Cytokines are a diverse group of soluble mediators consisting of short-lived small polypeptides or glycoproteins that play an important role in regulating both the immune and inflammatory responses. This group is composed of interleukins (ILs), interferons (IFNs), growth factors, and

chemokines [7, 17]. TNF-α and IL-1 are cytokines that play essential roles in the immediate immune response of the body to infection, by exerting various effects on hematopoiesis, immune responses, inflammation, and metabolism. Moreover, they trigger the production of other cytokines, chemokines, lipid mediators, and reactive oxygen species (ROS) [17]. They also induce the expression of leukocyte and endothelial cell adhesion molecules, recruit leukocytes, and stimulate neutrophils for phagocytosis, degranulation, and oxidative burst activity [18, 19]. Chemokines are a distinct group of small polypeptides that act as cytokine-like polypeptides that act as ligands for G protein-coupled, 7-transmembrane segment receptors, and have a critical function in the immune response by triggering migration of immune and inflammatory cells [17]. Toll-like receptors (TLRs) represent a significant class of receptors that have the ability to identify both pathogen-associated molecular patterns (PAMPs) from the external environment and damage-associated molecular patterns (DAMPs) from within the body [7, 17]. TLRs activate immune cells to distinguish between self and non-self, establish connections between innate and adaptive immunity [7] and promote subsequent innate and adaptive immune responses [18]. Human TLRs encompass a minimum of 10 receptors that recognize a diverse range of microbial ligands [17]. TLRs are present on all innate immune cells, including macrophages, natural killer (NK) cells, dendritic cells (DCs), circulating leukocytes like monocytes and neutrophils, adaptive immune cells such as T and B lymphocytes, and non-immune cells such as fibroblasts, epithelial, and endothelial cells and [7, 20]. The primary characteristics for differentiating different TLRs are their specific ligand binding properties, signal transduction mechanisms, and subcellular localization [7, 21]. Functionally, TLRs can be classified into two groups: I. Cell membrane TLRs (TLR1, TLR2, TLR4, TLR5, TLR6, and TLR10) and are found on the cell surface, II. Intracellular TLRs or nucleic acid sensors (TLR3, TLR7, TLR8, and TLR9) and are in endoplasmic reticulum (ER), endosomes, and lysosomes [7].

TLR Activation

TLRs are transmembrane proteins of type I that contain 20-27 extracellular leucine-rich repeats (LRR) responsible for recognizing PAMP/DAMP [7]. These proteins also have transmembrane domains and intracellular toll-interleukin 1 (IL-1) receptor (TIR) domains required for downstream signal transduction pathways activation [22]. The glycan moieties present in the extracellular domains of TLR act as binding sites for ligands [14]. The induction of cytokine production by TLR is crucial in recruiting other innate and adaptive immune components [17]. During innate immune responses, TLR-dependent signaling pathways are effectively regulated by several negative regulators [7]. TLR signaling encompasses at least two different pathways [23]. The initial signaling pathway, known as the MyD88-dependent pathway, is crucial for TLR2, 4, 5, 7, 8, and 9 [24], resulting in the synthesis of inflammatory cytokines [25]. On the other hand, the second pathway, called the TRIF-dependent pathway, involves the TIR domain-containing adaptor protein inducing IFN-β and is activated by TLR3 and 4. It is linked to the induction of interferon type-1 [26]. TLR signaling cascade that is dependent on MyD88 involves the activation of IL-1R-associated protein kinases (IRAK), which then induces TNF receptor-associated factor 6 (TRAF6)'s E3 ubiquitin ligase activity [2]. TRAF6 undergoes self-ubiquitination and conjugates ubiquitin chains onto other signaling molecules involved in activating TAK1, a ubiquitin-dependent kinase, and TAB2, which is a TAK1-binding protein [27, 28]. TAK1 is activated by TAB2, which acts as an adaptor that links TAK1 and TRAF6. This, in turn, activates the downstream kinase IKK [7]. The phosphorylation of the NF-κB inhibitor IκBα by IKK leads to the degradation of IκBα in a ubiquitin-dependent manner and the subsequent activation of nuclear factor kappa-B (NF-kB) [29]. Upon TLR activation, pro-inflammatory transcription factors such as activator protein 1 (AP-1) [7, 30], interferon regulatory factor 3 (IRF3), and nuclear factor kappa-B (NF-kB) undergo nuclear translocation. These

transcription factors are responsible for activating specific genes that encode pro-inflammatory cytokines, chemokines, type 1 interferon, and antimicrobial peptides [7, 13, 31-33]. NF-kB, a crucial transcription factor, plays a significant role in mediating macrophage inflammatory responses induced by both the MyD88- and TRIF-dependent pathways [17, 34]. It is also associated with septic and aseptic inflammation and is a crucial tumor promoter [35] (Fig. 1). In this dissertation, we will focus on the binding of PAMPs to TLRs at the upstream signaling of cytokine production.

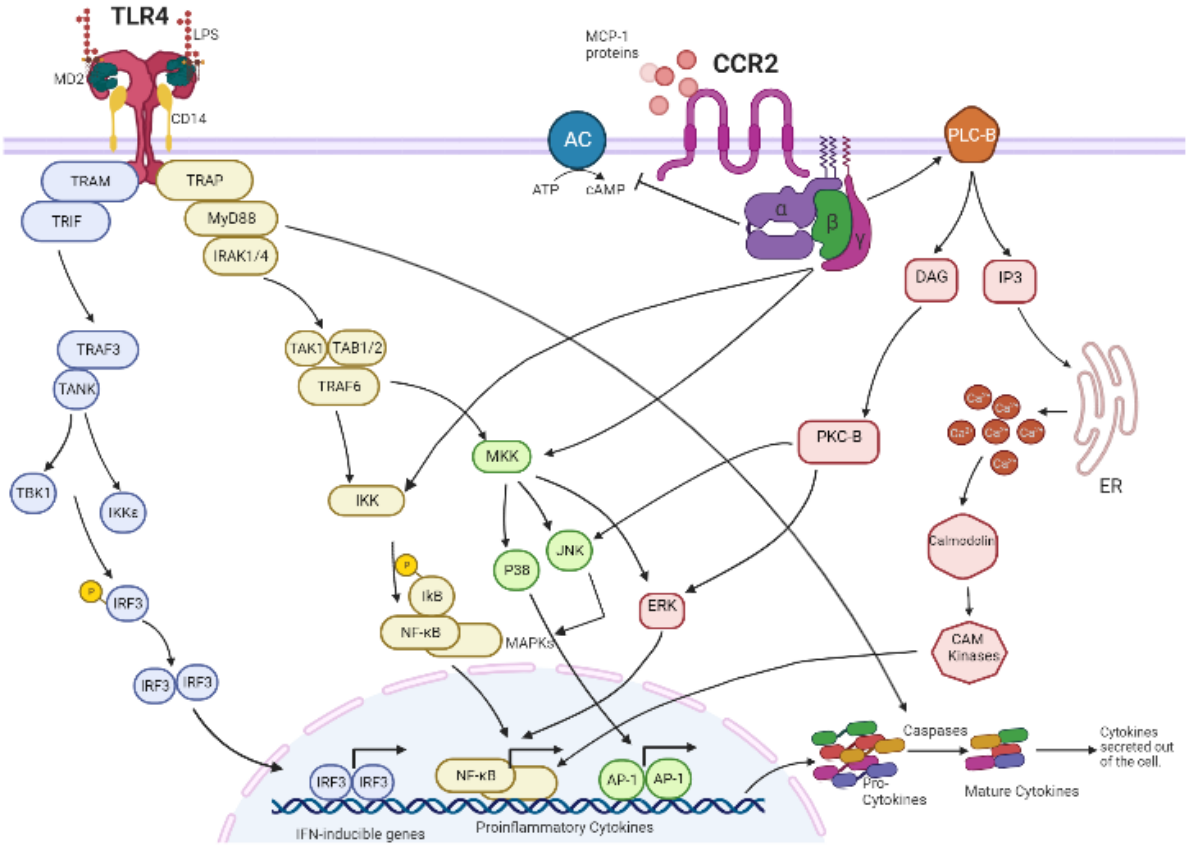

Figure. 1: TLR4 signaling induced by LPS to produce cytokines and chemokines.

Macrophages

Macrophages, the phagocytic innate immune cells responsible for combating infections, rely on NF-κB to regulate their function [2]. Upon activation by various PAMPs and DAMPs, macrophages

secrete cytokines and chemokines [36]. These activated macrophages can differentiate into different phenotypes, including M1 and M2 macrophages [37]. M1 macrophages are responsible for inducing inflammation by producing pro-inflammatory cytokines like TNF-α and IL-6, while M2 macrophages produce anti-inflammatory cytokines such as IL-10 and IL-13 to reduce inflammation [38, 39].

Inflammasomes

In response to pathogen-associated molecular patterns (PAMPs) and damage-associated molecular patterns (DAMPs), intracellular multi-protein complexes called inflammasomes are formed, characterized by the activation of inflammatory caspases. Well-known inflammasome receptors are NLRP1, NLRP3, NLRC4, and AIM2 [2, 13]. Following activation, the inflammasome receptors undergo oligomerization and recruit pro-caspase 1, leading to the processing of pro-caspase 1 and its conversion into active caspase 1 [2]. Once activated, caspase 1 cleaves pro-IL-1b and pro-IL-18, resulting in the generation of mature forms of these pro-inflammatory cytokines. This process leads to the secretion of these cytokines [40]. Inflammasomes are essential components of the innate immune system's defense against pathogenic infections and contribute to the regulation of the intestinal microbiota composition as well [2, 41].

Dysregulated Inflammation

Although short-term activation of the innate immune system is beneficial and serves as crucial defensive mechanisms of the host against infection, excessive activation of Toll-like receptors (TLRs) is harmful as it disturbs immune homeostasis by causing prolonged production of pro-inflammatory cytokines and chemokines [7]. This elevated immune response increases the

susceptibility to autoimmune diseases, chronic inflammatory disorders, as well as infectious and tumor-associated diseases, such as systemic lupus erythematosus, rheumatoid arthritis, cancer, sepsis, Alzheimer's disease, chronic hepatitis B virus, Behcet's disease, Obesity, diabetes type 1, and type 2 diabetes mellitus (T2DM) [42-47]. Furthermore, dysregulated activation of the inflammasome is implicated in a range of autoimmune and inflammatory diseases [48]. The involvement of the NF-κB signaling pathway in the regulation of the inflammasome is now well-established, playing a role in the onset and progression of inflammatory diseases [2, 48].

Inflammation in Cancer

Chronic and persistent inflammation can elevate the likelihood of developing cancer [15]. One of the signaling pathways that plays a significant role in tumor angiogenesis is NF-κB, which is crucial for the activation of tumor angiogenesis. The activation of NF-κB is increased in the majority of cancer types [6]. NF-κB comprises a group of inducible transcription factors that are triggered by PAMPs and DAMPs through activated pattern recognition receptors [2]. It plays a pivotal role in orchestrating immune and inflammatory responses [49]. Furthermore, NF-κB serves as a crucial connection between inflammation and cancer by virtue of its capacity to increase the expression of tumor-promoting cytokines such as IL-6 or TNF-α, and survival antiapoptotic molecules including Bcl-xL, Bcl2, and inhibitor of apoptosis (IAP) [6, 50]. NF-κB is involved in multiple stages of tumor progression, encompassing cell survival, proliferation, angiogenesis, metastasis, and apoptosis. Its functions and mechanisms are diverse and intricate [15, 50]. The NF-κB pathway mediates cancer development by influencing the signal transduction within the tumor microenvironment. NF-κB exhibits the ability to induce the expression of chemokines not only in stromal cells, tumor cells, and immune cells within the tumor microenvironment but also to

activate itself within each of these cells, leading to the transcriptional upregulation of cytokines. This, in turn, promotes tumor proliferation and metastasis [6]. Previous research suggests that even in the absence of an underlying inflammatory condition, cancer development depends on an NF-kB-regulated inflammatory response [50]. Consequently, human malignancies are often accompanied by sterile chronic inflammation [15]. Additionally, inflammation and NF-κB contribute to the initiation of tumorigenesis by stimulating the generation of reactive oxygen species and reactive nitrogen species, which in turn lead to DNA damage and the formation of carcinogenic mutations [6, 51]. Chronic inflammation and NF-κB activation also induce aneuploidy, chromosomal instability, and epigenetic alterations, thereby facilitating the development and advancement of tumors [51].

Inflammation in Wound Healing

The process of wound healing is characterized by its dynamic nature and involves intricate interactions among extracellular matrix molecules, resident cells, soluble mediators, and infiltrating leukocytes [52]. The normal process of wound healing encompasses four interconnected phases, namely homeostasis, inflammation, proliferation, and tissue remodeling, which occur simultaneously and in close proximity [52, 53]. In the early stages of wound healing, the extracellular matrix (ECM) facilitates the recruitment of platelets and leukocytes [53]. The presence of damaged tissue, as well as aggregated platelets and leukocytes entrapped within the blood clot, activate the coagulation pathways, resulting in the stabilization of the fibrin and platelet clot [52]. This clot acts as a scaffold and serves as chemoattractants, promoting the migration and proliferation of immune cells that orchestrate the inflammatory cell response [54, 55]. Chemokines, along with bacterial products like lipopolysaccharides, lipoteichoic acids, and formyl-methionyl peptides, are critical in mediating cell recruitment during the repair process in bacterially infected wounds [52]. The

presence of these molecules in the wounds facilitates the infiltration of various innate and adaptive immune cells, including neutrophils, macrophages, mast cells, Langerhans cells, as well as T and B cells [53]. These immune cells collaborate to eliminate bacteria and foreign pathogens at the site of infection. Moreover, these immune cells play a role in clearing the debris of damaged cells and clots while releasing a variety of growth factors and cytokines [56]. These factors contribute to cell proliferation and facilitate the synthesis of extracellular matrix molecules by the resident skin cells. During the phases of proliferation and tissue remodeling, the wound undergoes epithelialization, and newly formed granulation tissue emerges [52]. This granulation tissue comprises endothelial cells, fibroblasts, and macrophages, which work together to cover and fill the wound area, facilitating the restoration of tissue integrity. It is crucial for the synthesis, remodeling, and deposition of structural extracellular matrix molecules to take place in order to facilitate tissue formation and progression towards the healing state [5]. The acute inflammatory phase is recognized as a pivotal stage in safeguarding against infections and exerts significant influences on the tissue-repair process. By establishing an optimal environment for cell migration, proliferation, and differentiation, acute inflammation contributes to the maintenance of homeostasis. Resolution of the inflammation is imperative for successful repair following tissue injury. However, in cases of non-healing wounds, the normal progression through the phases of wound repair is impeded, resulting in a persistent state of chronic inflammation [57].

Chronic and Non-Healing Wounds

Normal inflammation during wound healing is beneficial to the host and can be resolved in a timely manner. However, dysregulated inflammatory response often results in impaired healing, poor tissue restoration and function, and increased scarring [2, 52, 53]. Clinically, chronic wounds are those

that have not gone through the orderly phases of healing but are trapped in pathologic inflammation, persistent infections, and necrosis, and remain intractable to carry out the normal repair process [7, 53, 58] (Fig. 2). The vast majority of chronic wounds fall into three main categories: venous ulcers, pressure ulcers, and diabetic ulcers, with a smaller fourth group secondary to arterial ischaemia [59, 60]. On the other hand, chronic inflammation, a hallmark of the non-healing wound, predisposes tissue to cancer development. Inflammation, fibroplasia, and angiogenesis are cardinal events that are intimately linked to wound repair. Thus, the chronic inflammatory microenvironment of the non-healing wound could be a risk factor for malignant transformation [52]. Chronic wound management remains an issue, as the ongoing inflammation in these wounds is very difficult to control. Another factor that can delay wound healing is infection of the wound. If the infection is not controlled in a timely fashion, a biofilm can form [53].

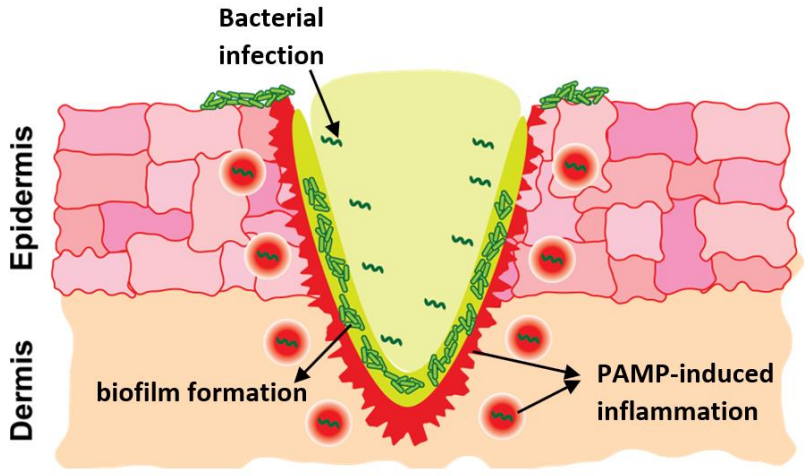

Figure. 2: Microbial factors that impede normal wound healing process and transform acute wounds into chronic wounds.

Infection in Chronic Wounds

Following skin injury, microorganisms typically present on the skin surface can infiltrate the underlying tissues. When replicating organisms cause harm to the host within a wound, this is

termed invasive infection, which significantly delays the healing of chronic wounds [53] (Fig. 3). The high-level exudate in chronic wounds creates a moist and nutrient-rich environment that promotes bacterial colonization and propagation. Furthermore, the presence of bacteria and endotoxins increases the severity of the inflammatory response [61]. During the early phase of chronic wounds, Gram-positive bacteria, notably *Staphylococcus aureus*, are predominant. In later stages, Gram-negative bacteria such as *Pseudomonas aeruginosa* become more common [62]. These bacteria produce virulence factors and endotoxins, which stimulate the expression of pro-inflammatory cytokines, exacerbating chronic inflammation [61]. The presence of multiple types of microorganisms in a wound results in microbial diversity and heterogeneity, which further complicates the wound-healing process [53]. Within a polymicrobial environment, different species interact dynamically, altering bacterial behavior and promoting increased virulence, ultimately contributing to delayed wound healing [63]. When microorganisms coexist within a biofilm, they can engage in microbial synergy, which gives them a competitive edge [64].

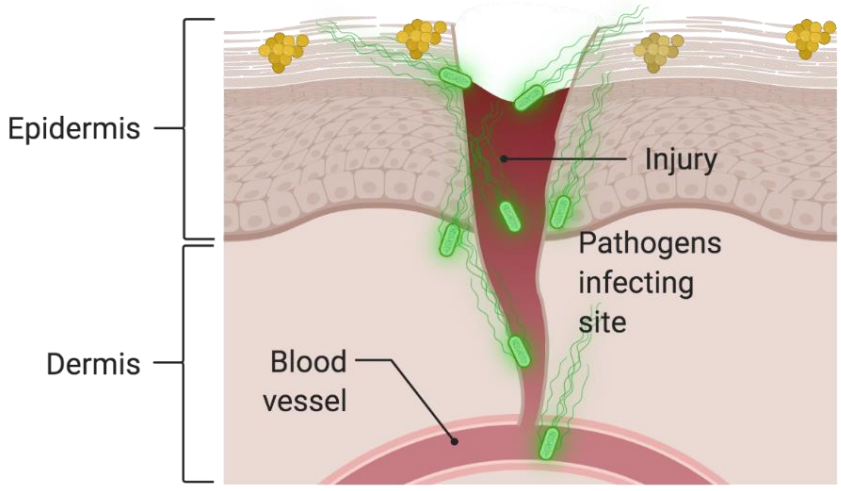

Figure. 3: Cutaneous wound healing. Microbial pathogens can infect wounds and impede the healing process.

Biofilm in Chronic Wounds

Biofilms are bacterial communities that form structured populations and adhere to the surface of wounds by embedding themselves in a matrix of capsular polysaccharide substance known as exopolysaccharide [65] (Fig. 4). The exopolysaccharide matrix shields bacteria from the host defense and antimicrobial adjuvants [53]. This, in turn, activates pro-inflammatory macrophages and neutrophils in the host immune system, triggering the accumulation of cytokines like TNF-α and IL-6, as well as matrix metalloproteinases (MMPs), which sustains the inflammation [66]. This worsens the chronic inflammation and perpetuates the cycle of impaired wound healing [67]. Chronic wounds have a higher prevalence of biofilms, with nearly 60% of these wounds exhibiting this phenomenon. In contrast, only 10% of acute wounds contain biofilms [53]. Eradicating biofilms poses significant challenges, primarily due to the exopolysaccharide matrix of biofilms that acts as a mechanical barrier, hinders the diffusion of antibiotics and immune cells, and makes biofilm elimination more difficult [68, 69]. As a result, leukocytes face difficulty entering biofilm and producing reactive oxygen species that are necessary to eliminate bacteria through the normal wound healing process, thereby decreasing bacterial phagocytosis [7]. Additionally, the polymicrobial nature of biofilms in chronic wounds promotes genetic exchange, which contributes to the rapid development of antibiotic resistance and results in increased heterogeneity and additional resistance in the wound [70]. Antimicrobial therapy can also trigger the development of thicker mucoid-like biofilm phenotypes as an evolutionary response. These mechanisms can ultimately lead to resistance in chronically treated infected wounds [71].

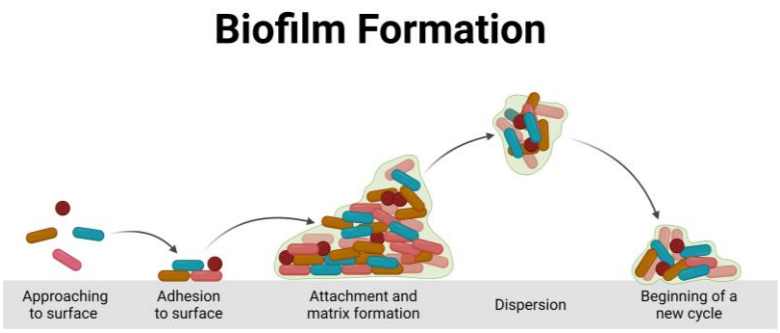

Figure. 4: Stages of biofilm formation.

Matrix metalloproteinases (MMPs) in Chronic Wounds

Impaired wound healing can also be attributed to the dysregulation of matrix metalloproteinases (MMPs), which play a crucial role in proper epithelialization and keratinocyte proliferation in wounds. Under normal circumstances, MMPs are secreted in small amounts by immune cells, fibroblasts, and keratinocytes in response to local mediators such as cytokines and growth factors involved in wound healing [53]. However, when MMP secretion is dysregulated, they can impair epithelialization and are strongly associated with the development of chronic wounds [72]. In chronic wounds, proinflammatory cytokines such as interleukin (IL)-1β and tumor necrosis factor alpha (TNF)-α, are known to be powerful stimulators of MMP expression and have been shown to reduce the expression of tissue inhibitor of metalloproteinases. As a result, an environment is created where MMP activity is relatively excessive [52]. The upregulation and activity of various MMP classes, including collagenases (MMP-1, MMP-8), gelatinases (MMP-2, MMP-9), stromelysins (MMP-3, MMP-10, and MMP-11), and the membrane type MMP (MT1- MMP) increases extracellular matrix (ECM) degradation and impairs normal wound healing processes such as migration, proliferation, and collagen synthesis of fibroblasts. Consequently, the degradation products of ECM further induce inflammation, leading to a self-perpetuating cycle [52, 53].

Chronic Wound Healing Therapies

The estimated number of patients with chronic wounds in the United States is around 4.5 million, leading to significant economic, psychologic, and social burdens [73, 74]. The incidence of risk factors associated with chronic wounds, such as age and obesity, has been on the rise which contributes to the growing market size of wound closure products [74, 75]. The importance of addressing the unmet medical need of non-healing chronic wounds is recognized by the US Food and Drug Administration (FDA). The FDA acknowledges that there is a lack of available innovative products for non-healing chronic wounds and overcoming barriers to product development in this area is crucial. Such barriers may include limited availability of biological models, difficulties in drug delivery, challenges in executing clinical trials, and restricted commercial viability. From 2020 to 2021, the Division of Dermatology and Dentistry (DDD), through a Science Strategies program assessed areas of unmet need and activity in the product development pipeline for wound healing [76]. Due to high unmet need with relatively limited research and funding, non-healing chronic wounds were identified as an area of priority. The unique complexities of the wound environment, such as degradative enzymes, hypoxia, ischemia, oxidative stress, bacterial infection, and the critical involvement of inflammatory cells, pose significant challenges in drug delivery. These factors act as obstacles in the development of therapeutics that can effectively maintain their efficacy [77, 78]. In clinical settings, the management of chronic wounds typically involves the implementation of debridement to eliminate infected and nonviable tissue, as well as the application of non-specific wound dressings [75]. Generic wound dressings that are commercially available include hydrogels, wet gauze, foam dressings, films, and hydrocolloids. These dressings facilitate the healing process of wounds by creating gas exchange, moisture, heat insulation, exudate drainage, infection barrier, and mitigating skin irritation or friction caused by contact with

clothing or devices like wheelchairs [75, 79, 80]. However, specific, and more advanced commercially available wound dressings like cellular and acellular skin substitutes are expensive, not easily accessible, and typically employed in specialized settings [73, 81-83]. In spite of the significant impact on public health, there is a lack of innovative products specifically designed for treating non-healing chronic wounds. While the FDA has cleared over 70 wound dressing products for managing wounds and promoting natural healing processes, these technologies are not specifically intended for chronic non-healing wound treatment [76]. By this it means that there are too many reasons that wounds become chronic and current wound healing technologies are not able to address them. The majority of drug and/or biologic products designed for treating chronic wounds tend to show a lack of efficacy during Phase 2 and 3 trials. Until now, only one product named becaplermin gel, along with two moderately effective cell-based therapies including Dermagraft and Apligraf (developed by Organogenesis, Canton, MA) have been granted approval by the FDA for treating chronic non-healing wounds. Moreover, there has been no FDA-approved small-molecule drug specifically designated for the treatment of non-healing chronic wounds [84-88].

It has been increasingly accepted that in chronic wounds, the inflammatory phase is probably the most disrupted process [81, 89-91]. Therefore, disrupting the proinflammatory cycle is essential for effective therapy aimed at healing chronic wounds [52]. A successful treatment for chronic and non-healing wounds should not only eliminate existing biofilms and prevent the formation of new ones, but also establish a favorable microenvironment for wound healing, which includes mitigating inflammation and oxidative stress [53, 92, 93] (Fig. 5). The disproportionate and imbalanced inflammation that characterizes chronic wounds represents a promising target for novel immunomodulation approaches to regulate diseases with abnormal tissue remodeling, including

chronic inflammatory conditions, healing disorders, and cancer [52]. In the potential immunomodulation approaches, neutrophil and monocyte recruitment as well as macrophage polarization can be modulated to address the persistent inflammation present in chronic wounds. Disrupting the cycle of leukocyte influx and the secretion of leukocyte-recruiting chemokines in chronic wounds can be achieved by neutralizing pro-inflammatory chemokines and cytokines [53].

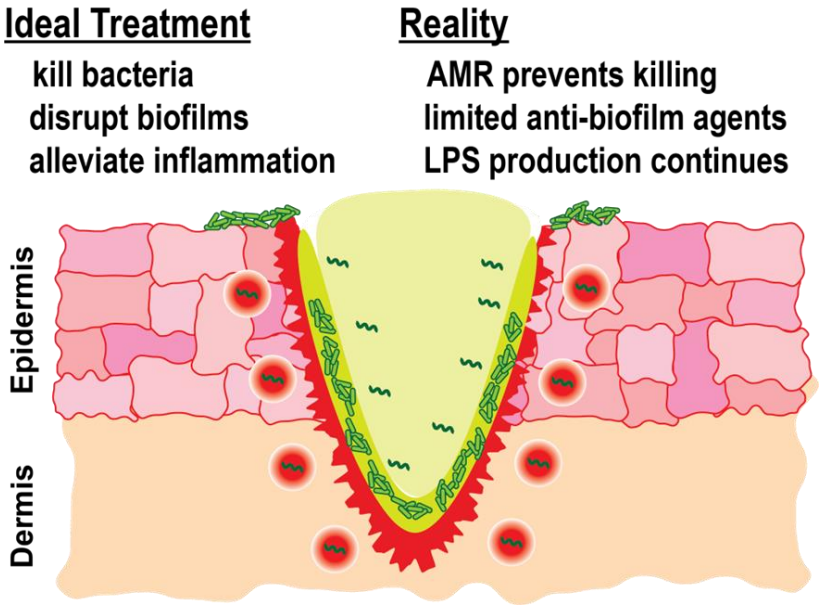

Figure. 5: Different criteria that a potential agent should possess against chronic wounds vs. reality of the available products for non-healing wounds.

Innovation: Branched Polyethylenimine (BPEI) and PEGylated BPEI

Polyethylenimines (PEI) are polymers with repeating amine groups separated by ethyl moieties and are available in different molecular masses from 500-Da up to 1,000,000-Da and higher [94]. PEIs are present in linear and branched forms. Linear PEIs (LPEI) are long chain polymers that are made of only secondary amines. However, branched PEIs (BPEI) are flexible polymers and contain primary, secondary, and tertiary amine groups. The primary amines of BPEI are protonated at neutral pH, which contributes to the highly cationic nature of the polymer. PEIs are utilized

across diverse industrial, environmental, and research contexts. The applications of PEIs include paper industry, water treatment, coating industry, chelating agents for heavy metals, dye-fixation agents, detergents, and cosmetics [95]. In biochemical research laboratories, PEIs have been used for a variety of reasons such as purification of proteins, adhesions for cell tissue culture plate, and transfection agents for gene therapy [96-99]. These successful applications prove PEIs as a promising agent for other biological purposes. We have previously identified low molecular weight 600 Da branched polyethylenimine (600 Da BPEI) (Fig. 6 top) as a broad-spectrum antibiotic potentiator that can overcome antibiotic resistance and eradicate biofilms of multidrug resistant strains of Gram-positive and Gram-negative bacteria including methicillin resistant *Staphylococcus aureus* (MRSA), methicillin resistant *Staphylococcus epidermidis* (MRSE), *Pseudomonas aeruginosa*, and carbapenem resistant *Enterobacteriaceae* (CRE) etc [65, 100-108]. However, the toxicity concerns arising from the presence of primary amines 600 Da BPEI are significant and need to be addressed. The in vivo toxicity concerns are resolved by covalently conjugating a low-molecular-weight polyethylene glycol (350 MW PEG) moiety to 600 Da BPEI, resulting in PEG-BPEI (Fig. 6 bottom). Additionally, we have shown that the PEGylated derivative possesses the potentiator characteristics of BPEI against the MDR strains and their biofilms [65, 108-111]. Regardless of the BPEI ability to facilitate the uptake of drugs and lower drug influx barriers as an antibiotic potentiator against bacterial biofilms and planktonic cells, therapeutic benefits of 600 Da BPEI and PEG-BPEI can further go beyond. In this work, we continue to investigate 600 Da BPEI and its PEGylated derivative as anti-PAMP and anti-DAMP molecules to help mitigate overproduction of inflammatory response. Overall, we envision BPEI and PEG-BPEI as topical agents for acute and chronic wounds because we propose that the potentiator molecules are multi-functional agents

that can address bacterial infection and biofilms, reduce inflammation, and successfully speed up wound healing.

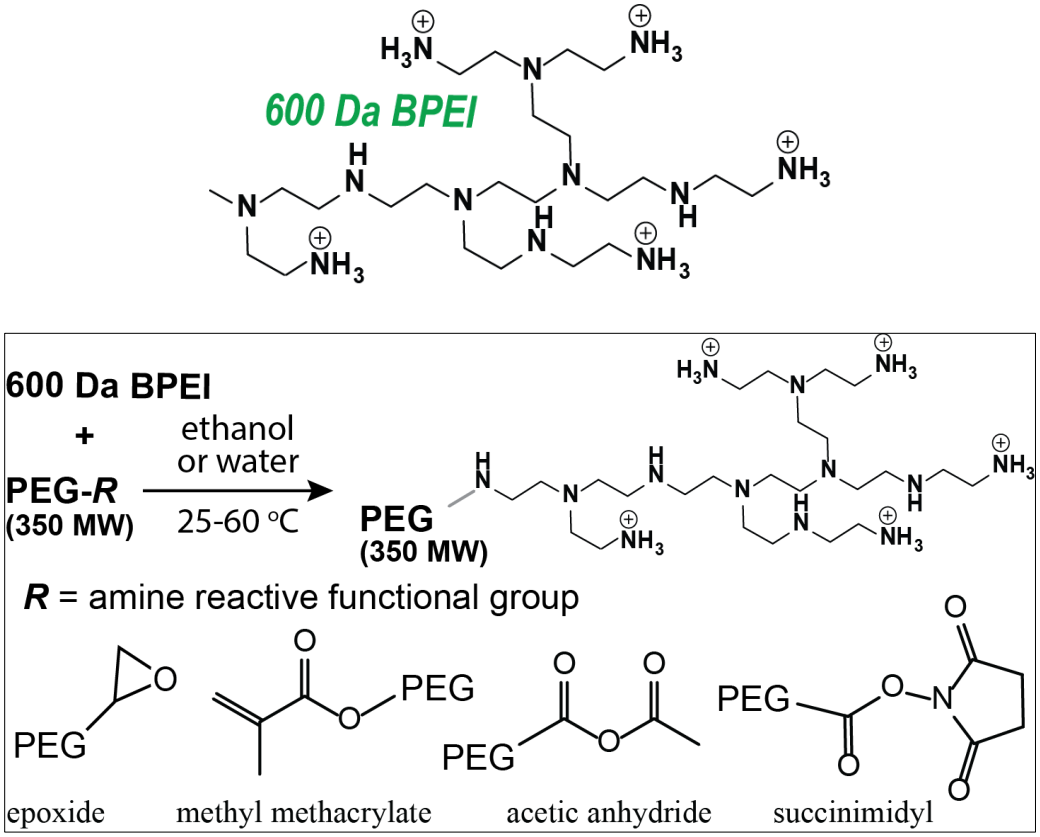

Figure. 6: BPEI structure (top), PEG-BPEI synthesis reaction (bottom)

Chapter 2: Neutralizing *S. aureus* PAMPs-triggered Immune Response in Human Macrophage Cells

Background and Significance of Research

Each year, millions of pressure ulcers and diabetic chronic wounds occur. Chronic wounds with high morbidity and mortality rates affect millions of people around the world, emerging as a threat to healthcare systems. Approximately, 6.5 million have chronic skin ulcers in the United States and there is an extensive economic burden on the healthcare setting and on society due to skin repair failing and non-healing ulcers [68, 69]. In diabetic patients, these ulcers lead to lower limb amputation and inflict significant pain, which ultimately results in reducing the quality of life for patients. Moreover, more than 1.25 million burn victims in the United States annually suffer from slow or non-healing wounds and are at increasing risk of invasive infections [112].

The slow healing of diabetic wounds and pressure ulcers is exacerbated by excessive inflammation when tissue cells detect danger signal molecules and, in response, cause the activation and accumulation of immune cells [2, 49, 50]. Inflammation is the first response to infection and injury caused by harmful stimuli, such as infected pathogens, damaged cells, or irritants [113, 114]. It is an essential protective immune response involving immune cells, blood vessels, and molecular mediators to eliminate the infected pathogens, removes necrotic cells, and clear damaged tissues[114]. However, dysregulated immune activation results in hyper-production of cytokines and systemic inflammation culminating in recurrent infection and tissue necrosis, septic shock, multiorgan failure, and death [115-117]. *Staphylococcus aureus* (*S. aureus*) is a Gram-positive bacterium that can cause serious infections such as skin and soft tissue infections, bloodstream

infections, and life-threatening septicemia. It is also an aggravator of the inflammatory skin disease atopic dermatitis (AD) [118-120]. *S. aureus* infections cause approximately 20,000 deaths a year in the US[119]. When through a tissue injury, the skin barrier is breached by *S. aureus* pathogens, an efficient immune response is initiated. This response involves both innate and recruited immune cells and eventual clearance of infection [118, 119].

The immunostimulant agents or Pathogen Associated Molecular Pattern molecules (PAMPs) of *S. aureus* bacteria are cell wall components lipoteichoic acid (LTA), and peptidoglycan (PGN)[121]. LTA is the major PAMP of *S. aureus* bacteria that is mainly released from bacterial cells following bacteriolysis induced by immune cells lysozymes, cationic bactericidal peptides from plasma and from neutrophils, phospholipase A2, elastase, and cathepsins, or beta lactam antibiotics [117, 122]. LTA is an amphiphilic polymer composed of a hydrophilic chain of poly glycerol-phosphate units, substituted with D-alanine and/or sugars that are covalently attached to the cytoplasmic membrane of *S. aureus* via a hydrophobic glycolipid anchor [121-124]. The backbone chain of LTA extends into the peptidoglycan to the outer surface of bacterial cell [125]. As an adhesion molecule, LTA facilitates the binding of bacteria to eukaryotic cells, their colonization, and tissues invasion [117].

LTA binds to immune cells either non-specifically via establishing phosphodiester units with membrane phospholipids, or specifically via LPS binding protein (LBP), glycosylphosphatidylinositol-anchored membrane protein CD14, nuclear protein high-mobility group box 1 (HMGB1), and TLR2 interaction [126, 127]. By binding to the target cells, LTA activates the innate immune system via inducing the production of proinflammatory cytokines such as Tumor Necrosis Factor alpha (TNF-α), Interleukin-1 (IL-1), Interleukin-8 (IL-8), Interleukin-12

(IL-12), and anti-inflammatory cytokine interleukin-10 (IL-10) [122]. After interaction with TLR2, LTA activates mitogen-activated protein kinase (MAPK), which induces associations with myeloid differentiation primary response 88 (MYD88), interleukin-1 receptor (IL-1R)-associated kinases (IRAKs), and TNF-receptor-associated factor 6 (TRAF6). LTA activates target genes using the extracellular signal-regulated kinase (ERK) pathway by the phosphorylation of ERK-1, MEK1/2, and c-Raf [126]. LTA can trigger the production of proinflammatory cytokines, nitric oxide (NO), the activation of nuclear transcription factor NF-kB and other proinflammatory mediators [124, 128, 129]. Through these mechanisms, LTA is involved in the pathophysiology of inflammation and post-infectious outcome thus suggesting that LTA is one of the major virulence factors of *S. aureus* [122].

In Gram-positive bacteria, the cell membrane is covered with thick peptidoglycan layers combined with LTA and lipoproteins that activate TLR2 and the downstream inflammatory signal transduction [125]. PGN, which predominates the cell wall of Gram-positive bacteria, is an alternating β (1, 4) linked N-acetylmuramyl and N-acetylglucosaminyl glycan whose residues are cross-linked by short peptides [127]. *S. aureus* cell wall is composed of 50% peptidoglycan (PGN) by weight [130] (Fig. 7). Like LTA, PGN binds to the CD14 protein and induces activation of the transcription factor NF-kB in host cells like macrophages [127]. PGN from *S. aureus* can be found in systemic circulation and induces the release of TNF-a and IL-6 in human immune cells. In an animal model, injection of *S. aureus* PGN contributes to the pathophysiology of multiple organ injury in sepsis [125]. Important findings have shown that a synergism with LTA and PGN results in higher cytokine levels, tissue damage, and causes septic shock and multiorgan failure in animals [117, 125, 131].

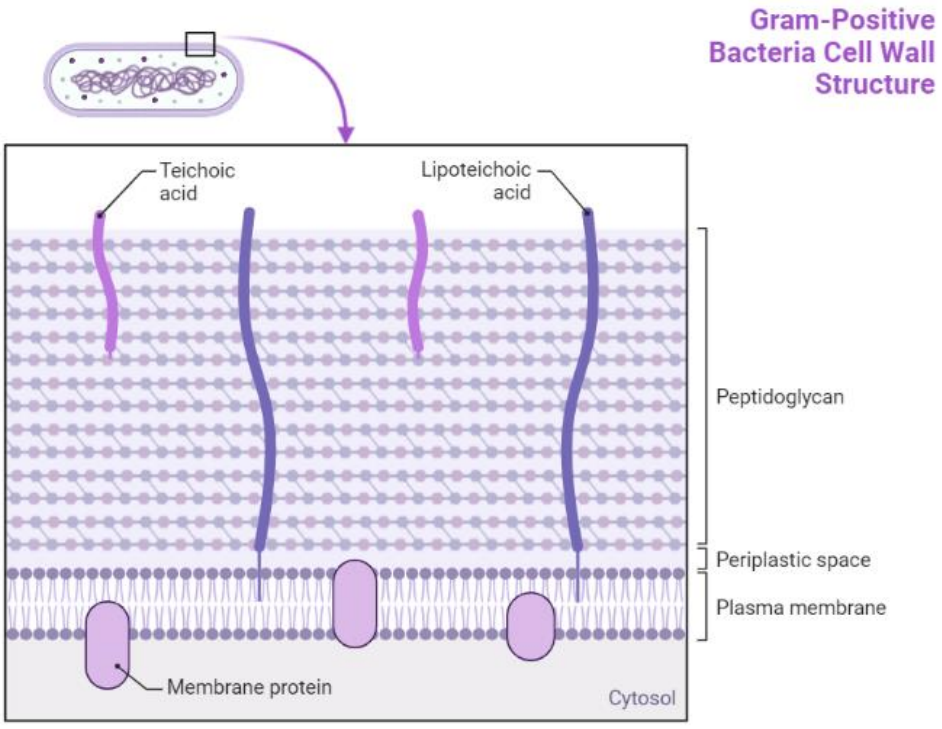

Figure.7: Structure of Gram-positive cell wall and LTA molecule.

There is an unmet need for developing technology that alleviates wound infection and improves healing. Ideal wound healing drugs should be effective against factors that impair the healing process such as reducing the chances of a prolonged inflammation at the wound site and restoring the optimal inflammatory response and minimize the development of antibiotic resistance and biofilm formation. However, successful compounds are elusive. Recent studies in our lab show that 600 Da branched polyethyleneimine (BPEI) and its less cytotoxic derivative PEG350-BPEI can facilitate the uptake of drugs and lower drug influx barrier by overcoming antimicrobial resistance and eradicating biofilms in methicillin-resistant *S. aureus*, methicillin-resistant *S. epidermidis*, *P. aeruginosa*, *E. coli*, and carbapenem-resistant *Enterobacteriaceae* bacteria [65, 101-111].

THP-1 macrophages are key cellular components of innate immunity and express several receptors include pattern recognition receptors (PRRs), such as the Toll-like receptors (TLRs). THP-1 macrophages recognize *S. aureus* bacteria via LTA and PGN and the pathogen recognition triggers a variety of pro-inflammatory responses [132].

In the current study, the ability of BPEI and PEG-BPEI potentiator molecules have been investigated as anti-PAMP molecules to reduce the production of TNF-α cytokine caused by *S. aureus* LTA and PGN in human THP-1 macrophage cells. We envision BPEI and PEG-BPEI as broad-spectrum multi-purpose agents against inflammatory PAMPs, biofilms, and antibiotic resistance mechanisms and thus, therapeutic agents for use in chronic skin or soft-tissue infections (SSTIs).

Contributions

This work was made possible due to the guidance and contributions of Dr. Karen Wozniak, Ph.D and Ms. Aysha Nair at Oklahoma State University. We would also like to thank Dr. Phil Bourne and the Protein Production Core (PPC) at the University of Oklahoma, Ms. Tra D. Nguyen, Ms. Savannah C. Morris, Mr. Zongkai Peng, and Mr. Yunpeng Lan.

Methods

Cell culture

THP-1 human monocyte-like cell line was purchased from Sigma (St. Louis, MO, ECACC, 88081201) and maintained in RPMI 1640 medium containing L-glutamine and sodium bicarbonate (Sigma, St. Louis, MO, R8758), supplemented with 10% heat-inactivated fetal bovine serum (FBS) (HyClone Laboratories, Logan, UT, SH30066.03), and 1% Pen Strep (PS) (10000 U/ml penicillin and 10000 µg/ml streptomycin, Gibco™ 15140122), at 37 °C and 5% CO2 (v/v) in a humidified incubator. The cells were suspension and grown in T-75-cm2 culture flasks (Corning, 431464) and sub-cultured every 5-6 days by three to five times dilution. Likewise, RAW 264.7 murine macrophage-like cells were purchased from American Type Culture Collection (ATCC, TIP-71) and maintained in DMEM (1X) medium (gibco, 11965-084), supplemented with FBS and PS. The cells were adherent and grown in tissue culture dishes (fisherbrand, FB012924) and sub-cultured every 2-3 days.

LTA, PGN, and HKSA treatments of THP-1 cells

Before treatments, THP-1 cells were seeded onto 96-well plates (Greiner Bio-one, Stuttgart, Germany) at 2×10^6 cells/mL in RPMI 1640 complete medium (1% Pen Strep, and 10% FBS) and incubated overnight at 37 °C and 5% CO2. The day after, the THP-1 cells were stimulated with 25 µg/ml of LTA (purified lipoteichoic acid from *S. aureus*; TLR2 ligand, InvivoGen, tlrl-pslta) for 4 h, or 25 µg/ml of PGN (peptidoglycan from *S. aureus*; TLR2 ligand, InvivoGen, tlrl-pgns2) for 6 h. Whole-cell heat-killed *S. aureus* bacteria (HKSA, heat killed *S. aureus*; TLR2 ligand, InvivoGen, tlrl-hksa) were also used for stimulation at 10^8 cells/mL final concentration for 6 h. Concentrations of treatments were selected based on the optimum production of TNF-α cytokine.

LTA, PGN, and HKSA were reconstituted in LAL-grade water (InvivoGen). After stimulation, supernatants were collected at certain timepoints by centrifugation. To protect TNF-α cytokine protein from degradation by endogenous proteases released during protein extraction, halt protease inhibitor cocktail (Thermo Scientific, 87786) was used. Immediately after supernatant collection, 10μL of protease inhibitor was added per one milliliter of supernatant to produce a 1X final concentration. Cell medium was frozen at − 20 °C until analysis. Untreated cells were used as controls.

Time-point assays of LTA, PGN, and HKSA

To explore at what time point the *S. aureus* PAMPs have the most inflammatory effect on TNF-α cytokine secretion, we did a time-point assay for each PAMP. THP-1 cells were plated in 96-well plates at 2×10^6 cells/mL in RPMI complete medium. After 24 h incubation, the THP-1 cells were treated with 25 μg/ml of LTA, or 25 μg/ml of PGN, or 10^8 cells/mL of HKSA cells. All the solutions were prepared in endotoxin-free water. The plates were then incubated for 2, 4, 6, 8, and 24 h, and supernatants were collected at the end of each time-point. To protect TNF-α cytokine protein from degradation by endogenous proteases released during protein extraction, halt protease inhibitor cocktail was used at the final 1X concentration. Time durations of treatments were selected based on the optimum production of TNF-α cytokine. Cell medium was frozen at − 20 °C until analysis. Untreated cells were used as controls.

Neutralizing immune response induced by *S. aureus* PAMPs by BPEI, PEG-BPEI, and Polymyxin B

The effect of BPEI and its derivative PEG350-BPEI against PAMP-induced TNF-α cytokine production was determined. Briefly, THP-1 cells were plated in 96-well plates at 2×10^6 cells/mL in RPMI complete medium and incubated overnight. The day after, different concentrations of BPEI were prepared in endotoxin-free water. For LTA neutralizing experiment, the THP-1 cells were treated with either LTA alone, combinations of an equivalent amount (25 μg/ml) of LTA with each of the BPEI concentrations, and BPEI concentrations alone. The latter was used as negative control and the cells treated with LTA alone represented the positive control. The combo conditions were incubated for 30 minutes before being added to THP-1 cells. Untreated cells were also prepared as control. Then, supernatants were collected after 4 hours of incubation. Same experiments were performed for PGN and HKSA except that the supernatants were collected at 6 h time-point. In HKSA neutralizing experiment, combo conditions were added to the cells immediately without prior incubation. We performed the same experiments for investigating the mitigating effects of PEG350-BPEI and polymyxin B as well. Three independent experiments (n = 3) were performed for all analysis.

Enzyme-Linked Immunosorbent Assay (ELISA) measurements

Concentrations of TNF-α cytokine were determined using DuoSet ELISA kits (R&D Systems, DY210) in THP-1 cell supernatants treated by each of the *S. aureus* PAMPs along with either BPEI, PEG-BPEI, or polymyxin B. A 96-well plate was coated with 100 μl per well of TNF-α specific capture antibody diluted in endotoxin-free PBS (Endotoxin-free Dulbecco's PBS 1X, Milipore Sigma, TMS-012-A) and incubated overnight at room temperature. The day after, each well was washed three times with 300 μl of washing buffer. Next, the plate was blocked with 300 μl of reagent diluent (R&D Systems, DY995) and incubated at room temperature for a minimum

of 1 h and then washed three times with washing buffer. Subsequently, 100 µl of standards or collected supernatants was added to the plate and incubated at room temperature for 2 h, followed by washing. Then, 100 µl of TNF-α specific detection antibody was added and the plate was incubated for 2 h at room temperature and then washed. After that, 100 µl of streptavidin-HRP was added, and the plate was incubated for a minimum of 30 min at room temperature in dark, followed by washing. Then, 100 µl of substrate solution (equal volume of hydrogen peroxide and tetramethylbenzidine (R&D Systems, DY999)) was added and the plate was once again incubated in dark at room temperature till the color developed. Reaction was stopped by adding 50 µl of 2 N sulfuric acid as stop solution. The absorbance of each well was immediately determined using a microplate reader set at 450 nm. For wavelength correction, the reading was set to 540 nm as well. Optical imperfections in the plate were corrected by subtracting readings at 540 nm from readings at 450 nm.

Cell stimulation, RNA extraction, and cDNA synthesis

For total RNA isolation, THP-1 cells were seeded at 2×10^6 cells/mL in RPMI 1640 complete medium and incubated overnight at 37 °C and 5% CO2. After 17 hours of incubation, the cells were stimulated by LTA alone, LTA and either BPEI or PEG-BPEI, and BPEI or PEG-BPEI concentrations alone. The solutions were prepared in endotoxin-free water. The combo conditions were incubated for 30 minutes before being added to THP-1 cells. Untreated cells were used as control. Each sample consisted of twelve wells. After stimulation, total cellular RNA was extracted from THP-1 cells using the Quick RNA MiniPerp Kit (Zymo Research, Irvine, CA, USA), according to the manufacturer's protocol. DNase I treatment (Zymo Research, Irvine, CA, USA) was executed to remove any genomic DNA. The concentration of the RNA samples was determined spectrophotometrically using Nanodrop (Thermo Fisher Scientific Inc., Waltham, MA,

USA) and then the RNAs were reverse transcribed to cDNA using Verso cDNA synthesis kit: (ThermoFisher, USA) based on the manufacturer's protocol. Three independent experiments (n = 2) were performed for all analysis.

qPCR

Quantitative real-time PCR analysis was performed using Roche 480 Lightcycler detection system and the qPCR products were detected with the PowerTrack SYBR Green master mix (appliedbiosystems). Human GAPDH primers (housekeeping gene) (Hs02786624_g1)
and human TNF-a primers (Hs00174128_m1) were purchased from ThermoFisher. Three independent experiments (n = 2) were performed for all analysis. Fold-change values were calculated according to delta delta Ct method (ΔΔCt) to compare gene expression levels between GAPDH and TNF-α genes.

Cytotoxicity assay

THP-1 macrophage cells were seeded onto 96-well plates (5000-10000 cells/cm^2) and allowed to incubate overnight. The cells were then treated with different concentrations of BPEI (7576, 3030, 1515, 151.5, and 15.15 μM), PEG-BPEI (4785, 1914, 957, 95.7, 9.57 μM), and polymyxin B (1511, 1134, 756, 75.6, and 7.56) for 48 h. All the tested compounds were prepared in a 10 mM Tris-HCl buffer. Polymyxin B was used as a positive control and cells that were only treated with Tris-HCl considered as negative control. At the end of the incubation period, 10 μL of 0.15 mg/mL of Resazurin dye was added to the wells as a redox indicator. The plate was then incubated for 3 h and fluorescence signals were detected at 570 nm (excitation) and 600 nm (emission). The same mammalian cell cytotoxicity assay was performed for RAW 264.7 mouse macrophages. Six

replicate measurements were performed for each compound concentration condition, and the average reported.

Statistical Analysis

All experiments were performed in triplicate and the presented data are representative results of the means ± standard error of the mean (SEM). Differences in cytokine production were analyzed using one-way ANOVA with Tukey's post-test. A 95% confidence value with a p-value consisting of $p < 0.05$ was considered statistically significant. Data were analyzed using GraphPad Prism 6.01 software (GraphPad Software Inc., USA) and Adobe Illustrator.

Results

Optimization of TNF-α protein production induced by LTA, PGN, HKSA

Lipoteichoic acid (LTA) and peptidoglycan (PGN) are *S. aureus* PAMPs that are known to be TLR2 receptor agonists. In order to mimic simultaneous bacterial infection and inflammation propagated by the PAMPs, we treated THP-1 cells with various concentrations of LTA or PGN (100 ng/mL, 1 μg/ml, 10 μg/ml and 25 μg/ml) for 24 h. Then, levels of TNF-α cytokine were measured in cell supernatants. Treatment of THP-1 cells with either 25 μg/ml of LTA or PGN provoked strong TNF-α secretion. However, when cells were treated with lower concentrations of the PAMPs, release of TNF-α was similar to non-treated cells (data is not shown). Therefore, the concentration of 25 μg/ml of LTA and PGN was selected to induce the highest secretion of TNF-α cytokine. To more closely mimic the conditions of a natural infection caused by pathogenic bacteria, heat-killed *S. aureus* (HKSA) were used to stimulate TNF-α production. HKSA bacteria retain the structural components of the cell wall, including LTA, PGN, and other molecules. This structural integrity can activate different components of the immune system, including toll-like receptors (TLRs) and pattern recognition receptors (PRRs) that provide a more comprehensive and complex immune stimulus compared to isolated components such as LTA. This can lead to a broader and more representative immune response.

Different concentrations of HKSA were used to stimulate THP-1 cells and we found the concentration of 10^8 cells/mL of HKSA to produce the highest TNF-α protein level. Next, we wanted to explore if the production of TNF-α cytokine was time-dependent. We treated THP-1 cells with 25 μg/ml of LTA for 4, 8, and 24 h. For cells stimulated with either 25 μg/ml of PGN or

10^8 cells/mL of HKSA we investigated 2, 4, 6, 8 and 24 h time-points. Supernatants were collected at the end of each time point and the level of TNF-α was measured using ELISA. Untreated cells were incubated for each of the time points as control. As shown in Fig. 8, each of the Gram-positive PAMPs showed a time-dependent manner in inducing TNF-α cytokine secretion. For LTA (Fig. 8A) and PGN (Fig. 8B), secretion of TNF-α was found to be highest at 4 h incubation. After that the level of the cytokine decreased gradually (Fig. 8A and 8B). Therefore, 4 hours of incubation for THP-1 cells treated with 25 μg/ml of LTA was used to produce the ultimate amount of TNF-α cytokine. For PGN, the optimized condition was 25 μg/ml of the PAMP for 4-6 hours of incubation. For HKSA, TNF-α secretion was significantly higher at 8 h (Fig. 8C). Since, 6 h incubation also gave large TNF-α production, the time-point was finalized to produce optimal amount of the cytokine induced by heat-killed *S. aureus* bacteria. In all the time-point assays, levels of TNF-α protein were the lowest at 24 h which is probably due to the TNF-α protein turnover to maintain the balance of the protein within cells and ensure its proper function and cellular homeostasis.

Given the reported synergistic effect of lipoteichoic acid and peptidoglycan in inducing inflammation[117, 125, 131, 133], we anticipated a stronger and more pronounced inflammatory response for TNF-α production induced by heat-killed *S. aureus* bacteria (HKSA) compared to their individual effects. The findings presented in Fig. 8C suggest that the coexistence of LTA and peptidoglycan significantly amplifies inflammatory signaling pathways and subsequently enhances the immune response in THP-1 cells. None of the untreated cells in each time-point showed any signal for TNF-α production in ELISA.

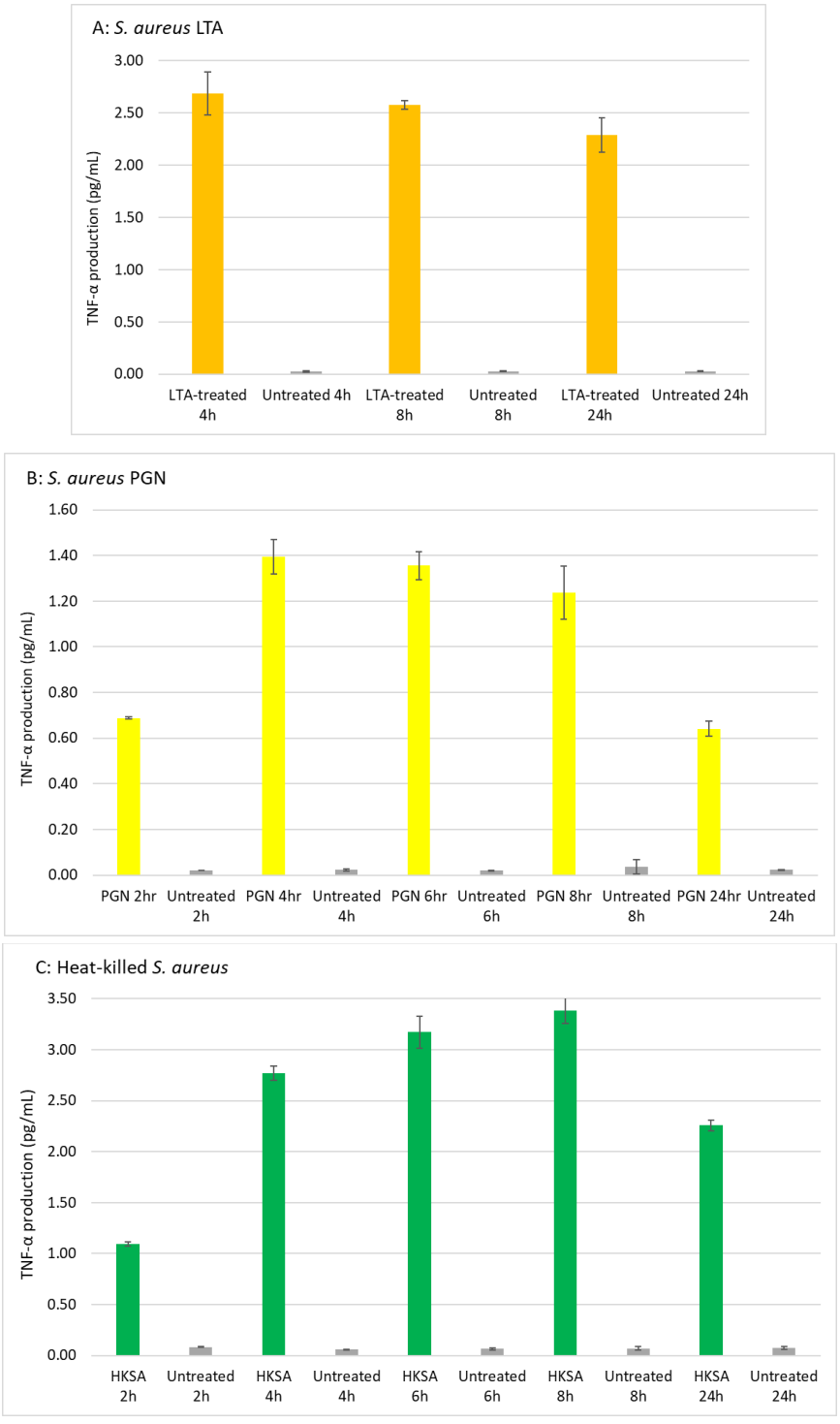

Figure 8. Results for timepoint assay of TNFα production induced by *S. aureus* PAMPs. THP-1 cells were treated with A) 25 µg/ml of LTA, B) 25 µg/ml of PGN, and C) 10^8 cells/mL of HKSA cells. The cells were then incubated for 2, 4, 6, 8, and 24 h, and supernatants were collected at the end of each time-point. Levels of TNFα cytokines were quantified using ELISA. Untreated cells were used as controls. Timepoints that resulted in the highest secretion of TNFα protein were selected as the optimum timepoints for stimulating THP-1 cells with the respective PAMPs.

Modulation of inflammatory effects of *S. aureus* PAMPs with different cationic compounds

To examine whether BPEI and PEG-BPEI have any antagonistic effect on the production of the immune response, THP-1 cells were treated with combinations of various *S. aureus* PAMPs including LTA, PGN, or HKSA and either BPEI or PEG-BPEI. First, human macrophage cells were stimulated using LTA alone, as well as combinations of LTA with varying concentrations of BPEI. On the other hand, each of the concentrations of BPEI was applied to the cells independently to see if BPEI itself can induce any TNF-α cytokine production. Results in Fig. 9A demonstrated that treatment of THP-1 cells with LTA provoked strong TNF-α secretion. However, interaction between LTA and all applied concentrations of BPEI was antagonistic since pre-neutralization stimulated significantly lower TNF-α secretion than LTA alone. Interestingly, a 1:1 ratio mixture of 25 μg/mL of LTA and 25 μg/mL of BPEI resulted in 86% reduction in TNF-α release. Despite a slightly lower reduction in TNF-α production observed in the combinations of 25 μg/mL of LTA with higher concentrations of BPEI, the neutralizing effect remained remarkably high, reaching approximately 80%. Notably, the treatment of cells with different concentrations of BPEI alone yielded TNF-α release levels comparable to those of non-treated cells (Fig. 9A).

To examine whether smaller concentrations of BPEI are effective against LTA-induced immune response, we applied 2, 5, 7, and 10 μg/ml of BPEI concentrations to neutralize LTA. As Fig. 9B shows, the LTA-induced TNF-α production in THP-1 cells treated with combinations of LTA and BPEI was reduced in a dose-dependent manner from 2 to 10 μg/mL. At a concentration of 10 μg/mL, BPEI exhibited the greatest level of inhibition, resulting in a 30% reduction in the production of TNF-α cytokines. This experiment demonstrated the ability of BPEI to neutralize

the immune response induced by LTA, particularly when the concentration of the pathogen-associated molecular pattern was more than twice as high as that of the BPEI inhibitor.

Next, we investigated if LTA can be neutralized with PEGylated derivative of BPEI as well. We observed that PEG-BPEI potentiator molecule (Fig. 9C) showed similar results as Fig. 9B. As shown in Fig. 9C, combinations of PEG-BPEI concentrations and LTA demonstrate a dose-dependent manner in disrupting the LTA-induced TLR activation. Although PEGylation of the amines of 600 Da BPEI reduced the neutralization ability of 600 BPEI against LTA, this BPEI derivative (PEG-BPEI) shows significant reduction in TNF-α secretion from 25% to up to 60% at its highest concentration level (100 μg/mL).

Our next question was to compare the neutralizing activity of our polymer potentiators (BPEI and PEG-BPEI) to polymyxin B as an existing FDA-approved drug in the market. While polymyxin B is primarily an antibiotic rather than an anti-inflammatory drug, it possesses Gram-negative endotoxin-binding effects. Therefore, polymyxin B can disrupt TLR activation and can suppress TNF-α activity[134].We investigated polymyxin B and LTA interactions on TNF-α secretion (Fig. 9D). Combinations of polymyxin B and LTA showed significant reducing effect in cytokine production. Despite polymyxin B nearly completely blocking the immune response at the highest concentrations, its neutralizing effect at 25 μg/mL was only 40%, which is less than half of the effect exhibited by BPEI at the same concentration (Fig. 9D).

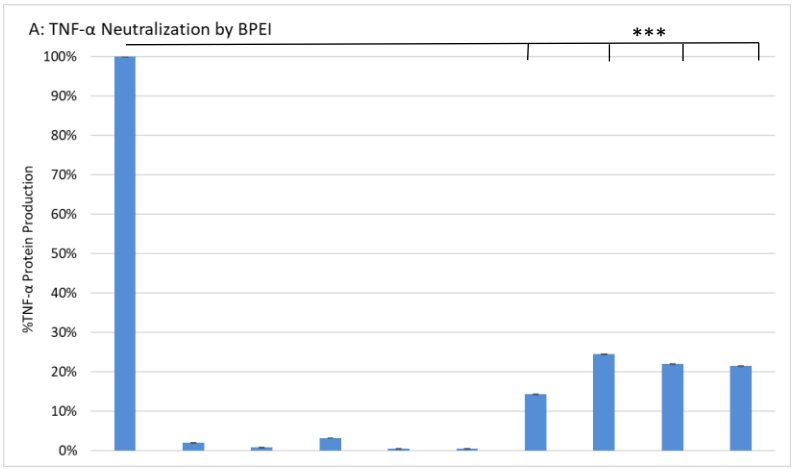

LTA 25 µg/mL	+	-	-	-	-	-	+	+	+	+
Untreated	-	+	-	-	-	-	-	-	-	-
BPEI 25 µg/mL	-	-	+	-	-	-	+	-	-	-
BPEI 50 µg/mL	-	-	-	+	-	-	-	+	-	-
BPEI 75 µg/mL	-	-	-	-	+	-	-	-	+	-
BPEI 100 µg/mL	-	-	-	-	-	+	-	-	-	+

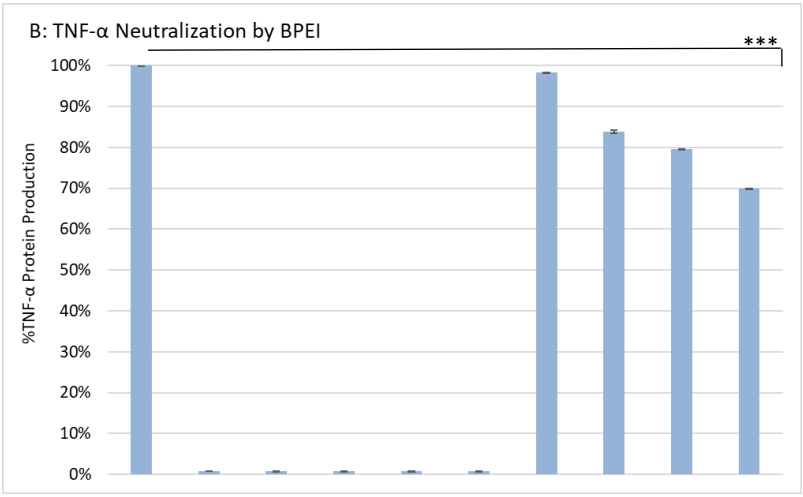

LTA 25 µg/mL	+	-	-	-	-	-	+	+	+	+
Untreated	-	+	-	-	-	-	-	-	-	-
BPEI 2 µg/mL	-	-	+	-	-	-	+	-	-	-
BPEI 5 µg/mL	-	-	-	+	-	-	-	+	-	-
BPEI 7 µg/mL	-	-	-	-	+	-	-	-	+	-
BPEI 10 µg/mL	-	-	-	-	-	+	-	-	-	+

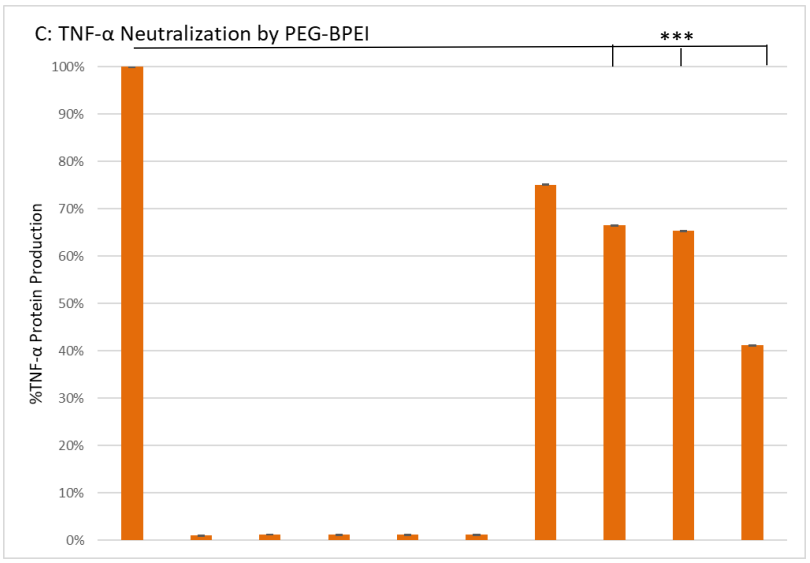

LTA 25 µg/mL	+	-	-	-	-	-	+	+	+	+
Untreated	-	+	-	-	-	-	-	-	-	-
PEG-BPEI 25 µg/mL	-	-	+	-	-	-	+	-	-	-
PEG-BPEI 50 µg/mL	-	-	-	+	-	-	-	+	-	-
PEG-BPEI 75 µg/mL	-	-	-	-	+	-	-	-	+	-
PEG-BPEI 100 µg/mL	-	-	-	-	-	+	-	-	-	+

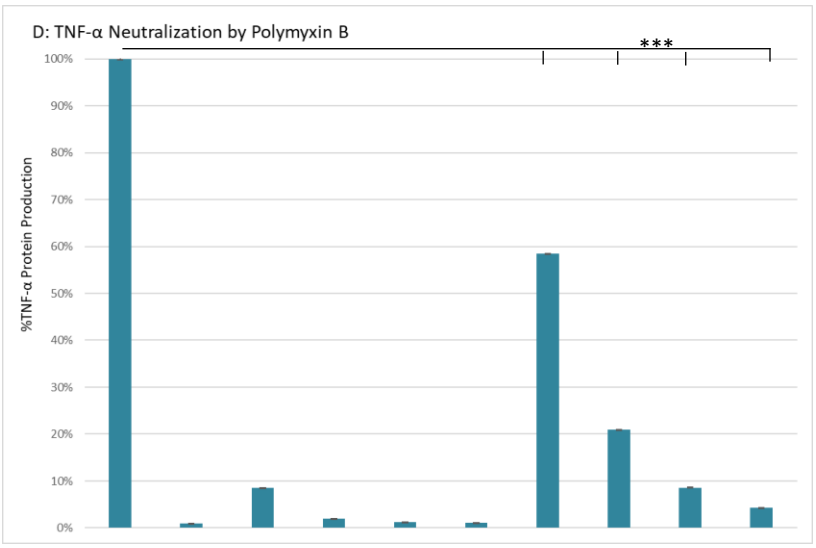

LTA 25 µg/mL	+	-	-	-	-	-	+	+	+	+
Untreated	-	+	-	-	-	-	-	-	-	-
Polymyxin B 25 µg/mL	-	-	+	-	-	-	+	-	-	-
Polymyxin B 50 µg/mL	-	-	-	+	-	-	-	+	-	-
Polymyxin B 75 µg/mL	-	-	-	-	+	-	-	-	+	-
Polymyxin B 100 µg/mL	-	-	-	-	-	+	-	-	-	+

Figure 9. Results for neutralizing immune response induced by *S. aureus* LTA. THP-1 cells were treated with an equivalent amount of LTA and concentrations of A) and B) BPEI, C) PEG-BPEI, and D) polymyxin B. Levels of TNFα cytokines were quantified using ELISA. Untreated cells were used as controls. All experiments were performed in triplicate and the presented data are representative results of the means ±

standard error of the mean (SEM). A 95% confidence value with a p-value consisting of $p < 0.05$ was considered statistically significant.

Subsequently, we evaluated the impact of BPEI on attenuating the TNF-α production induced by peptidoglycan (PGN), the other cell wall component of *S. aureus*. As illustrated in Fig. 10, macrophage cells treated solely with PGN displayed notable activation of TLR after 6 hours of incubation. Although BPEI concentrations partially neutralized PGN and mitigated the secretion of TNF-α, the overall reduction in cytokine levels did not significantly differ from the immune response elicited by PGN (Fig. 10A). Treatment of THP-1 cells with different concentrations of PEG-BPEI and an equivalent amount of PGN resulted in a higher TNF-α reduction than its precursor molecule, 600 Da BPEI (Fig. 10B). To our surprise, the outcomes of neutralizing PGN with polymyxin B were even more unfavorable (Fig. 10C). At combination concentrations of 25 μg/mL of PGN and 50 and 75 μg/mL of polymyxin B, the levels of TNF-α production exceeded 100% (data is not shown), surpassing those observed in the positive control. We hypothesize that all the cationic compounds examined in this study, including BPEI, PEG-BPEI, and polymyxin B, employ electrostatic interactions to bind with LTA and PGN and modify the characteristics of the Gram-positive cell wall components to activate TLRs and induce cytokine production. However, as evidenced by the results presented in Fig. 3, it appears that BPEI, PEG-BPEI, and polymyxin B may not form robust interactions with PGN, hindering their ability to effectively neutralize it.

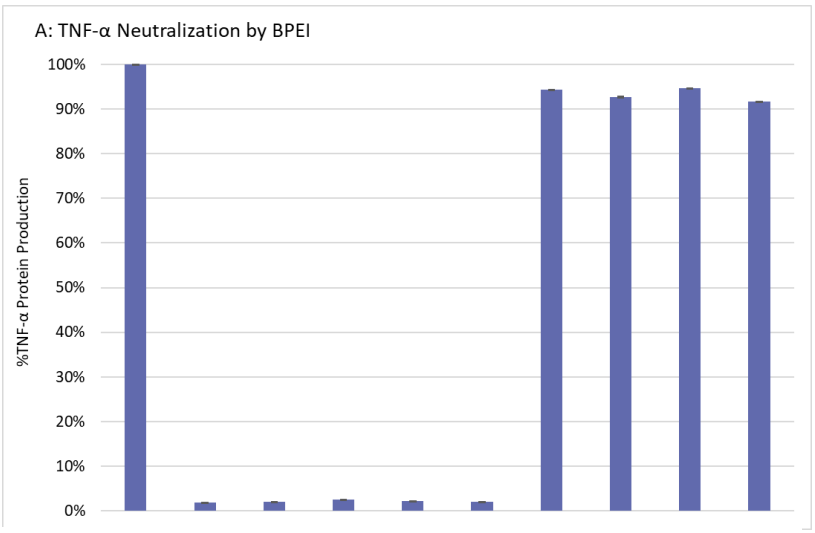

PGN 25 µg/mL	+	-	-	-	-	-	+	+	+	+
Untreated	-	+	-	-	-	-	-	-	-	-
BPEI 5 µg/mL	-	-	+	-	-	-	+	-	-	-
BPEI 10 µg/mL	-	-	-	+	-	-	-	+	-	-
BPEI 15 µg/mL	-	-	-	-	+	-	-	-	+	-
BPEI 20 µg/mL	-	-	-	-	-	+	-	-	-	+

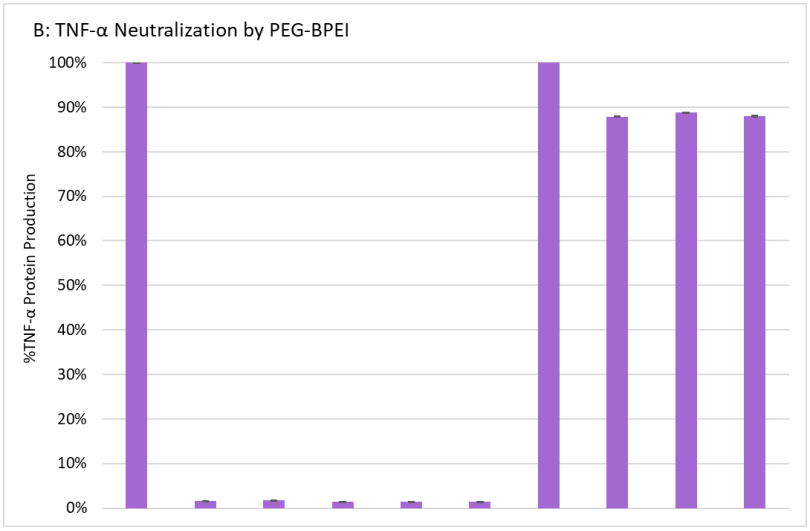

PGN 25 µg/mL	+	-	-	-	-	-	+	+	+	+
Untreated	-	+	-	-	-	-	-	-	-	-
PEG- BPEI 5 µg/mL	-	-	+	-	-	-	+	-	-	-
PEG-BPEI 10 µg/mL	-	-	-	+	-	-	-	+	-	-
PEG-BPEI 15 µg/mL	-	-	-	-	+	-	-	-	+	-
PEG-BPEI 20 µg/mL	-	-	-	-	-	+	-	-	-	+

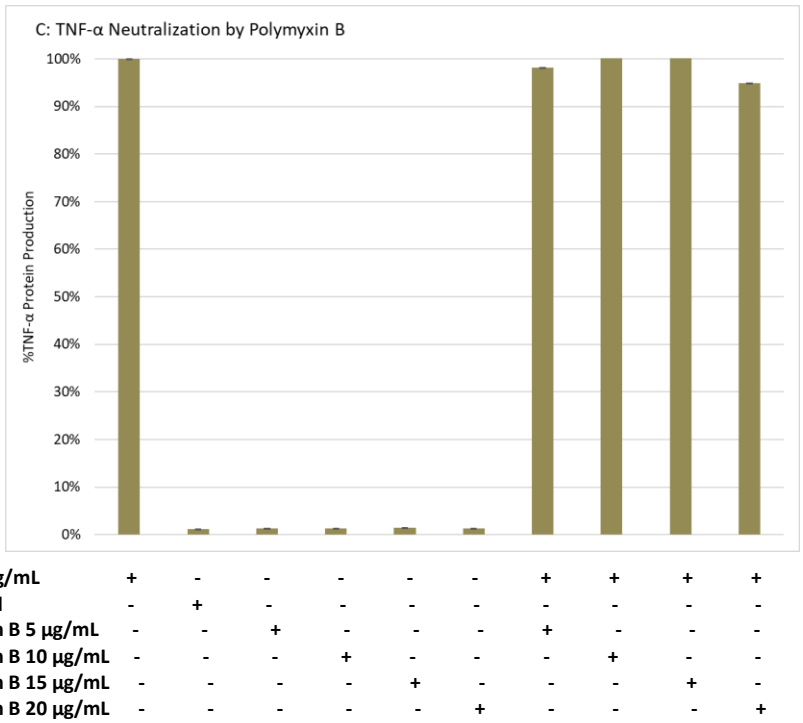

Figure 10. Results for neutralizing immune response induced by *S. aureus* peptidoglycan (PGN). THP-1 cells were treated with an equivalent amount of PGN and concentrations of A) BPEI, B) PEG-BPEI, and C) polymyxin B. Levels of TNFα cytokines were quantified using ELISA. Untreated cells were used as controls. All experiments were performed in triplicate and the presented data are representative results of the means ± standard error of the mean (SEM). A 95% confidence value with a p-value consisting of $p < 0.05$ was considered statistically significant.

We also assessed the ability of BPEI and PEG-BPEI to neutralize the induction of TNF-α production by heat-killed *S. aureus* bacteria (HKSA). We applied concentrations of 100 ng/mL, and 1-15 μg/mL of BPEI and PEG-BPEI to neutralize HKSA-triggered TNF-α production in THP-1 cells. Taking into account that lipoteichoic acid and peptidoglycan together can have greater effect in inducing inflammatory responses, we anticipated that the neutralizing ability of BPEI and PEG-BPEI on TNF-α secretion induced by heat-killed *S. aureus* bacteria would be diminished in comparison to their individual effects. Unexpectedly, a concentration of 15 μg/mL of BPEI resulted in a 40% decrease in TNF-α production, as depicted in Fig. 11A. Moreover, BPEI exhibited a 10% reduction in the inflammatory response at concentrations of 100 ng/mL and 10 μg/mL, also shown in Fig. 11A. On the other hand, PEG-BPEI demonstrated a more robust mitigating effect in HKSA-induced TNF-α production compared to BPEI, resulting in reductions of 60% and approximately 20% at concentrations of 15 μg/mL and 10 μg/mL, respectively (Fig. 11B). We did not pursue further investigations involving higher concentrations of BPEI and PEG-BPEI to neutralize the immune response stimulated by HKSA. While it was not feasible to quantify the concentrations of LTA and PGN present in 10^8 cells/mL of HKSA bacteria for direct comparison with 25 μg/mL of each of LTA and PGN used in this study (Fig. 8), we consider the observed neutralizing effects of BPEI and PEG-BPEI on HKSA-induced inflammation response to be of greater value. This is due to the fact that heat-killed whole *S. aureus* bacteria contain a wide range of antigens and molecular patterns capable of activating various components of the immune system, including toll-like receptors (TLRs) and pattern recognition receptors (PRRs). This can lead to a more comprehensive immune response that closely mirrors the conditions of a natural infection, unlike the utilization of isolated components such as LTA and PGN. Additionally, the structural components and antigens present in heat-killed *S. aureus* bacteria

remain intact, reducing the risk of utilizing chemically isolated LTA and PGN that may be damaged or impure for immune response stimulation. Finally, we employed polymyxin B as a commercially available reference drug to mitigate the inflammation response triggered by HKSA, allowing us to compare the results with those obtained using our branched polyethyleneimines, BPEI and PEG-BPEI. In contrast to what we expected, polymyxin B exhibited a maximum reduction of only 12% in the HKSA-induced TNF-α production (Fig. 11C).

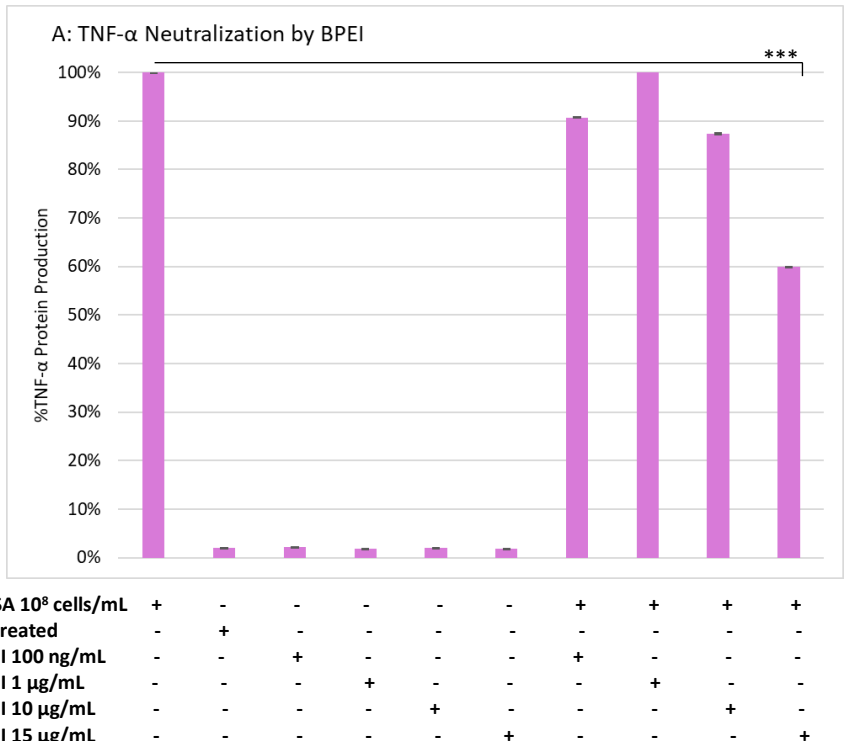

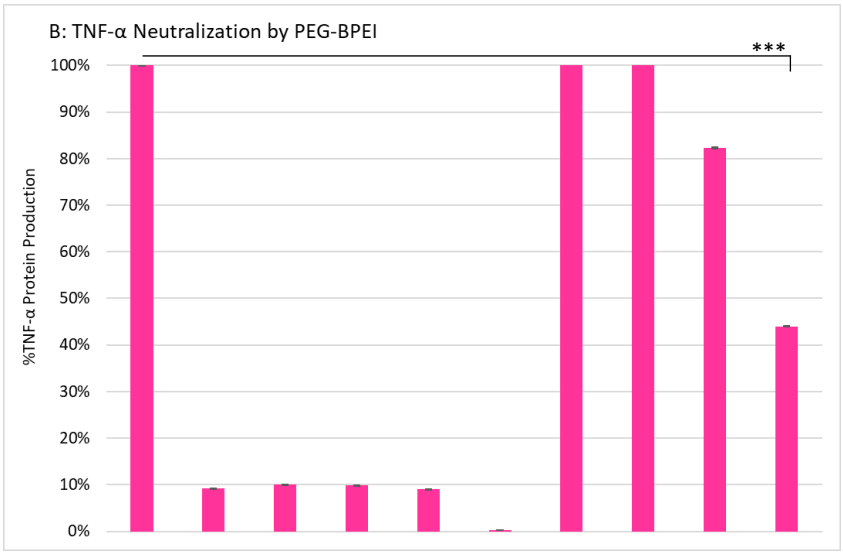

HKSA 10^8 cells/mL	+	-	-	-	-	-	+	+	+	+
Untreated	-	+	-	-	-	-	-	-	-	-
PEG-BPEI 100 ng/mL	-	-	+	-	-	-	+	-	-	-
PEG-BPEI 1 µg/mL	-	-	-	+	-	-	-	+	-	-
PEG-BPEI 10 µg/mL	-	-	-	-	+	-	-	-	+	-
PEG-BPEI 15 µg/mL	-	-	-	-	-	+	-	-	-	+

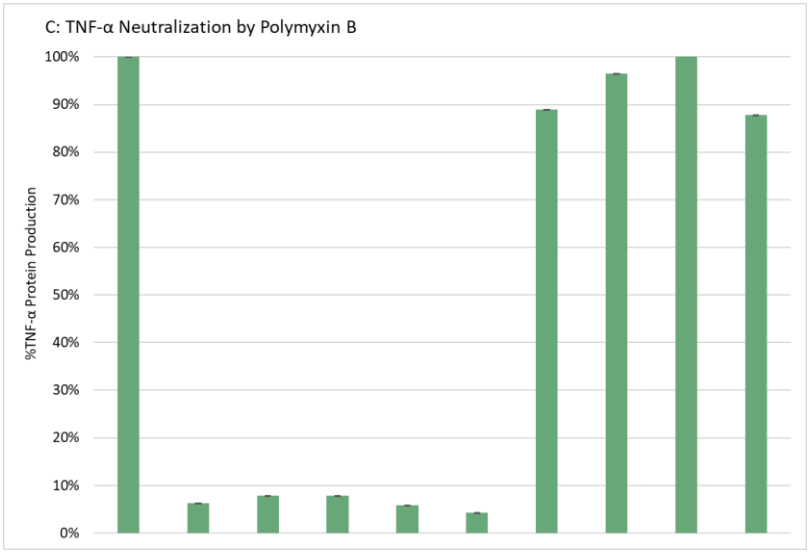

HKSA 10^8 cells/mL	+	-	-	-	-	-	+	+	+	+
Untreated	-	+	-	-	-	-	-	-	-	-
Polymyxin B 100 ng/mL	-	-	+	-	-	-	+	-	-	-
Polymyxin B 1 µg/mL	-	-	-	+	-	-	-	+	-	-
Polymyxin B 10 µg/mL	-	-	-	-	+	-	-	-	+	-
Polymyxin B 15 µg/mL	-	-	-	-	-	+	-	-	-	+

Figure 11. Results for neutralizing immune response induced by heat-killed *S. aureus* bacteria (HKSA). THP-1 cells were treated with an equivalent amount of HKSA and concentrations of A) BPEI, B) PEG-BPEI, and C) polymyxin B. Levels of TNFα cytokines were quantified using ELISA. Untreated cells were used as controls. All experiments were performed in triplicate and the presented data are representative

results of the means ± standard error of the mean (SEM). A 95% confidence value with a p-value consisting of $p < 0.05$ was considered statistically significant.

Confirmation of mitigating effects of BPEI and PEG-BPEI in LTA-induced inflammation response by RT-PCR and qPCR assays

To investigate the potential impact of BPEI and PEG-BPEI on LTA-induced TNF-α cytokine mRNA expression, we conducted neutralization experiments using these branched polyethylenimines. Initially, THP-1 cells were exposed to 25 μg/ml of LTA for varying durations (1, 2, 6, and 8 hours) to determine the time point at which LTA could induce the highest levels of TNF-α gene expression. Fig. 12A illustrates the initial expression of TNF-α mRNA within one hour of THP-1 cell incubation. This early gene expression notably declined at the 6-hour time point and was completely absent after 8 hours of incubation. Hence, we focused on a one-hour incubation period to reach the highest levels of TNF-α mRNA levels induced by LTA. Subsequently, THP-1 cells were exposed to various treatments, including LTA alone and combinations of LTA with different concentrations of BPEI. Cells treated with BPEI concentrations and untreated cells were used as negative controls. Following a 1-hour stimulation, total cellular RNA was extracted, reverse transcribed into cDNA, and subjected to quantitative real-time PCR analysis. As depicted in Fig. 12B, BPEI treatment exhibited a significant inhibitory effect on the expression profile of the TNF-α gene. These qPCR findings were consistent with the results obtained from the ELISA experiments (Fig. 12A). According to the data in Fig. 12B, BPEI at a concentration of 25 μg/ml suppressed TNF-α mRNA production by 75%. Although higher concentrations of BPEI resulted in a lesser reduction in TNF-α gene expression, they still caused a considerable decrease of 44% to 55% in the expression of the gene (Fig. 12B). The RT-PCR experiments were also conducted for PEG-BPEI. The results, as depicted in Fig. 12C,

demonstrated that this derivative of BPEI effectively inhibited the expression profile of the TNF-α gene in a dose-dependent manner, in accordance with the findings obtained from the ELISA assays (Fig. 9C). At the lowest PEG-BPEI concentrations, there was a noticeable decrease of up to 40% in the mRNA levels of the TNF-α cytokine gene. Intriguingly, at a concentration of 75 µg/ml of PEG-BPEI, the downregulation reached 70% of mRNA production, and at 100 µg/ml, only a minimal 6% expression of the TNF-α gene was observed (Fig. 12C). Taken together, these results verified results of ELISA analysis and suggested that BPEI and PEG-BPEI can mitigate the production of inflammation response via the downregulation of signal transduction associated with the TNF-α cytokine production.

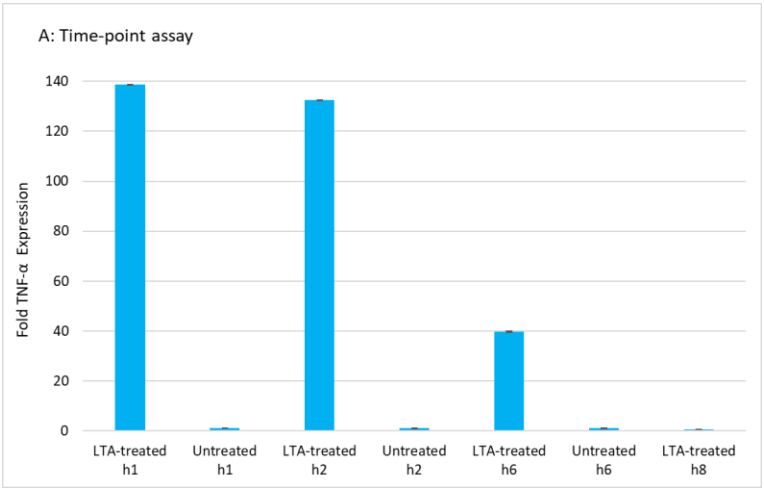

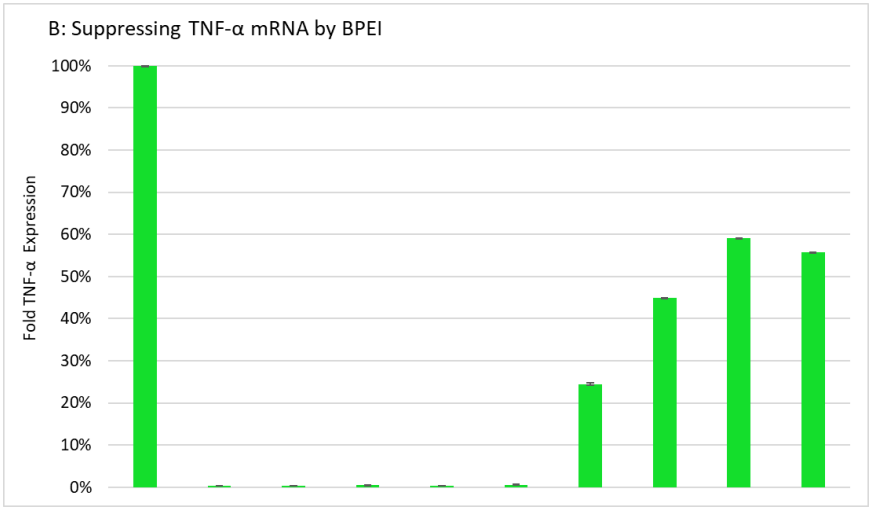

LTA 25 µg/mL	+	-	-	-	-	-	+	+	+	+
Untreated	-	+	-	-	-	-	-	-	-	-
BPEI 25 µg/mL	-	-	+	-	-	-	+	-	-	-
BPEI 50 µg/mL	-	-	-	+	-	-	-	+	-	-
BPEI 75 µg/mL	-	-	-	-	+	-	-	-	+	-
BPEI 100 µg/mL	-	-	-	-	-	+	-	-	-	+

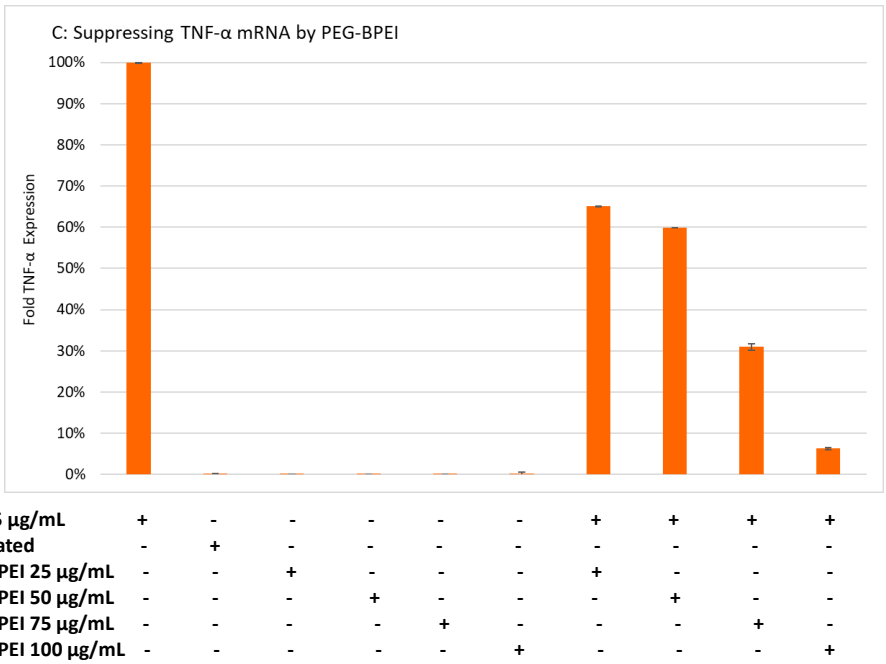

Figure 12. qPCR results for neutralizing immune response induced by *S. aureus* LTA. A) THP-1 cells were treated with 25 µg/ml of LTA and incubated for 1, 2, 6, and 8 h. Total cellular RNA was extracted, reverse transcribed to cDNA and then quantitative real-time PCR analysis was performed to detect the levels of TNFα mRNA. B) THP-1 cells were treated with an equivalent amount of LTA and concentrations of BPEI. Then, TNFα gene expression was quantified using qPCR. C) THP-1 cells were treated with an equivalent amount of LTA and concentrations of PEG-BPEI. Then, TNFα gene expression was quantified using qPCR. Untreated cells were used as controls. All experiments were performed in duplicate, and the presented data are representative results of the means ± standard error of the mean (SEM). A 95% confidence value with a p-value consisting of $p < 0.05$ was considered statistically significant. To normalize the fold-changes between different experiments, their values were expressed as percentages.

BPEI and PEG-BPEI prevents cytotoxicity in human and murine macrophages

To test the cytotoxicity of 600 Da BPEI, PEG 350-BPEI, and Polymyxin B used in the previous experiments, RAW 264.7 murine and THP-1 human macrophage cells were incubated for two days in the presence of different concentrations of BPEI, PEG-BPEI, and Polymyxin B. The

The latter compound was used as a positive control as it has high cytotoxicity effects on eukaryotic cells. The concentration at which each compound reduced cell viability by 50%, IC50, was calculated to determine the dose-response relationship (Fig. 13A). As Fig. 13A shows, the IC50 for low molecular weight BPEI in RAW 264.7 cells were determined to be 874.1 µM (equivalent

to 577 μg/mL of BPEI), whereas for Polymyxin B, it was 66.44 μM (equivalent to 88 μg/mL of Polymyxin B). This striking contrast indicates that low-MW BPEI exhibits negligible cytotoxicity, as it requires a concentration over 6.5 times larger than that of Polymyxin B to produce a similar cytotoxic effect. The IC50 for PEG-BPEI was 916 μM (equivalent to 958 μg/mL of PEG-BPEI) (Fig. 13A). Hence, PEG-BPEI demonstrated minimal cytotoxicity, making it a prospective candidate for further *in vivo* experimentation. The concentration of BPEI and PEG-BPEI employed in this cytotoxicity assessment is approximately 50-fold higher compared to the maximum quantity, 100 μg/mL, utilized in ELISA and qPCR experiments.

Similarly, THP-1 macrophages were exposed to concentrations of BPEI and PEG-BPEI using a concentration range of 0.01-5 mg/mL. As anticipated, the findings from the Resazurin assay indicated that BPEI had minimal impact on cell viability, and similarly, the treatment with PEG-BPEI also exhibited negligible effects (Fig. 13B). The IC50 were determined for BPEI and PEG-BPEI, resulting in values of 853.3 μM and 2661 μM, respectively. Notably, the IC50 for BPEI in THP-1 cells was similar to that observed in RAW 264.7 cells. Interestingly, the IC50 for PEG-BPEI was three times higher in RAW 264.7 cells, indicating the enhanced safety profile of PEG-BPEI when administered to human macrophage cells. Overall, these results show that the BPEI and PEG-BPEI branched polyethyleneimines do not cause any appreciable cytotoxicity against eukaryotic cells until they reach a threshold of 340 μg/mL for BPEI and 833.3 μg/mL for PEG-BPEI which are much higher than the concentrations that used in TNF-α neutralization experiments in this study (Fig. 13B).

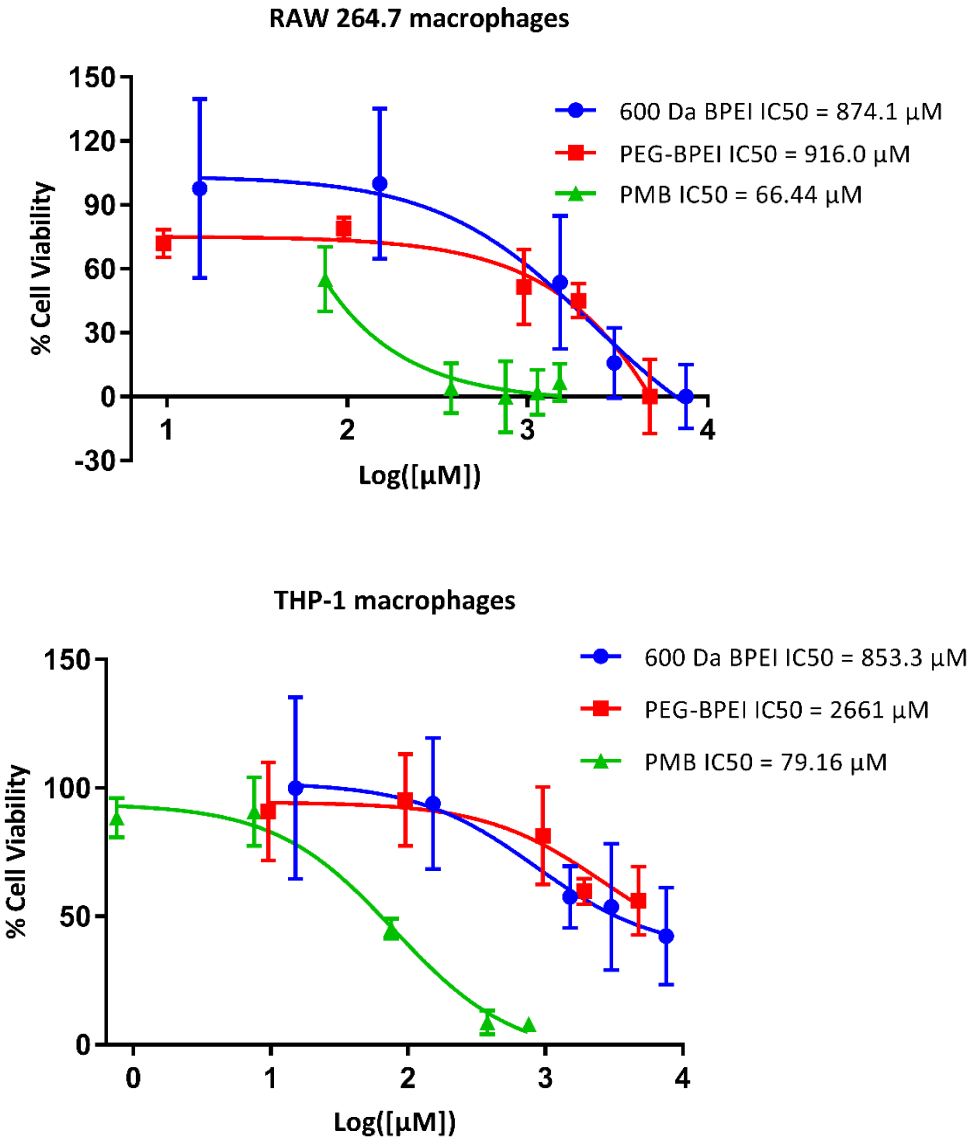

Figure 13. Cytotoxic effect of BPEI, PEG-BPEI, and polymyxin B on A) RAW 264.7 murine macrophages and B) THP-1 human macrophages.

Discussion

From a clinical perspective, chronic wounds are characterized by a disruption in the typical sequence of healing phases [7]. Instead, they become trapped in a state of pathological inflammation, persistent infections, necrosis, and exhibit a resistance to the normal repair process. In general, because of the ongoing inflammation in chronic wounds the clinical management for these wounds continues to present a challenge [53]. Within clinical settings, the management of chronic wounds commonly involves the utilization of debridement to remove infected and nonviable tissue, along with the application of non-specific wound dressings [74]. Nevertheless, these technologies do not have a specific focus on the treatment of chronic non-healing wounds [76]. The FDA acknowledges that there is a lack of available innovative products for treating non-healing chronic wounds and emphasizes that it is crucial to overcome barriers to product development in this area [76]. To date, the FDA has only approved one product called becaplermin gel, along with two moderately effective cell-based therapies, Dermagraft and Apligraf (developed by Organogenesis, Canton, MA), for the treatment of chronic non-healing wounds. Furthermore, there is currently no small-molecule drug approved by the FDA specifically for treating non-healing chronic wounds [84-88].

Considering the substantial impact of the proinflammatory phase on the progression of chronic wound healing [81, 89, 91], the extracellular and intracellular components of the inflammatory response are attractive therapeutic targets for novel immunomodulation approaches [17]. These approaches hold potential for regulating conditions characterized by abnormal tissue remodeling, such as chronic inflammatory disorders, healing disorders, and even cancer [52]. *Staphylococcus aureus* (*S. aureus*) is a Gram-positive bacterium that causes serious infections in skin and soft tissues [118-120]. It can also initiate a large variety of proinflammatory cytokines in wounds by its

immunostimulatory pathogen associated molecular pattern components, LTA and PGN[121]. The PAMP molecules bind to TLR2 in macrophage cells to induce activation of nuclear factor kappa B, a transcription factor involved in TNF-α, IL-1, IL-6, IL-8, and IL-10 cytokine generation [35, 117]. Therefore, as expected, the treatment of THP-1 cells with LTA or PGN resulted in the induction of TNF-α cytokine production, with LTA showing a more pronounced effect (Fig. 8A and Fig. 8B).

A recent study demonstrated that heat-killed whole cell preparations derived from *S. aureus* can activate the transcription factor NF-kB in a TLR2 and CD14-dependent manner [131]. In Fig. 8C, we confirmed this finding by demonstrating that whole *S. aureus* bacteria induce the production of TNF-α cytokines in THP-1 cells expressing TLR2. These results align with previous reports highlighting the synergistic effects of LTA and PGN in enhancing the generation of proinflammatory agonists [117]. The inhibition of TLR signaling pathways has been identified as a promising therapeutic approach to attenuate undesirable chronic inflammatory loop associated with various diseases such as non-healing wounds [7, 22]. The ongoing clinical development of TLR blockade strategies encompasses several approaches [7, 9] such as comprehensive inhibition of TLR activity through the utilization of neutralizing antibodies, soluble TLR extracellular domains (ECDs), natural antagonists, and small molecule inhibitors [17]; targeting downstream signaling pathways that are activated as a result of TLR stimulation by using small molecules and microRNA inhibitors that hinder MyD88/TRAF/IRAK complex formation, MAPK, or IKK activity; and employing PAMP antagonists, including LTA inhibitors such as antibodies, phospholipids, cationic immunoglobulins, and cationic peptides [7, 117, 135]. Some of these compounds have reached phase II clinical trials and the results are currently awaited, whilst others, particularly those

targeting common signaling pathways such as MAPK, have proved to be of limited efficacy [9, 136]. Regarding the LTA inhibitors, there are currently no established clinical guidelines for employing proven strategies to neutralize LTA activity *in vivo*. It is advised to avoid the exclusive use of antibiotics, such as beta-lactams, that trigger bacteriolysis and induce release of large quantities of LTA [117, 137, 138].

Current available therapeutic adjuvants for treatment of inflammatory disorders include non-steroidal anti-inflammatory drugs and anti-TNF-α and anti-IL-1β antibodies such as infliximab, alemtuzumab, adalimumab, itanercept, anakinra, etc. However, these are narrow-spectrum macromolecules, which have severe interactions and side effects such as sepsis, increase in upper respiratory disorders, reactivation of latent tuberculosis, lupus-like syndrome [114, 139].

On the other hand, an effective treatment for chronic and non-healing wounds should encompass not only the eradication of bacterial infections and existing biofilms but also the establishment of a favorable wound microenvironment for wound healing by mitigating inflammation and oxidative stress. This involves a universal therapeutic that can address factors that impede wound healing [53, 92, 93]. Previous studies in our lab have utilized laser scanning confocal microscopy images to illustrate the attachment of BPEI to teichoic acids within the cell wall of methicillin-resistant *Staphylococcus aureus* (MRSA) bacteria [100]. According to the microscopy data, BPEI was located within the cell wall region of the bacteria, indicating a potential interaction between BPEI and the major components of the Gram-positive cell wall, teichoic acids. The interaction was similarly detected through nuclear magnetic resonance (NMR) investigations involving combined solutions of BPEI and wall teichoic acids (WTA) extracted from Gram-positive *Bacillus subtilis* bacteria, as

compared to NMR spectra of teichoic acid alone. The NMR data indicated a phosphate:amine binding resulting from the WTA:BPEI interactions, likely facilitated by the electrostatic attraction between the abundant cationic primary amines of BPEI and the anionic phosphate groups of WTA [100].

In general, teichoic acids encompass two types: lipoteichoic acids (LTAs), which are secured in the bacterial membrane through a glycolipid anchor, and WTAs, which are covalently linked to peptidoglycan. These integral cell wall constituents consist of an anionic chain comprising repeating units of polyglycerolphosphate or polyribitolphosphate. As a result, the Gram-positive envelope acquires a significantly negative surface net charge [140, 141]. Taking this into account, this research focused on examining the polycationic characteristics of BPEI and PEG-BPEI, aiming to establish robust electrostatic interactions with the polyanionic phosphate groups found in lipoteichoic acid molecules (LTA). We suggest the same mechanism of interaction involving the primary amines of BPEI with the phosphate groups of LTA, which aligns with the findings of the earlier study [100]. Illustrated in Fig. 9, both BPEI and its PEGylated derivative demonstrated the ability to neutralize LTA molecules and alleviate the production of TNF-α cytokines. Our rationale is that the cationic polymers can modify the characteristics of Gram-positive cell wall components by modifying the molecular structure and/or introducing steric bulk through the branched polymer. Such interference can impede the attachment of LTA to TLR receptors, block the signal transduction through TLR, and consequently prevent the initiation of TNF-α cytokine production (Fig. 14). Additionally, we examined the impact of BPEI and PEG-BPEI binding to another constituent of the Gram-positive cell wall, peptidoglycan, on the generation of an inflammatory response. Nevertheless, as depicted in Fig. 10, peptidoglycan activation of TLR signaling was only

partially neutralized by the polyethylenimines. This partial neutralization can likely be attributed to the structural composition of peptidoglycan, which contains fewer ionic groups in comparison to teichoic acids. Consequently, there was an insufficient formation of electrostatic interactions between the cationic components of BPEI and PEG-BPEI polymers and the anionic acidic groups of peptidoglycan, hindering effective neutralization of the molecule [142].

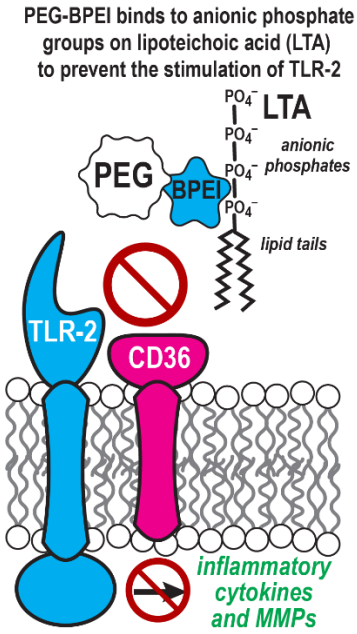

Figure 14. Proposed mechanism of action of LTA and PEG-BPEI interactions. LTA molecules activate TLR2 receptor and induce the downstream signaling cascade that ultimately produces inflammatory cytokines. Cationic PEG-BPEI binds with LTA through electrostatic interactions and prevents it from activating TLR2 receptor. This eventually results in mitigated cytokine production.

Moreover, our findings demonstrate that heat-killed whole *S. aureus* bacteria (HKSA) elicit a more pronounced inflammatory response in THP-1 cells compared to LTA and PGN individually, as shown in Fig. 8. This can be attributed to the presence of both LTA and PGN in the cell wall of *S. aureus* bacteria, which likely exhibit a greater effect in inducing TNF-α production. It is intriguing to note that the combined administration of HKSA with either BPEI or PEG-BPEI resulted in a

substantial reduction of the immune response in THP-1 cells (Fig. 11A and 11B). The neutralization of intact bacterial cells in wound environments holds great significance as it may facilitate the creation of a conducive healing environment. This neutralization process may help to minimize inflammation, foster tissue regeneration, inhibit biofilm formation, and reduce the potential for secondary infections. Typically, wounds are exposed to a mixture of pathogenic bacteria and PAMPs. Hence, the development of a therapeutic agent capable of targeting all invading components that can cause wound infection and trigger immune responses becomes imperative. Likewise, intact bacterial cells inhibit tissue regeneration as they release toxins within wounds that can damage tissue cells and hinder their proliferation and migration capacities [143, 144]. Therefore, killing these cells is also important. An added benefit to killing bacteria is reducing biofilm formation, which impedes the healing process and enhances bacterial resistance against antibiotics and immune defenses [65].

Lastly, we assessed the impact of polymyxin B, an FDA-approved antibiotic known to possess certain anti-inflammatory properties. Polymyxin B, a cationic polypeptide, contains five primary amine groups that, at physiological pH, are protonated and bear a positive charge. This charge enables the antibiotic to bind effectively to the negatively charged endotoxin components of the Gram-negative bacterial cell wall. The inhibitory effects of polymyxin B on the release of inflammatory mediators, such as TNF-α and interleukin-6, have been observed in previous studies[134, 145]. In this study, while polymyxin B demonstrated a notable decrease in TNF-α cytokine release induced by LTA (Fig. 9D), its impact on TLR activation triggered by PGN and HKSA was not substantial (Fig. 10C and Fig. 11C). Consequently, minimizes the anti-inflammatory effectiveness of polymyxin B to Gram-negative bacteria.

It is noteworthy that polymyxin B exhibits significant cytotoxicity towards mammalian cells and carries a black box warning due to its potential for neurotoxicity and nephrotoxicity. The warning highlights the risk of polymyxin B-induced neurotoxicity, which can lead to respiratory paralysis resulting from neuromuscular blockade. These adverse reactions and side effects render polymyxin B a drug of last resort [146-149]. Our study further confirmed this fact by demonstrating the pronounced cytotoxic effect of polymyxin B on human and murine macrophage cells, while simultaneously observing negligible cytotoxicity in the cells treated with low-molecular-weight BPEI and PEG-BPEI, as illustrated in Fig. 13.

In recent investigations conducted within our laboratory [64, 99-110], it has been revealed that branched polyethyleneimine (BPEI) with a molecular weight of 600 Da, along with its safer derivative known as PEGylated BPEI (PEG350-BPEI), exhibit several beneficial properties. These compounds have shown the potential to enhance the uptake of drugs, reduce barriers to drug influx, and counteract antibiotic resistance mechanisms. Moreover, BPEI and PEG350-BPEI potentiators possess an additional advantage in their ability to disrupt biofilms formed by *Staphylococci, P. aeruginosa*, and carbapenem-resistant *Enterobacteriaceae* bacteria expressing KPC and NDM-1 [65, 100-111].

In this study, we present compelling evidence demonstrating the capacity of 600 Da BPEI and PEG350-BPEI to effectively mitigate the production of inflammatory responses in human THP-1 macrophage cells, while exhibiting minimal cytotoxicity. Our findings indicate that both BPEI and PEG350-BPEI possess anti-inflammatory properties against the Gram-positive cell wall components and intact *S. aureus* bacteria. Based on these outcomes, we envision BPEI and PEG-

BPEI as versatile topical agents for application in acute and chronic wounds. Not only do these agents actively prevent the release of cytokines, but they also disrupt antibiotic resistance mechanisms and interfere with the biofilm matrix. This multifaceted approach holds the potential to speed up the wound healing process.

Chapter 3: Effect of BPEI and PEG-BPEI to mitigate inflammation induced by Gram-negative bacterial and fungal PAMPs

Background and Significance

Wound healing and recovery after burn encompass a complicated pathophysiological process proceeding by inflammation, proliferation of cells, contraction of the skin at the wound site, collagen metabolism, and complex interaction with the extracellular matrix and cytokines [150-153]. By constantly monitoring the environment, immune cells provide a strong barrier against microbial pathogens. However, in case of injury and disease, the skin barrier is breached, and opportunistic microorganisms can become pathogenic and can cause infections. Chronic wounds are especially prone to infection. Clinical studies have shown that up to 90% of diabetic foot ulcers leading to lower limb amputation are caused by chronic infections [153]. Unlike acute wounds, which progress through the inflammatory phase and eventually heal, chronic wounds stagnate in the inflammatory phase [154]. This is due in part to the presence of polymicrobial communities in chronic wounds, which include bacteria and fungi. These microbes contribute to the overproduction of cytokines, which in turn perpetuates inflammation [155-157]. The persistent inflammation in chronic wounds can lead to delayed healing, deepening and expansion of the wound, and a significant decrease in the quality of life for those affected [158-160]. Chronic wounds are a major global health problem which affect millions of people around the globe and cost healthcare systems billions of dollars each year[161]. Medical deficiencies in wound healing lead to over 38 million cases of chronic wound infections, which are closely linked to unfavorable disease prognoses [162]. Indeed, how to prevent and treat wound infection is a serious clinical issue. In the absence of robust anti-inflammatory drugs, a new line of therapeutic agents should be introduced. Ideally, it should be a single

compound with multifunction properties that reduce cytokine production, diminish persistent infection and biofilms, and helps infectious wounds treatment [163].

The innate immune system is the first line of defense against pathogen invasion through an evolutionarily conserved pathogen recognition system [164]. Unlike the adaptive immunity that recruits T-cells and specific antibodies against antigens, innate immune response relies on pathogen-associated molecular patterns (PAMPs) recognition[165]. In mammals, a family of Toll-like receptors (TLRs) is a key component of the innate immune system that is responsible for recognizing PAMPs and generating the subsequent immune response. Some examples of the PAMPs include bacterial lipoproteins, lipopolysaccharide (LPS), non-methylated CpG DNA, and fungal glucan (Zymosan) [166-168].

Lipopolysaccharide (LPS) is an abundant glycolipid component present on the outer leaflet of Gram-negative bacteria (Fig. 15). During a Gram-negative infection, the immune system's response to the highly conserved lipid A component of LPS is a severe generalized inflammation clinically manifested as the systemic inflammatory response syndrome (SIRS) and endotoxin shock. Toll-like receptor 4 (TLR4) primarily recognizes, and is activated by LPS endotoxin, leading to signaling events that eventually culminate with the release of inflammatory cytokines [169, 170].

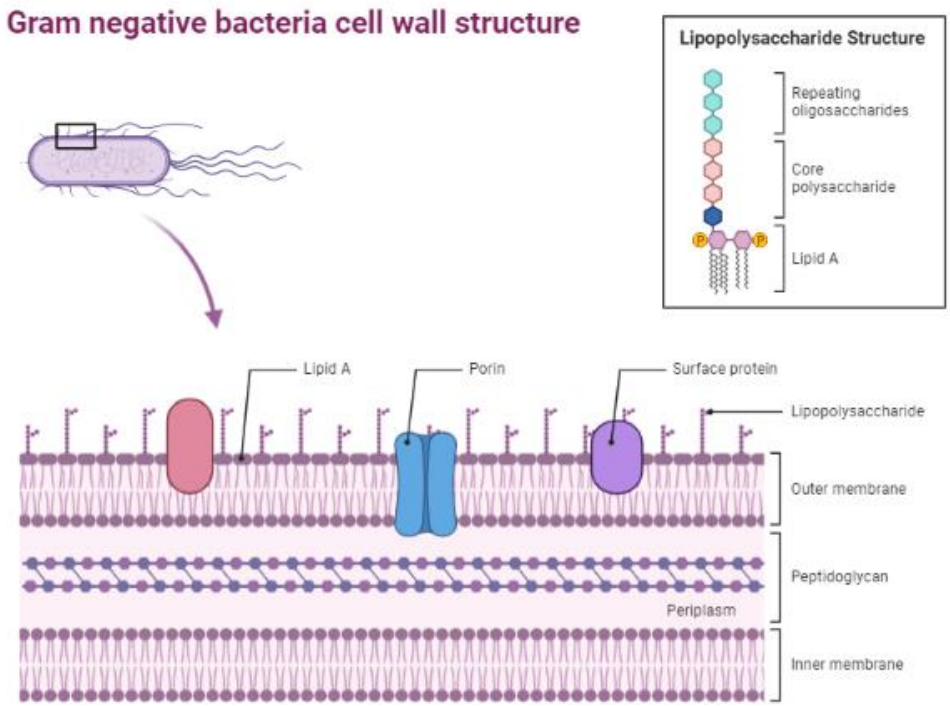

Figure 15. Structure of Gram-negative cell wall and LPS molecule.

TLR4 activation requires interaction with several co-receptors and through a series of consecutive steps. LPS first combines with LPS-binding protein (LBP) and then LBP transfers LPS molecule to cluster of differentiation 14 (CD14) protein. CD14 in turn chaperones the formation of LPS and myeloid differentiation factor 2 (MD2) complex [169]. TLR4 is not able to bind LPS directly and the adaptor protein MD2 is required. MD2 directly recognizes and binds the lipophilic part (lipid A) of LPS to form a discrete aggregate. It non-covalently associates to TLR4 to form the final activated heterodimer of LPS/MD2/TLR4 that in its turn induces the downstream intracellular signal (Fig. 16). The interactions between MD2, lipid A sugars and fatty acid chains of LPS, and the two TLR4 on the extracellular side promotes the dimerization of TLR4. Activation of downstream signaling events initiated by TLR4 in response to LPS all take advantage of adapter proteins to operate including myeloid differentiation factor 88 (MyD88), TIR domain-containing

adaptor-protein (TIRAP), TIR domain-containing adapter-inducing interferon (TRIF), and TRIF-related adapter molecule (TRAM) [171, 172]. LPS response mediated by TLR4 can be divided into two categories: an early MyD88-dependent response, and a delayed MyD88-independent response. The early response, which is dependent on MyD88 and TIRAP leads to the transcription of nuclear factor-kB (NF-kB) (TLR4/MyD88/NF-kB pathway). The later LPS response makes use of TRIF and TRAM and leads to the late activation of NF-kB and IRF3 transcription factors (TLR4/TRIF/IRF3 pathway) and subsequently the production of pro-inflammatory cytokines, chemokines and other pro-inflammatory proteins such as inducible NO synthase (iNOS) [169, 171, 173, 174] (Fig. 1). The pro-inflammatory cytokines such as TNF-α, IL-6, IL-8, and IFN-β act locally but are released systemically and initiate the storm of cytokines that cause vital tissues damage [166].

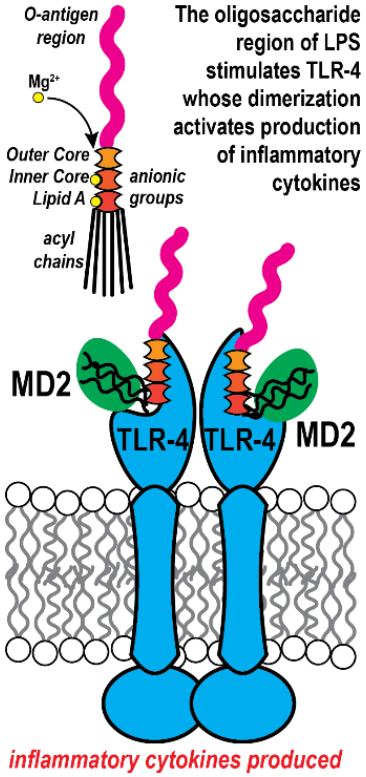

Figure 16. LPS molecules activate TLR4 receptor and induce the downstream signaling cascade that ultimately produces inflammatory cytokines. TLR4 activation requires interaction with several co-receptors and through a series of consecutive steps. LPS first combines with LPS-binding protein (LBP) and then LBP transfers LPS molecule to cluster of differentiation 14 (CD14) protein. CD14 in turn chaperones the formation of LPS and myeloid differentiation factor 2 (MD2) complex.

Fungal pathogens, which include *Candida albicans*, *Cryptococcus neoformans*, and *Aspergillus fumigatus*, can cause invasive fungal infections that are a major global health burden [167, 168, 175]. These pathogens cause over 1 million confirmed fatalities annually, along with 100 million infections in mucosal tissues and 1 billion infections on the skin [175]. The innate immune system identifies fungal cells as foreign invaders by detecting distinct molecular patterns associated with fungal pathogens (PAMPs) [167, 176]. At the surface of fungal cells, various fungal PAMPs are present, such as glucans (β- and α-linked), chitin, chitosan, mannans, galactosaminogalactan, and fungal DNA [167, 168] (Fig. 17). These critical fungal cell wall components are identified by pattern recognition receptors (PRRs) including TLRs (particularly TLR2 and TLR4), C-type lectin receptors (CLRs) such as Dectin-1 and Dectin-2, and galectin family proteins that are present on the surface of host cells [168, 175, 177]. Zymosan, derived from the cell wall of *Saccharomyces cerevisiae*, is composed protein and repeating glucose units linked by β-1,3-glycosidic bonds. Zymosan stimulates macrophages through the activation of TLR2. This activation leads to the induction of NF-kB signaling pathway and the subsequent production of various inflammatory cytokines such as TNF-α, IL-6, IL-8 [178-183]. Zymosan is also recognized by Dectin-1 receptor which is expressed on the surface of macrophages, dendritic cells, and neutrophils [177, 179, 184].

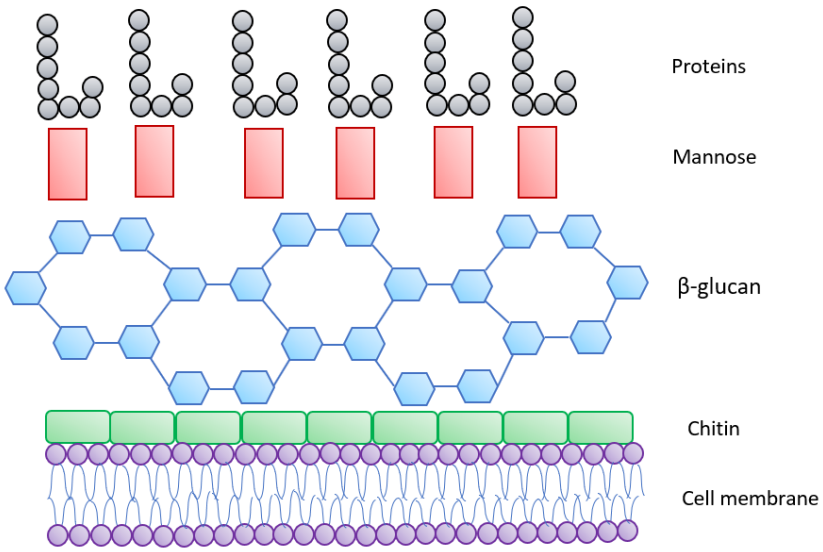

Figure 17. Structure of fungal cell wall.

In this work, we demonstrated the ability of 600 Da branched polyethylenimine (BPEI) and its less toxic PEGylated derivative (PEG-BPEI) to mitigate TNF-α cytokine production induced by LPS of Gram-negative bacteria and fungal zymosan in THP-1 macrophage cells. The significance of utilizing low molecular weight BPEI potentiators Gram-negative and fungal PAMPs becomes more evident when considering their ability to disrupt biofilms and combat antibiotic resistance in *Pseudomonas aeruginosa*, *Staphylococcus aureus*, *Escherichia coli*, and carbapenem-resistant *Enterobacteriaceae* [65, 100-111].

Contributions

This work was made possible due to the guidance and contributions of Dr. Karen Wozniak, Ph.D and Ms. Aysha Nair at Oklahoma State University. We would also like to thank Dr. Phil Bourne and the Protein Production Core (PPC) at the University of Oklahoma, Ms. Tra D. Nguyen, Mr. Zongkai Peng, and Mr. Yunpeng Lan.

Methods

Cell culture

THP-1 human monocyte-like cell line was purchased from Sigma (St. Louis, MO, ECACC, 88081201) and maintained in RPMI 1640 medium containing L-glutamine and sodium bicarbonate (Sigma, St. Louis, MO, R8758), supplemented with 10% heat-inactivated fetal bovine serum (HyClone Laboratories, Logan, UT, SH30066.03), and 1% Pen Strep (10000 U/ml penicillin and 10000 µg/ml streptomycin, Gibco™ 15140122), at 37 °C and 5% CO2 (v/v) in a humidified incubator. Cells were grown in T-75-cm2 culture flasks (Corning, 431464) and sub-cultured every 5 or 6 days by three to five times dilution.

Preparation of heat-killed *P. aeruginosa* bacteria

P. aeruginosa bacterial stocks were purchased from American Type Culture Collection (ATCC BAA-47, a PAO1 strain). A heat-killed preparation of bacteria (HKL) was prepared by growing bacterial cultures in cation-adjusted Mueller–Hinton broth (CAMHB) media) overnight at 37°C on a rotator. Cultures in log-phase growth were harvested and bacteria concentration was enumerated by measuring their optical density at 600 nm. Then, the cells were centrifuged, and washed three times in PBS. The recovered bacteria were resuspended in PBS and incubated at 85°C for 5 minutes. Then, the bacterial cells were cooled down for 20 minutes at room temperature. After two additional washes in PBS, the absence of viable colonies was confirmed by lack of growth on nutrient agar plates. Optical density (OD) of the heat-killed *P. aeruginosa* (HKPA) was measured at 600 nm one more time to confirm their concentration. The HKPA was kept at −20°C.

LPS, HKPA, and zymosan treatments of THP-1 cells

Before treatments, THP-1 cells were seeded onto 96-well plates (Greiner Bio-one, Stuttgart, Germany) at 2×10^6 cells/mL in RPMI 1640 complete medium (1% Pen Strep, and 10% FBS) and incubated overnight at 37 °C and 5% CO2. The day after, the THP-1 cells were stimulated with 100 ng/ml of *E. coli* O26:B6 LPS (eBioscience™ Lipopolysaccharide (LPS) Solution, Invitrogen, 00-4976-93) for 8 h, or 100 ng/ml of *E. coli* O111:B4 LPS (Lipopolysaccharides, from *Escherichia coli* O111:B4, Sigma, L2630) for 4 h, or 100 ng/ml of *K. pneumoniae* LPS (Lipopolysaccharides, from *Klebsiella pneumoniae*, Sigma, L4268) for 2 h, or 1 μg/ml of *P. aeruginosa* LPS (Lipopolysaccharides, from *Pseudomonas aeruginosa* 10, Sigma, L8643) for 6 h, or 25 μg/ml of Zymosan (cell wall from *Saccharomyces cerevisiae*; TLR2 and Dectin-1 ligand, InvivoGen, tlrl-zyn) for 6 h. Whole-cell heat-killed *P. aeruginosa* bacteria BAA47 (HKPA) were also used for stimulation at 10^5 cells/mL final concentration for 2 h. All the solutions were prepared in endotoxin-free water. Concentrations of treatments were selected based on the optimum production of TNF-α cytokine. LPS, HKPA, and Zymosan were reconstituted in LAL-grade water (InvivoGen). After stimulation, supernatants were collected at certain timepoints. To protect TNF-α cytokine protein from degradation by endogenous proteases released during protein extraction, halt protease inhibitor cocktail (Thermo Scientific, 87786) was used. Immediately after supernatant collection, 10μL of protease inhibitor was added per one milliliter of supernatant to produce a 1X final concentration. Cell medium was frozen at − 20 °C until analysis. Untreated cells were used as controls.

Time-point assays of LPS, HKPA, and zymosan

To explore at what time point the Gram-negative and fungal PAMPs have the most inflammatory effect on TNF-α cytokine secretion, we did a time-point assay for each PAMP. THP-1 cells were plated in 96-well plates at 2×10^6 cells/mL in RPMI complete medium. After 24 h incubation, the THP-1 cells were treated with 100 ng/ml of *E. coli* O26:B6 LPS, or 100 ng/ml of *E. coli* O111:B4 LPS, or 100 ng/ml of *K. pneumoniae* LPS, or 1 μg/ml of *P. aeruginosa* LPS, or 25 μg/ml of Zymosan, or 10^5 cells/mL of HKPA. The solutions were prepared in endotoxin-free water. The plates were then incubated for 2, 4, 6, 8, and 24 h, and supernatants were collected at the end of each time-point. To protect TNF-α cytokine protein from degradation by endogenous proteases released during protein extraction, halt protease inhibitor cocktail was used at the final 1X concentration. Time durations of treatments were selected based on the optimum production of TNF-α cytokine. Cell medium was frozen at − 20 °C until analysis. Untreated cells were used as controls.

Neutralizing immune response induced by LPS, HKPA, and Zymosan using BPEI

The effect of BPEI against the Gram-negative and fungal PAMPs-induced TNF-α cytokine production was determined. Briefly, THP-1 cells were plated in 96-well plates at 2×10^6 cells/mL in RPMI complete medium and incubated overnight. The day after, different concentrations of BPEI were prepared. For each neutralizing experiment, the THP-1 cells were treated with either PAMP alone, combinations of an equivalent amount of the PAMP with each of the BPEI concentrations, and BPEI concentrations alone. All the solutions were prepared in endotoxin-free water. The latter was used as negative control and the cells treated with PAMP alone represented the positive control. The combo conditions were incubated for 30 minutes before being added to

THP-1 cells. Untreated cells were also prepared as control. Then, supernatants were collected after certain hours of incubation. In HKPA neutralizing experiment, combo conditions were added to the cells immediately without prior incubation.

Enzyme-linked immunosorbent assay (ELISA) measurements

Concentrations of TNF-α cytokine were determined using DuoSet ELISA kits (R&D Systems, DY210) in THP-1 cell supernatants treated by each of the Gram-negative and fungal PAMPs along with BPEI. A 96-well plate was coated with 100 µl per well of TNF-α specific capture antibody diluted in endotoxin-free PBS (Endotoxin-free Dulbecco's PBS 1X, Milipore Sigma, TMS-012-A) and incubated overnight at room temperature. The day after, each well was washed three times with 300 µl of washing buffer. Next, the plate was blocked with 300 µl of reagent diluent (R&D Systems, DY995) and incubated at room temperature for a minimum of 1 h and then washed three times with washing buffer. Subsequently, 100 µl of standards or collected supernatants was added to the plate and incubated at room temperature for 2 h, followed by washing. Then, 100 µl of TNF-α specific detection antibody was added and the plate was incubated for 2 h at room temperature and then washed. After that, 100 µl of streptavidin-HRP was added, and the plate was incubated for a minimum of 30 min at room temperature in dark, followed by washing. Then, 100 µl of substrate solution (equal volume of hydrogen peroxide and tetramethylbenzidine (R&D Systems, DY999)) was added and the plate was once again incubated in dark at room temperature till the color developed. Reaction was stopped by adding 50 µl of 2 N sulfuric acid as stop solution. The absorbance of each well was immediately determined using a microplate reader set at 450 nm. For wavelength correction, the reading was set to 540 nm as well. Optical imperfections in the plate were corrected by subtracting readings at 540 nm from readings at 450 nm.

Statistical Analysis

All experiments were performed in triplicate and the presented data are representative results of the means ± standard error of the mean (SEM). Differences in cytokine production were analyzed using one-way ANOVA with Tukey's post-test. A 95% confidence value with a p-value consisting of $p < 0.05$ was considered statistically significant. Data were analyzed using GraphPad Prism 6.01 software (GraphPad Software Inc., USA) and Adobe Illustrator.

Results

Optimization of TNF-α protein production induced by Gram-negative and fungal PAMPs

The major component of outer leaflet of Gram-negative bacteria is called lipopolysaccharide (LPS), which has a crucial role in the interaction between the host and pathogen within the innate immune system. LPS acts as a potent immunostimulant endotoxin that can stimulate the immune system strongly, even when present in nanogram amounts [185, 186]. In order to optimize the secretion of TNF-α cytokine induced by the Gram-negative endotoxin, LPS molecules from different Gram-negative strains were selected to stimulate THP-1 cells. The macrophage cells were treated with 100 ng/ml of either *E. coli* O26:B6 LPS or *E. coli* O111:B4 LPS or *K. pneumoniae* LPS. In the case of *P. aeruginosa* LPS, 1 μg/ml of the molecules were utilized to treat THP-1 cells. Moreover. heat-killed *P. aeruginosa* bacteria BAA47 (HKPA) were prepared and used as intact bacterial components at the concentration of 10^5 cells/mL. To generate an immune response stimulated by a fungal PAMP, THP-1 cells were treated with 25 μg/ml of Zymosans. The plates were then incubated for 2, 4, 6, 8, and 24 h, and supernatants were collected at the end of each time-point. Untreated cells were incubated for each of the time points as control. Consequently, levels of TNF-α cytokine protein were measured in cell supernatants using ELISA. As shown in Fig. 18, each of the Gram-negative and fungal PAMPs showed a time-dependent manner in inducing TNF-α cytokine secretion. For *E. coli* O26:B6 LPS (Fig. 18A), *P. aeruginosa* LPS (Fig. 18D), and *E. coli* O111:B4 LPS (Fig. 18B), secretion of TNF-α was measured at the highest at 8, 6, and 4 h incubation, respectively. *K. pneumoniae* LPS (Fig. 18C) and HKPA (Fig. 18E) showed high immunostimulant potential by inducing the ultimate amount of TNF-α cytokines in THP-1 cells only 2 hours after incubation. In the case of zymosan, the highest levels of TNF-α were produced at the time-point 6 h (data is not shown). As expected, in almost all the time-point assays, levels

of TNF-α proteins were the lowest at 24 h similar to what was observed with time-point experiments for Gram-positive PAMPs in chapter 2. None of the untreated cells in each time-point assay showed any signal for TNF-α production in ELISA.

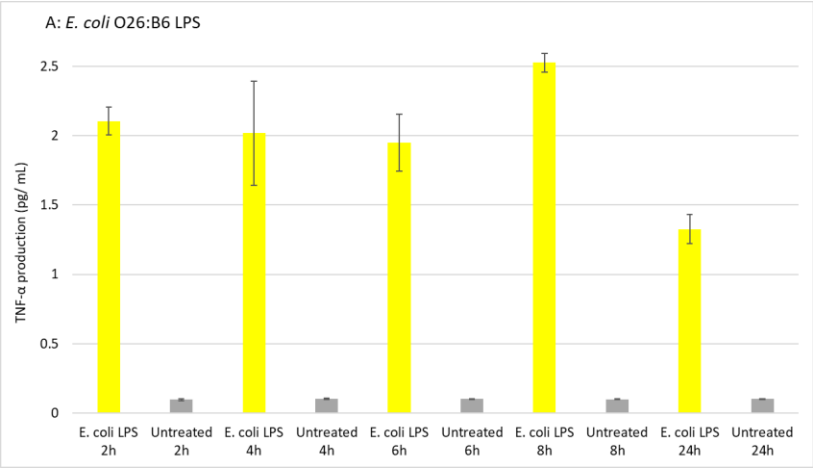

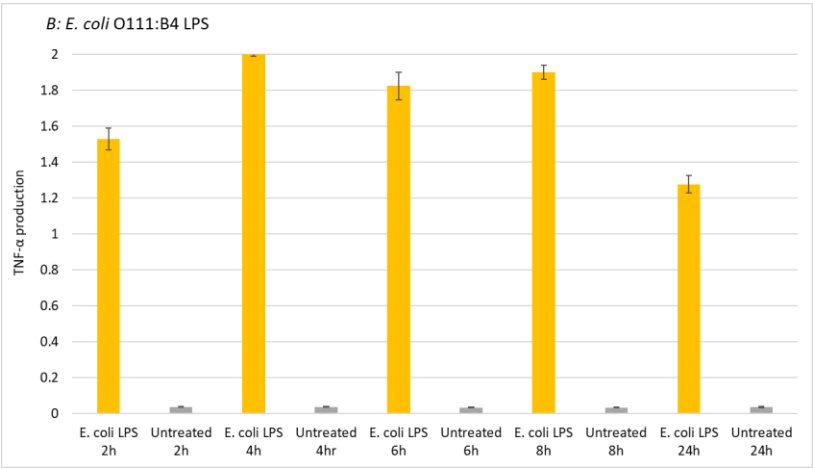

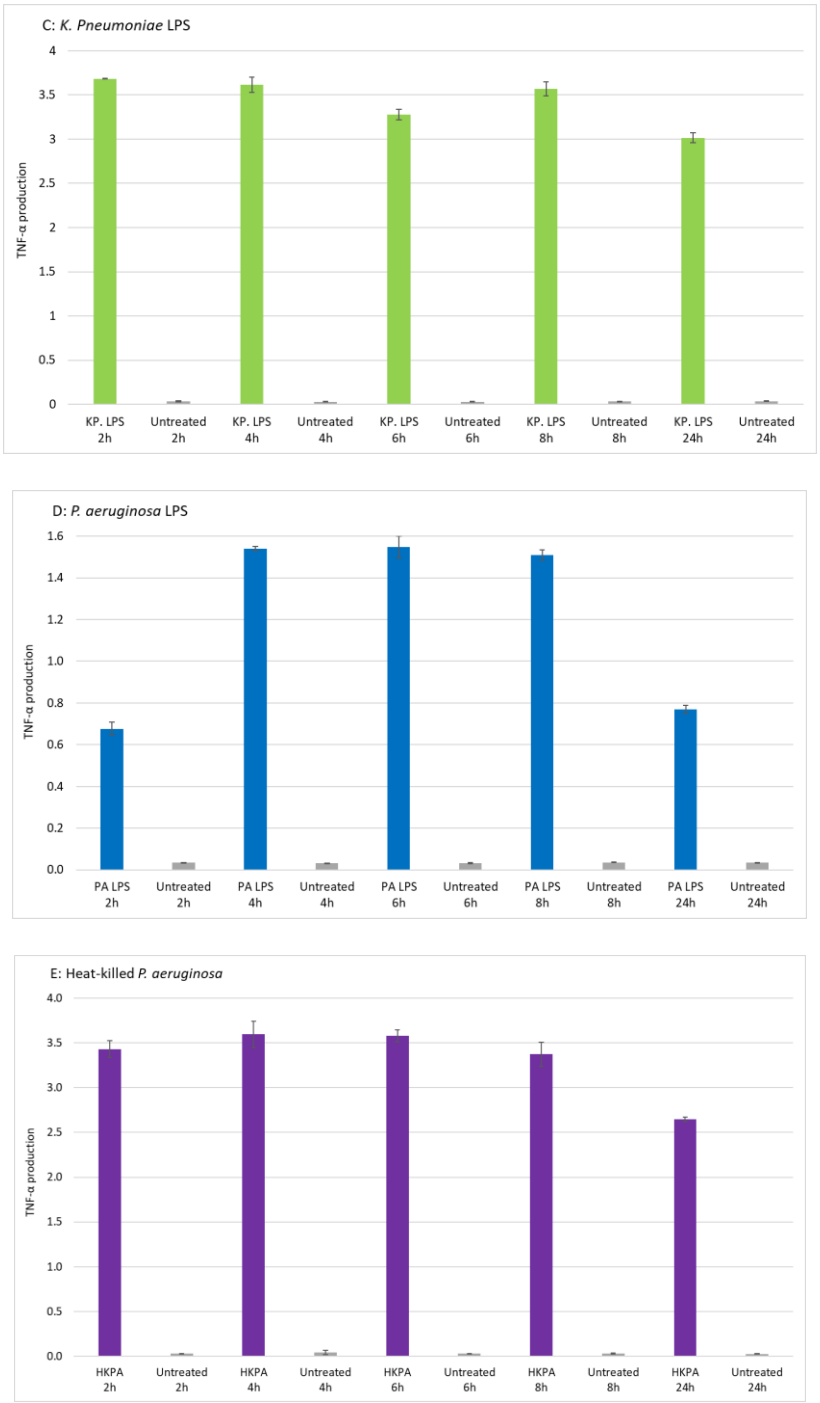

Figure 18. Results for timepoint assay of TNFα production induced by Gram-negative PAMPs. THP-1 cells were treated with A) 100 ng/ml of *E. coli* O26:B6 LPS, B) 100 ng/ml of *E. coli* O111:B4 LPS, C) 100 ng/ml of *K. pneumoniae* LPS, D) 1 µg/ml of *P. aeruginosa* LPS, E) 10^5 cells/mL of HKPA cells. The cells were then incubated for 2, 4, 6, 8, and 24 h, and supernatants were collected at the end of each time-point. Levels of TNFα cytokines were quantified using ELISA. Untreated cells were used as controls. Timepoints that resulted in the highest secretion of TNFα protein were selected as the optimum timepoints for stimulating THP-1 cells with the respective PAMPs.

Neutralizing the immunostimulatory effects of Gram-negative and fungal PAMPs with BPEI

Previous research conducted in our laboratory demonstrated the binding of 600 Da BPEI to *P. aeruginosa* LPS [106, 111]. Through the utilization of isothermal titration calorimetry, they directly quantified the enthalpy associated with the molecular binding interactions between 600 Da BPEI and *P. aeruginosa* LPS. The observed binding profile indicated an exothermic interaction between 600 Da BPEI and LPS, which is likely attributed to electrostatic interactions between the cationic amines of 600 Da BPEI and the anionic phosphates and carboxylate groups of LPS molecules [106, 111]. Based on this finding, in this study we aim to explore the antagonistic effect of 600 Da BPEI molecules on the generation of the inflammatory response triggered by Gram-negative LPS and fungal zymosan. Due to their distinct structural characteristics, LPS molecules were selected from various Gram-negative bacterial species [185].

THP-1 cells were treated with combinations of each of the PAMP molecules including *E. coli* O26:B6 LPS, *E. coli* O111:B4 LPS, *K. pneumoniae* LPS, *P. aeruginosa* LPS, HKSA, and zymosan with various concentrations of BPEI. Then, the amount of released TNF-α cytokines were measured using ELISA. The data shown in Fig. 19 demonstrates the modulation effect of BPEI on the production of TNF-α proteins stimulated with LPS molecules from two strains of *E. coli* bacteria. Against LPS molecules purified from *E. coli* O26:B6 bacteria, three concentrations of BPEI were employed including 10 ng/mL, 100 ng/mL, and 1 μg/mL. These concentrations corresponded to LPS to BPEI mass ratios of 0.1:1, 1:1, and 1:10, respectively. Although we did notice a decrease in the quantity of TNF-α cytokine resulting from all BPEI concentrations, the mitigating effect was modest (Fig. 19A). This suggests that BPEI possesses some antagonistic

effects on the immune response, yet it is unable to completely neutralize the LPS molecule. Likewise, when it comes to *E. coli* O111:B4 LPS, BPEI exhibited a brief reduction in the levels of induced TNF-α at a 1:1 ratio (Fig. 19B).

When *K. pneumoniae* LPS was used to treat THP-1 cells for two hours, it provoked a significant secretion of TNF-α as shown in Fig. 18C. This observation suggests that *K. pneumoniae* LPS may induce a more robust immune response compared to *E. coli* and *P. aeruginosa* LPS. Combinations of either 10 ng/mL or 100 ng/mL of BPEI molecules with 100 ng/mL of *K. pneumoniae* LPS resulted in a slight neutralization in the immune response (Fig. 20, top) although the neutralization effect became more pronounced when BPEI concentrations were increased, (Fig. 20, bottom). This finding indicates a dose-dependent relationship between BPEI and the disruption of TNF-α production induced by *K. pneumoniae* LPS.

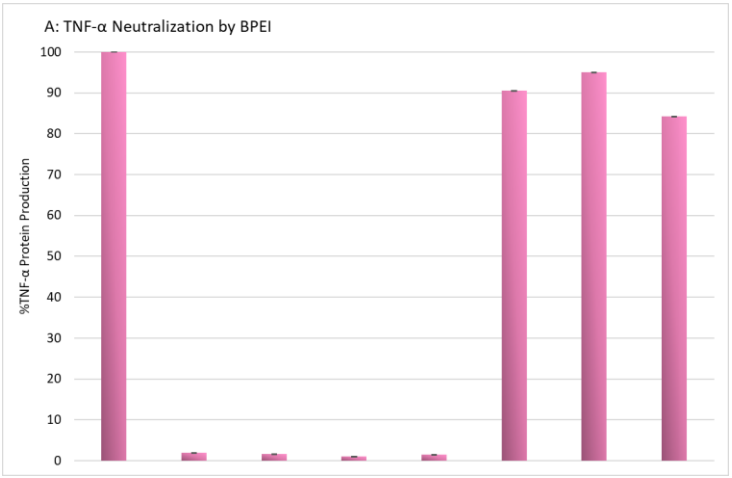

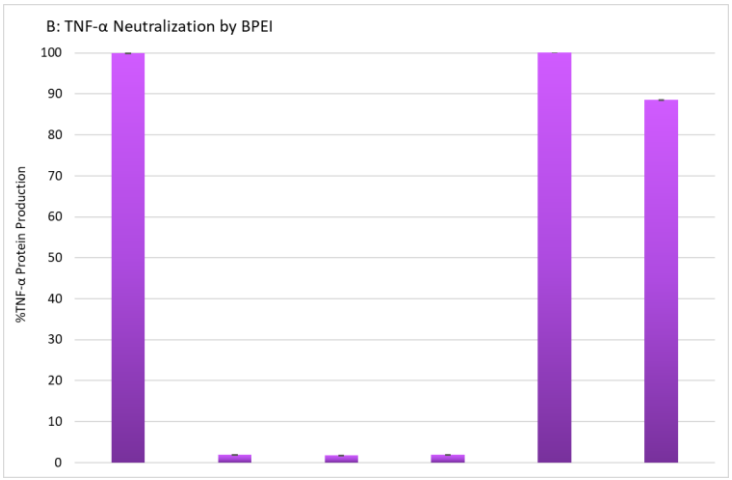

***E. coli* O111:B4 LPS 100 ng/mL**	+	-	-	-	+	+
Untreated	-	+	-	-	-	-
BPEI 10 ng/mL	-	-	+	-	+	-
BPEI 100 ng/mL	-	-	-	+	-	+

Figur[illegible]phage cells (THP-1 cells) in responses to combinations of 600-Da BPEI and A) *E. coli* O26:B6 LPS and B) *E. coli* O111:B4 LPS. Data are shown as an average of two biological replicates. Error bars denote standard deviation. Untreated cells were used as controls.

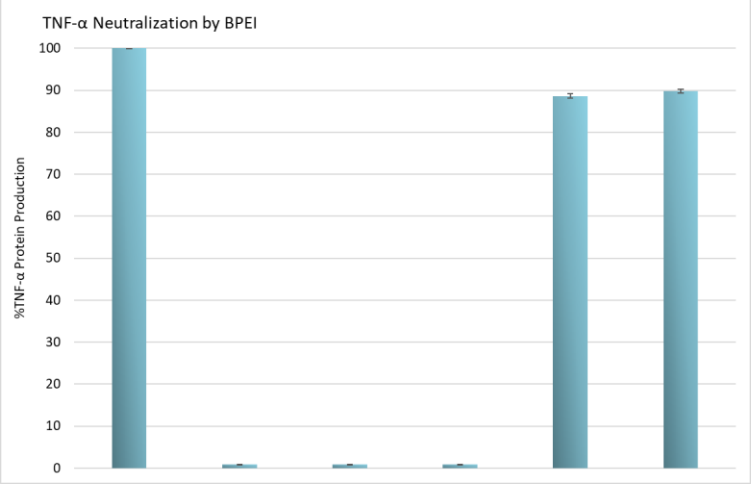

***K. pneumoniae* LPS 100 ng/mL**	+	-	-	-	+	+
Untreated	-	+	-	-	-	-
BPEI 10 ng/mL	-	-	+	-	+	-
BPEI 100 ng/mL	-	-	-	+	-	+

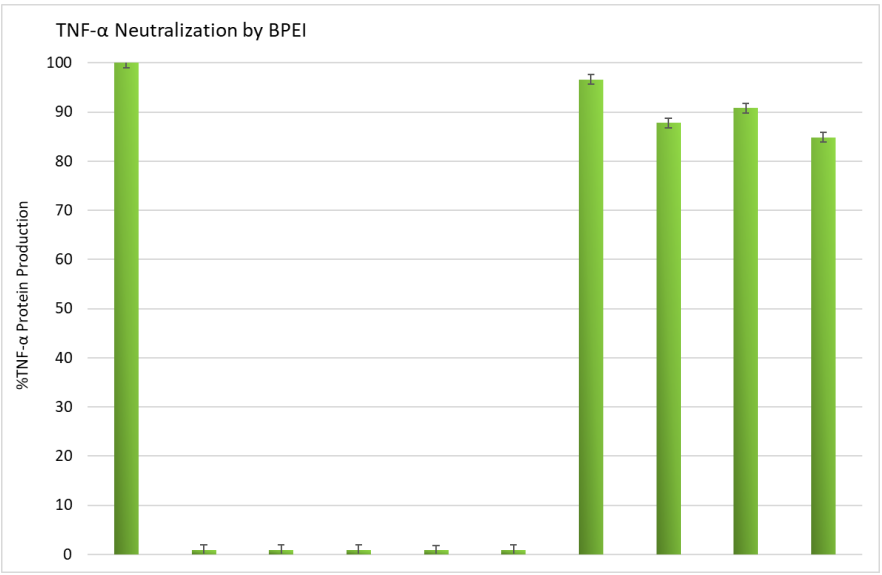

***K. pneumoniae* LPS 100 ng/mL**	+	-	-	-	-	-	+	+	+	+
Untreated	-	+	-	-	-	-	-	-	-	-
BPEI 25 µg/mL	-	-	+	-	-	-	+	-	-	-
BPEI 50 µg/mL	-	-	-	+	-	-	-	+	-	-
BPEI 75 µg/mL	-	-	-	-	+	-	-	-	+	-
BPEI 100 µg/mL	-	-	-	-	-	+	-	-	-	+

Figure 20. ELISA data show the amount of cytokine TNFα released by human macrophage cells (THP-1 cells) in responses to combinations of 600-Da BPEI and *K. pneumoniae* LPS. Data are shown as an average of three technical replicates. Error bars denote standard deviation. Untreated cells were used as controls.

Based on the previous study that was conducted in our lab [106, 111], which demonstrated a binding interaction between 600 Da BPEI and *P. aeruginosa* LPS, our hypothesis was that BPEI would effectively reduce the TNF-α secretion induced by *P. aeruginosa* LPS. However, contrary to our expectations, BPEI did not exhibit any reduction in TNF-α production in the experiment (Fig. 21A). Due to the commercially prepared nature of the LPS molecules, we suspect that the disparity in purifying protocols and varying purity levels of the *P. aeruginosa* LPS used in the two studies may account for the observed results. Future studies will involve application of laboratory purified *P. aeruginosa* LPS to further investigate the mitigating effect of BPEI against TNF-α secretion induced by the LPS. Nevertheless, it is likely that structural and/or compositional differences between the LPS from *E. coli* and *P. aeruginosa* may explain the observed differences in the ability

of BPEI to neutralize the LPS from these pathogens. For instance, the LPS from *P. aeruginosa* contains numerous anionic carboxylate groups in the O-antigen region (Fig. 23) that provide binding sites for interactions with BPEI. However, these binding sites are located away from the alkyl tail region that is the binding site for LBP and subsequent co-receptors that lead to TLR2 activation. In this scenario, BPEI binding with isolated and soluble LPS may not affect cytokine release. In contrast to this hypothesis, the LPS from *E. coli* does not contain anionic charges in the O-antigen region (Fig. 23) and thus BPEI will bind with the anionic sites of the inner core and lipid A regions. Here, BPEI can provide steric barriers to interfere with LBP binding and TLR2 activation.

Regarding intact whole bacterial cells, the LPS molecules are not isolated but instead reside in a dense monolayer to form the outer leaflet of the bacterial outer membrane. This arrangement exposes the O-antigen region to the extracellular environment where it can interact with the host cells. While whole cell bacteria are known to stimulate TLRs, the mechanism and identification of the signaling initiation is not well understood. It is very likely that LPS is involved, it is also possible that other bacterial cell surface molecules participate and provide redundancy in the recognition of the immune system. Therefore, when BPEI binds to whole cells it can interfere with the signaling cascade by limiting recognition of the LPS O-antigen or other nearby molecules on the cell surface. We measured the ability of BPEI to neutralize the production of TNF-α induced by heat-killed *P. aeruginosa* bacteria (HKPA). As shown in Fig. 21B and 21C, application of 100 ng/mL, 1 and 10 μg/mL of BPEI resulted in a small reduction in the immune response although increasing BPEI concentrations (50-150 μg/mL) resulted in up to ~ 30% reduction in TNF-α protein levels.

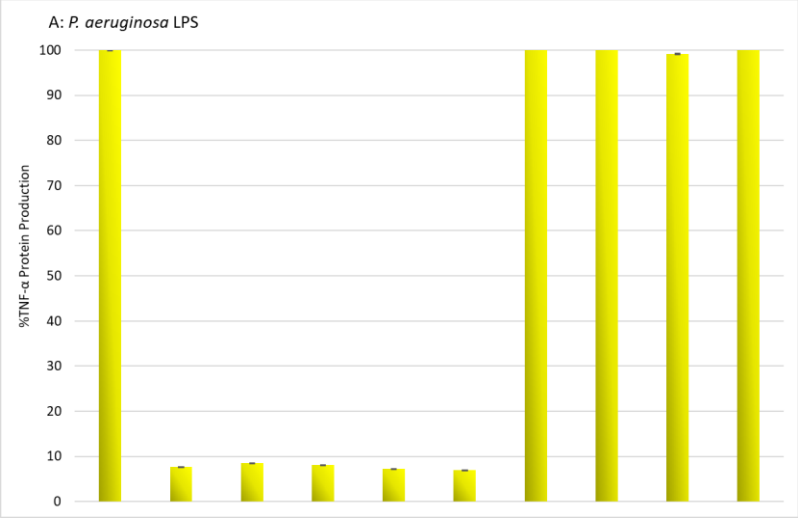

***P. aeruginosa* LPS 100 ng/mL**	+	-	-	-	-	-	+	+	+	+
Untreated	-	+	-	-	-	-	-	-	-	-
BPEI 100 ng/mL	-	-	+	-	-	-	+	-	-	-
BPEI 10 ng/mL	-	-	-	+	-	-	-	+	-	-
BPEI 1 µg/mL	-	-	-	-	+	-	-	-	+	-
BPEI 10 µg/mL	-	-	-	-	-	+	-	-	-	+

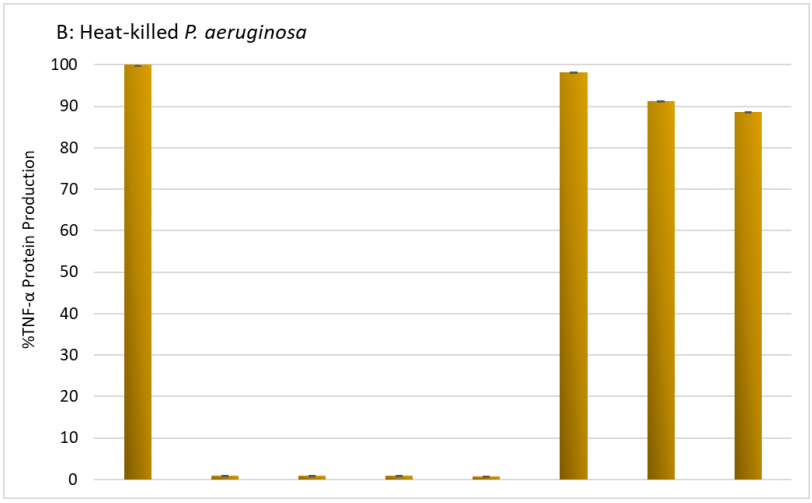

Heat-killed *P. aeruginosa* 10^5 cells/mL	+	-	-	-	-	-	+	+
Untreated	-	+	-	-	-	-	-	-
BPEI 100 ng/mL	-	-	+	-	-	-	+	-
BPEI 1 µg/mL	-	-	-	+	-	-	-	+
BPEI 10 µg/mL	-	-	-	-	+	-	-	-

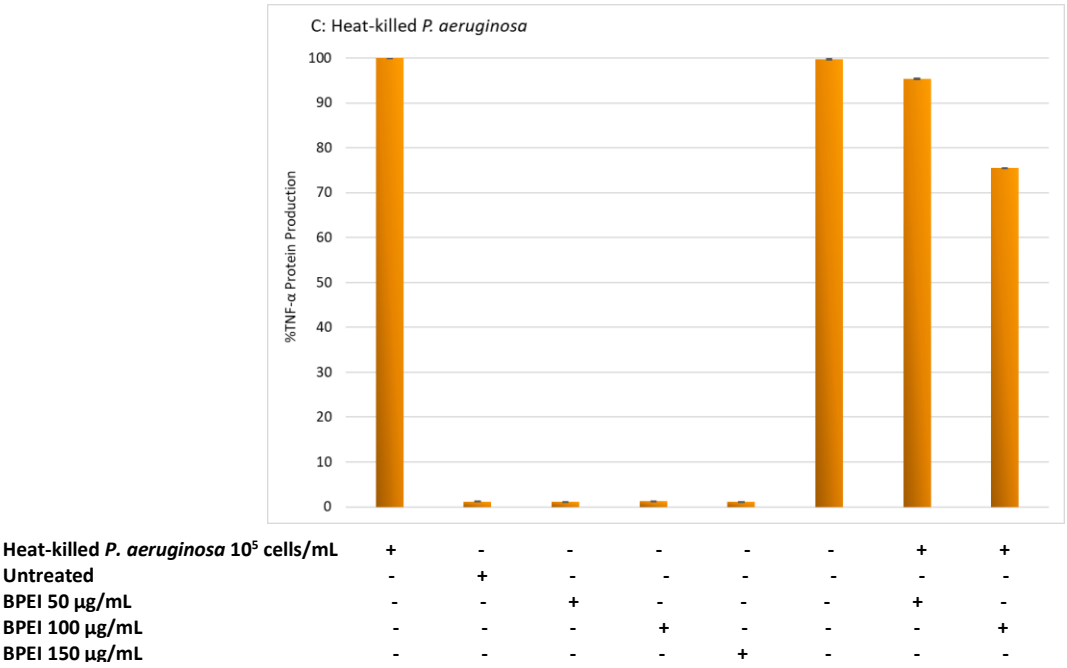

Figure 21. A) Time-point assay. ELISA data show the amount of cytokine TNFα released by human macrophage cells (THP-1 cells) in responses to combinations of 600-Da BPEI and B) *P. aeruginosa* LPS and C) heat-killed *P. aeruginosa* BAA-47 (HKPA). Data are shown as an average of two biological replicates. Error bars denote standard deviation. Untreated cells were used as controls.

Another objective was to examine the interaction between fungal zymosan and BPEI in relation to TNF-α secretion. Zymosan, a cell wall component derived from the yeast *S. cerevisiae*, can activate TLR receptors and induce the production of TNF-α[179, 180]. For this purpose, THP-1 cells were stimulated with different combinations of zymosan (25 µg/mL) and BPEI (ranging from 50 to 125 µg/mL). Interestingly, the results depicted in Fig. 22 revealed that 600 Da BPEI effectively neutralized zymosan, leading to a significant reduction in cytokine production. Furthermore, BPEI exhibited a dose-dependent pattern in mitigating the production of TNF-α protein, with a 50% reduction observed at a concentration of 125 µg/mL. The binding mechanism between branched polyethyleneimines and zymosan is presently unclear. Further investigations are needed to unravel the underlying interaction mechanism.

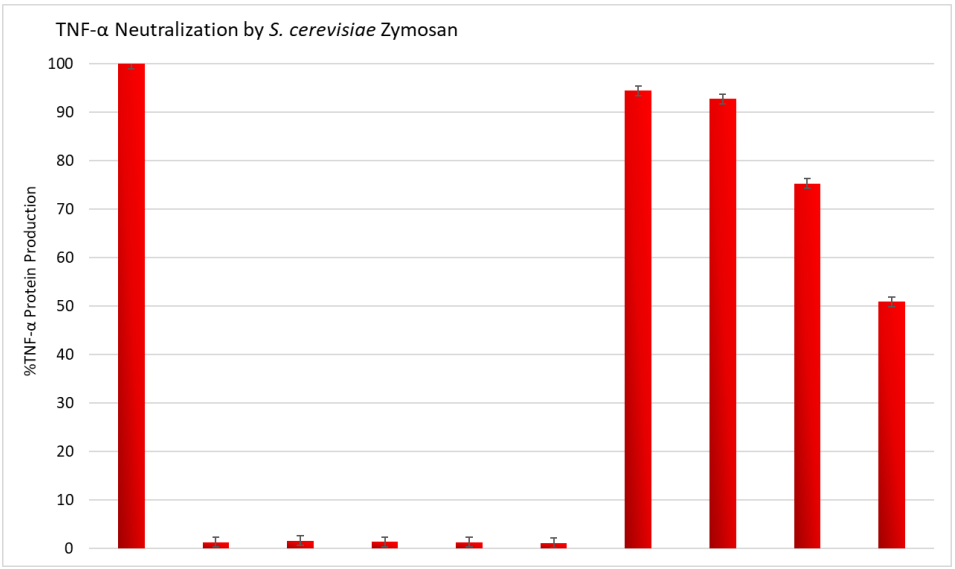

***S. cerevisiae* Zymosan 25 µg/mL**	+	-	-	-	-	-	+	+	+	+
Untreated	-	+	-	-	-	-	-	-	-	-
BPEI 50 µg/mL	-	-	+	-	-	-	+	-	-	-
BPEI 75 µg/mL	-	-	-	+	-	-	-	+	-	-
BPEI 100 µg/mL	-	-	-	-	+	-	-	-	+	-
BPEI 150 µg/mL	-	-	-	-	-	+	-	-	-	+

Figure 22. ELISA data show the amount of cytokine TNFα released by human macrophage cells (THP-1 cells) in responses to combinations of 600-Da BPEI and *S. cerevisiae* zymosan. Data are shown as an average of two biological replicates. Error bars denote standard deviation. Untreated cells were used as controls.

Discussion

Lipopolysaccharide (LPS) serves as a crucial component located in the outer membrane of Gram-negative bacteria. It plays a significant role in immune system interactions and the generation of immune responses. The LPS molecule is consisted of three components: lipid A, which is a hydrophobic portion responsible for anchoring LPS to the outer leaflet of the outer membrane; core oligosaccharide which along with lipid A helps maintain the integrity of the outer leaflet; and O-antigen polysaccharide, which is connected to the core and forms a polymer consisting of repeated oligosaccharide units that directly interact with the external environment [186-188]. While LPS structures in various Gram-negative species share common characteristics, there are also variations that contribute to the unique properties and pathogenicity of each bacterium. These modifications, particularly in the Lipid A component, play a significant role in the bacteria's pathogenicity and their interactions with the host immune system (Fig. 23) [185].

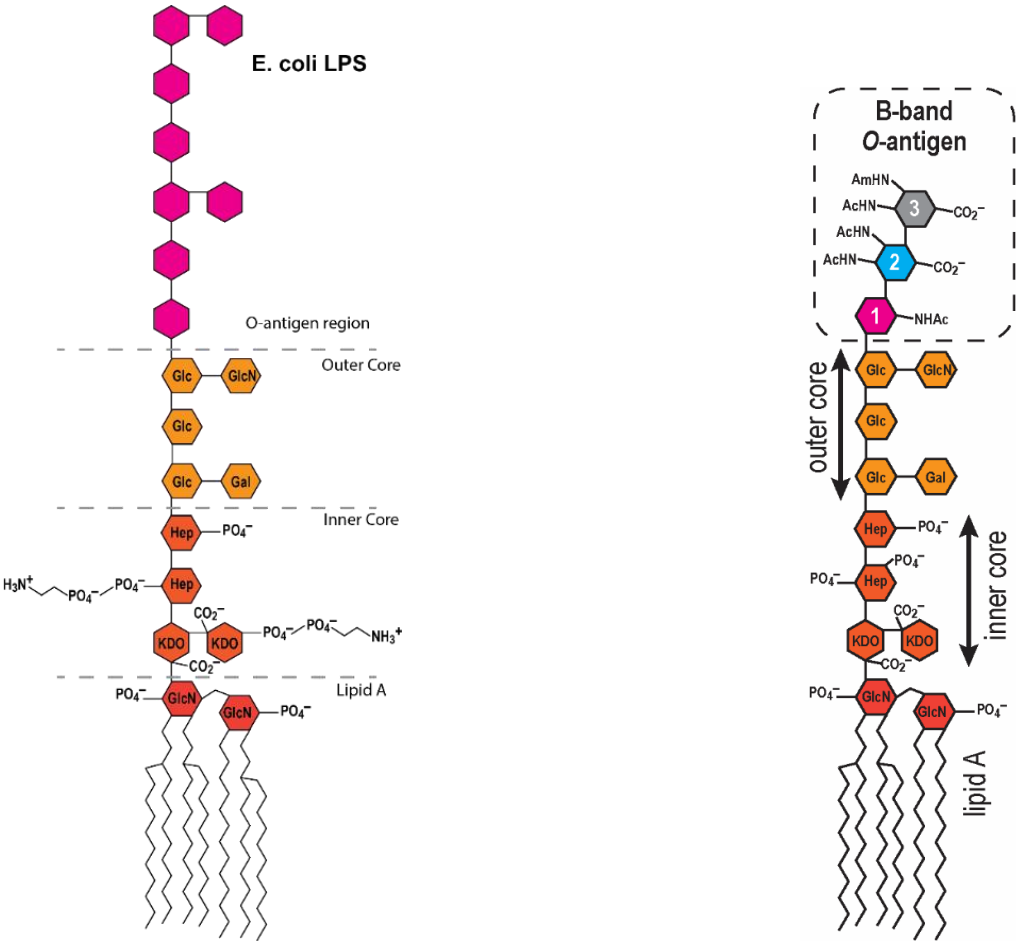

Figure 23. Lipopolysaccharide (LPS) structures from *E. coli* and *P. aeruginosa* bacteria. Both LPS molecules contain three main components: lipid A, a core oligosaccharide, and O-antigen. The O-antigen region in *P. aeruginosa* LPS contains several carboxyl groups which add to the negativity of the overall charge of the molecule. However, in the *E. coli* LPS structure, O-antigen is constituted of a polysaccharide chain attached to the core oligosaccharide and is free of charge.

LPS molecules activate TLR4 receptor and induce the downstream signaling cascade that eventually produce inflammatory cytokines [169, 170]. TLR4 activation requires interaction with several co-receptors through a series of consecutive steps. LPS first combines with LPS-binding protein (LBP) and then LBP transfers LPS molecule to cluster of differentiation 14 (CD14) protein. CD14 in turn chaperones the formation of LPS and myeloid differentiation factor 2 (MD2) complex [169] (Fig. 24). In this work, we demonstrated the ability of 600 Da branched

polyethyleneimine (BPEI) to mitigate TNF-α cytokine production induced by Gram-negative LPS in THP-1 macrophage cells. We proposed a mechanism of interaction between the cationic BPEI with the anionic groups of LPS which is shown in Fig. 24. BPEI through its cationic amines can electrostatically interact with the anionic groups of LPS molecule and prevents it from combining with co-receptors. This would eventually result in less TLR4 dimerization and mitigated cytokine production.

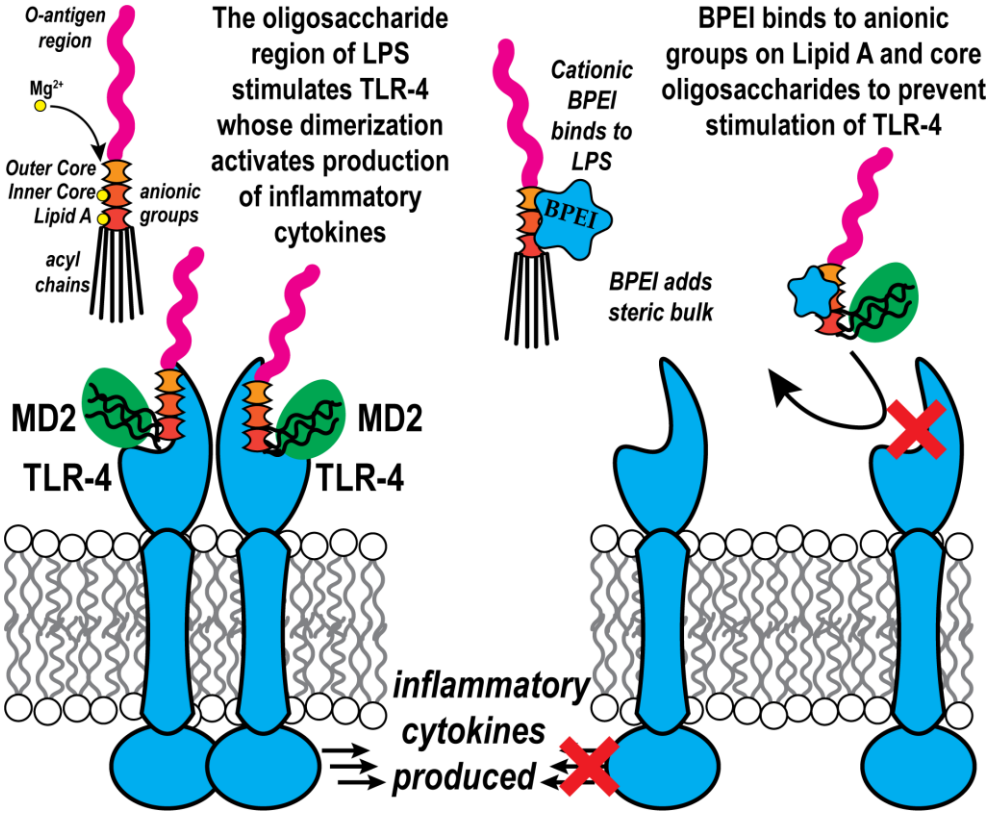

Figure 24. Proposed mechanism of action of LPS and BPEI interactions. LPS molecules activate TLR4 receptor and induce the downstream signaling cascade that ultimately produces inflammatory cytokines. TLR4 activation requires interaction with several co-receptors through a series of consecutive steps (left). Cationic BPEI binds with LPS through electrostatic interactions and prevents it from combining with co-receptors. This eventually results in less TLR4 dimerization and mitigated cytokine production (right).

Overall, the results of this study are representative of a qualitative investigation of the effect of 600 Da BPEI against Gram-negative LPS. This is due to the presence of inherent complexities in this work which prevented us from doing a more quantitative assessment of BPEI ability in neutralizing Gram-negative LPS induced-immune response. First of all, the molecular weight of LPS is not well understood in the literature which makes it impossible to measure the accurate molar ratio of LPS to BPEI. Also, the binding site of BPEI and LPS is unknown. We believe that the presence of LBP, CD4, and MD2 co-receptors that bind to LPS and prepare it to bind to TLR4 receptor are different than the BPEI binding site. These differences prevent BPEI from effectively neutralizing LPS. Also, the various structural characteristics of LPS molecules among different Gram-negative species create the possibility of different binding patterns with BPEI. This results in differing neutralizing trends of BPEI against the LPS molecules that vary among species. Again, we strongly believe that LPS sample purification and the purity levels among the various commercial LPS samples used in this research may pose additional factors that reduce the neutralizing properties of LPS.

Nevertheless, our findings in this study demonstrate the ability of 600 Da BPEI to effectively reduce the production of inflammatory responses induced by *S. cerevisiae* zymosan (Fig. 22). To the best of our knowledge, this is the first time that the release of inflammatory cytokines has been mitigated by combining zymosan glycoprotein with another compound. β-glucans possess multiple hydroxyl groups that facilitate bonding with reactive groups of other compounds, thereby modifying their water solubility, conformation, and capacity to form aggregates [189]. Based on this, we propose three mechanisms of interactions between BPEI and β-glucans molecules. First of all, we suggest that the deionization of hydroxyl (OH) groups in zymosan occurs in the presence of amine groups of BPEI. Zymosan is composed of a mixture of carbohydrates, including β-glucans

and mannans, as well as proteins [178, 179]. The β-glucan structure in zymosan contains hydroxyl (OH) groups attached to the glucose molecules which play a crucial role in stabilizing the overall structure through interstrand hydrogen bonding [190]. Under physiological pH conditions, the majority of hydroxyl groups (-OH) in the β-glucan backbone do not undergo significant deprotonation. This is because the pKa values of these hydroxyl groups are higher than the pH range typically found in physiological conditions. However, when cationic BPEI is present in the solution, the OH groups in the basic pH become deprotonated. The deprotonation of hydroxyl (OH) groups has the potential to influence the overall structure and properties of the β-glucan molecule, thereby potentially modifying its biological activity [190]. Moreover, the interaction of zymosan with BPEI can be attributed to cooperative hydrogen bonding between the hydroxyl groups on the β-glucan of zymosan and the amine groups on the BPEI. Since solubility of β-(1→3)-glucans increases in basic media [191], The interaction between BPEI and zymosan can result in the formation of aggregates, which, in turn, can disrupt the organized structure of zymosan and impact its biological activity. Lastly, we propose the possibility that BPEI can form conjugates with β-glucan, resulting in modifications to the zymosan molecule. The presence of functional hydroxyl and aldehyde groups in β-glucan enables it to undergo conjugation with other biomolecules that have a strong affinity for binding to β-glucan, such as proteins and amino acids [189]. Due to the shared presence of amine groups with amino acids, it is likely that the cationic compound BPEI utilizes a similar mechanism of interaction to form conjugates with β-glucan. Nevertheless, a comprehensive experimental investigation or specific understanding of the interactions involved is necessary to determine the precise behavior of β-glucan in the presence of cationic compounds like BPEI.

Chapter 4: Eradicating Biofilms of Carbapenem-Resistant *Enterobacteriaceae*

Background and Significance

Carbapenem-Resistant *Enterobacteriaceae* (CRE) cause severe infections including community-acquired pneumonia (CAP), ventilator-associated pneumonia (VAP), bloodstream infections (BSIs), complicated urinary tract infections (cUTIs), complicated intra-abdominal infections (cIAIs), and hospital acquired pneumonia (HAP) [192]. According to the World Health Organization, CRE is in the list of "Priority: Critical" pathogens. Likewise, the Centers for Disease Control and Prevention (CDC) requires an urgent and aggressive action against the immediate public health threat from CRE [193]. The danger exists because carbapenem antibiotics, normally prescribed for the treatment of *Enterobacteriaceae* infections, [194] are ineffective against CRE because these isolates commonly produce carbapenemase enzymes that degrade a wide range of antibiotics, including carbapenems and β-lactams [195]. The predominate carbapenemases are the *Klebsiella pneumoniae* carbapenemases (KPCs) [196-198]. A greater concern are metallo-β-lactamases (MBLs), such as New Delhi MBL (NDM-1), because they degrade more antibiotics than KPCs [196-198]. Numerous efforts are focused on the development of β-lactamase inhibitors to disable these enzymes and permit bacterial killing by carbapenem antibiotics, such as meropenem, imipenem, and ertapenem [199, 200]. Nevertheless, CRE infections continue to pose a threat to human health because, in part, new therapeutics do not address the ability of CRE to evade drug activity by encasing the bacterial cells in a biofilm matrix [201, 202].

Biofilms are structured populations of bacterial cells that adhere to the surfaces of the materials by embedding within a matrix of capsular polysaccharide substance known as exopolysaccharide [202-205]. This additional layer of protects CRE from host defenses and pharmaceutical antimicrobials [202-204]. Eradication of CRE biofilms requires high concentrations of antimicrobials, but the most likely scenario is the use of adjuvants that improve drug efficacy and lower the risk of drug cytotoxicity issues and severe side effects that arise with high doses [206, 207]. Therefore, successful treatment of CRE biofilm infections may require several agents: an antibiotic that is not affected by resistance factors, or a combination of antibiotic plus a compound that disables resistance factors, and finally an anti-biofilm agent. Recent studies in our lab show that 600 Da branched polyethyleneimine (BPEI) and its safer derivative – PEGylated BPEI (PEG350-BPEI) – can facilitate the uptake of drugs, lower drug influx barriers, and disable CRE resistance mechanisms [110, 208-210]. Another advantage of PEG350-BPEI potentiators is the ability to disrupt bacterial biofilms of Staphylococcal and *P. aeruginosa* bacteria [109, 211]. Here, we demonstrate the ability of 600 Da BPEI and PEG350-BPEI to eradicate biofilms of carbapenem-resistant *Enterobacteriaceae* expressing KPC and NDM-1. Activity was lower against the NDM-1 positive strain compared to the KPC positive strain; an effect attributed to greater biofilm production by the NDM-1 strain. Furthermore, inverted laser scanning confocal microscopy images show that BPEI disrupts the normal cell cycle of the CRE bacteria by inducing elongated cells, irregular cell division, and distortions in both size and shape of the cells.

Contributions

This work was made possible due to the guidance and contributions of Dr. Tingting Gu and Dr. Paterson Larson at Samuel Robert Noble Microscopy Laboratory, the University of Oklahoma.

Methods

Material

The bacterial strains used in this work, *Escherichia. coli* BAA-25922™ (a non-resistant laboratory reference strain), *E. coli* BAA-2452™ (a carbapenem resistant *Enterobacteriaceae* expressing metallo-β-lactamase NDM-1), and *E. coli* BAA-2340™ (a carbapenem resistant *Enterobacteriaceae* expressing *Klebsiella Pneumoniae* carbapenemase (KPC)) were purchased from the American Type Culture Collection. Chemicals including growth media were purchased from Sigma-Aldrich. 600 Da BPEI was purchased from Polysciences, Inc. PEG350-BPEI was synthesized and characterized as described in previously[111].

Inhibition of bacterial growth

The minimum inhibitory concentrations (MIC) of BPEI and its derivative PEG350-BPEI against *E. coli* BAA-2452™ (an NDM positive strain), *E. coli* BAA-2340™ (a KPC positive strain), and *E. coli* BAA-25922™ cells were determined. Briefly, serial dilutions of BPEI and PEG350-BPEI were prepared in Tris-HCl 0.05 M (pH=7) buffer and added into 96-well microtiter plates (Greiner Bio-one, Stuttgart, Germany) with cation-adjusted Mueller–Hinton broth (CAMHB) media. Then, bacterial cells from each *E. coli* strain were added (5×10^9 cells/mL), and the plate incubated overnight at 37 °C. The optical density of the cells was measured at 600 nm (OD_{600}) after 20 hours of growth. Each MIC value was the average of three separate trials.

Time dependence of bacterial growth

E. coli BAA-2452™ and *E. coli* BAA-2340™ cells were grown from overnight cultures (5×10^9 CFU/mL) using CAMHB supplemented with three separate concentrations of 600 Da BPEI treatments (64 μg/mL, 256 μg/mL, and 1024 μg/mL). Untreated cells were grown as control. Bacteria were incubated at 37 °C with shaking. The change in optical density for each sample was monitored at 600 nm (OD_{600}) over 24 hours.

Biofilm formation

Biofilm formation assays were performed as described by Naves P, *et al*. with a slight modification [212]. Four different broths were used including two minimal and two nutrient-rich media. M63 media (22 mM KH_2PO_4, 40 mM K_2HPO_4, 15 mM $(NH_4)_2SO_4$, 1mM $MgSO_4$, %0.4 arginine) [213], and M9 (12.8 g Na_2HPO_4, 3 g KH_2PO_4, 0.5 g NaCl, 1 g NH_4Cl, %20 glucose, 1 M $MgSO_4$, 1 M $CaCl_2$, %0.5 Thiamine) (adapted from ATCC Medium: 2511 M9 Minimal Agar/Broth) were the minimal media. The two rich broths included Luria–Bertani (LB) and CAMHB. All strains were grown from a cryogenic stock overnight at 37 °C. From overnight cultures (5×10^5 CFU/mL) 1.3 μL aliquots were inoculated in 130 μL of each broth media in 96 wells microtiter plates. These plates were then incubated for 24 hours at 37 °C to form established biofilms and afterwards supernatant was discarded. Growing biofilms for *E. coli* 2340 was met with unexpected challenges of producing consistent deposition of biomass in the microtiter plates. We found that the biofilms formed in MHB broth were established in a more consistent manner for the strain.

Biofilm disruption assay

Microtiter plates containing biofilms were rinsed with 150 µL sterile saline to remove planktonic bacteria followed by 20 minutes of air drying. Subsequently, 130 µL of a 1% crystal violet (CV) solution (Sigma-Aldrich, USA) was added to the wells for 20 minutes to stain the adhered cells. The supernatant was carefully removed by turning the plate over and removing the liquid with gentle shaking followed by washing to remove excess stain. Total volume of 100 µL of Tris-HCl 0.05 M (pH=7) buffer was added to each well of the 96-well biofilm plate followed by the addition of 600 Da BPEI, 32 µg/mL (5.33 nmol) or 64 µg/mL (10.66 nmol), and PEG350-BPEI, 32 µg/mL (3.4 nmol) or 64 µg/mL (6.8 nmol. The negative and positive controls were Tris-HCl buffer alone and 30% acetic acid, respectively. The plates were incubated at 25 °C for biofilm disruption. Disruption of the biofilm caused the biomass to disperse into solution, quantified by carefully transferring the supernatant to a new 96-well plate for 550 nm (OD_{550}) measurement. Eight technical replicates and two independent experiments were accomplished for each strain. Statistical analysis was conducted using Student's t-test by comparing the negative control to the other measured values.

Biofilm eradication

The potential of BPEI and PEG350-BPEI to eradicate CRE *E. coli* biofilms was investigated using the colony biofilm model. Briefly, bacterial cells were inoculated from a cryogenic stock overnight at 37 °C. Then, about 2 µL of the cell culture (1 col/mL (5×10^2 CFU) in CAMHB media) was transferred to sterilized 13-mm paper discs (Isopore^{TM}, Merck Millipore Lt, Ireland) which had been placed onto TSA plates. The plates incubated at 37 °C. After 24 hours, the paper discs had visible biomass of bacteria. Next, the discs were carefully transferred to a fresh Trypticase Soy

Agar (TSA) plate, treated with 100 µL of different concentrations of BPEI or PEG350-BPEI and incubated at 37°C for another 8 h. Biofilms treated with Tris-HCl buffer were considered as negative controls. Subsequently, the paper discs with treated biofilms were transferred into Eppendorf tubes with 1 mL of Tris-HCl buffer and were sonicated for 10 minutes. Then, a serial dilution of the cells was prepared up to eight times and plated on TSA agar. The plates were incubated overnight at 37°C and the viable cells were enumerated by colony counting. Viable cell counts were converted to log10 units, and standard deviations were calculated. Two technical replicates and three independent experiments were accomplished for each strain.

Inverted Confocal Laser Scanning Microscopy

Cultures of *E. coli* BAA-2452™, and *E. coli* BAA-2340™ cells treated with 256 µg/mL of BPEI were grown at mid-log growth phase at 37 °C with shaking. The cells were then pelleted by centrifugation at 6,000 × g for 40 minutes at 4 °C and the supernatant was removed. Then, 6 µM DAPI in phosphate-buffer saline (1X PBS, pH 7.2) was added to the cell pellet and incubated for 30 minutes at room temperature. Next, 0.03 µM Nile red was added to the cells for another 30 minutes at room temperature. The fluorescence dyes were then removed by centrifugating the cells at 12,000 × g for 5 minutes at room temperature. BPEI-untreated *E. coli* samples were also stained in a similar way and considered as negative control for imaging. The stained bacterial cells, either untreated or BPEI-treated were then fixed by 4% glutaraldehyde (GA) followed by a 10-fold dilution in 1X PBS. The cells were added to a microscope slide and imaged using a Leica Stellaris 8 FALCON inverted confocal microscopy with a 63x/1.4 NA oil objective. DAPI was excited by a Diode 405 nm laser line and Nile red was excited by a White Light Laser at 510 nm wavelength. Single optical sections were acquired of cells that had adhered to the coverslip with the pixel size

at 32.5 nm × 32.5 nm. TauGating was used to remove autofluorescent and enhance image quality. Image processing was performed using ImageJ Analysis Software. Each section was the representative image of four replicates.

Results and Discussion

Biofilm disruption assay

To elucidate the antibiofilm activity of BPEI and PEG350-BPEI, biofilm disruption assays against *E. coli* ATCC 25922, ATCC 2340, and ATCC 2452 were conducted using crystal violet staining. Biofilms were grown and stained with a 1% crystal violet (CV) solution. After washing, the plate was subjected to treatment by different concentrations of 600 Da BPEI and PEG350-BPEI. The biofilm-disrupting action of 600 Da BPEI and PEG350-BPEI against *E. coli* ATCC 2452 and *E. coli* ATCC 2340 are shown in Fig. 25A and 25B, respectively. The negative and positive controls were Tris-HCl buffer and 30% acetic acid, respectively. The crystal violet data in Fig. 25 show that the buffer had no effect on dispersing the *E. coli* biofilms and visual inspection confirmed that the biofilm layer remained intact on the plate. However, 30% acetic acid completely dislodged the biofilms into the solution. Likewise, 32 µg/mL and 64 µg/mL of 600 Da BPEI (5.33 and 10.66 nmol) and PEG350-BPEI (3.4 and 6.8 nmol) also dispersed the *E. coli* biofilms. These results illustrate that treating the bacterial cells with increasing concentrations of 600 Da BPEI and PEG350-BPEI increases the amount of the biomass dispersed into solution. Acetic acid was used as a positive control and the biofilm disruption data were normalized to the intensity of the OD_{550} data collected with the acetic acid treated samples. The OD_{550} values of the crystal violet absorbance in Fig. 25A show biofilms treated with 5.33 nmol of 600 Da BPEI and 3.4 nmol of PEG350-BPEI were partially dispersed into solution, whereas those exposed to 10.66 nmol of 600 Da BPEI and 6.8 nmol of PEG350-BPEI were completely disrupted. Treating *E. coli* 2452 biofilms with 5.33 and 10.66 nmol of BPEI and 3.4 and 6.8 nmol of PEG350-BPEI, resulted in a higher biofilm disruption than *E. coli* 2340. Fig. 25B shows that 600 Da BPEI (5.33 nmol) and PEG350-BPEI (3.4 and 6.8 nmol) were able to disperse over half of the biofilm. As expected, greater biofilm

disruption effects were seen at 10.66 nmol concentration of 600 Da BPEI and is similar to the dispersal obtained with 30% acetic acid. Fig. 25C shows the biofilm disruption of the laboratory reference strain *E. coli* ATCC 25922, which is non-pathogenic but often studied in *E. coli* anti-biofilm studies. Treatment of *E. coli* 25922 biofilms with different concentrations of 600 Da BPEI and PEG350-BPEI resulted in higher dispersal than that of 30% acetic acid. PEG350-BPEI (3.4 and 6.8 nmol) in particular, showed greater biofilm disruption than its precursor molecule, 600 Da BPEI. Chemical modification of 600 Da BPEI with a 350 MW PEG group increases the ability to disperse biofilms of *E. coli* 25922. However, the opposite effect is observed in the dispersal of *E. coli* 2452 (NDM-1 positive) and *E. coli* 2340 (KPC positive) biofilms. The reasons for this observation are unclear. Nevertheless, the aim of this work was to disperse *E. coli* biofilms with the same agent that disables CRE antibiotic resistance mechanisms[110]. Additionally, in a clinical setting, wounds are likely to be contaminated with multiple bacterial strains and/or species. Thus, the ability to disperse biofilms of different *E. coli* species is an asset of 600 Da BPEI and PEG350-BPEI regardless of the relative efficiency measured with *in vitro* studies.

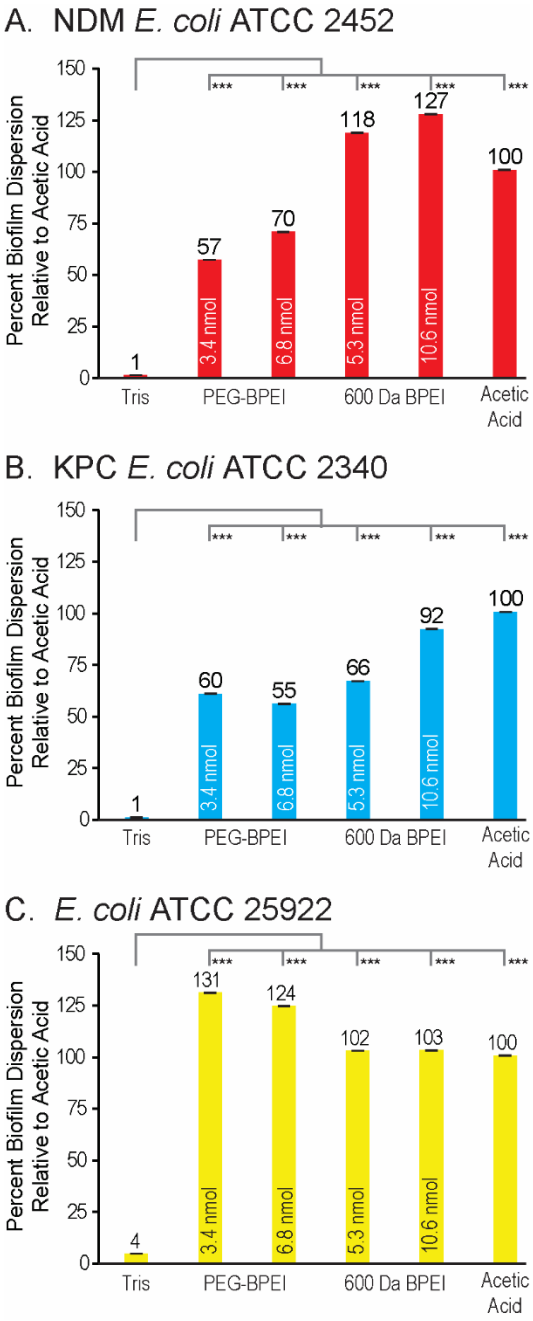

Figure 25. Biofilms of *E. coli* strains A) ATCC 2452 (NDM+), B) ATCC 2340 (KPC+), C) ATCC 25922 were stained with 1% crystal violet prior to treatment with two concentrations of 600 Da BPEI (5.33 and 10.66 nmol) and PEG350-BPEI (3.4 and 6.8 nmol). Treatment resulted in dispersion of the biomass into solution, which was quantified with OD_{550} measurement. The resulting intensity was used as a gauge of biofilm disruption. Measured values were compared to the negative control. Error bars represent standard deviation. Eight technical replicates and two independent experiments were accomplished for each strain. Statistical analysis with one-way ANOVA analysis generates $p < 0.001$ (99.99% confidence) denoted by ***.

Biofilm eradication

Antibiofilm activity of 600 Da BPEI and PEG350-BPEI was investigated further by implementing a biofilm killing model. Sterilized 13-mm paper discs were placed on TSA plates. Then, biofilms were grown for 24 hours on the paper discs for laboratory strain ATCC 25922 and CRE *E. coli* strains ATCC 2340 and ATCC 2452. Sterile 3-mm cellulose filtration discs were used to keep the biofilms hydrated during treatment. 600 Da BPEI and PEG350-BPEI were applied using 100 μL of increasing concentrations of 600 Da BPEI (1024 μg/mL, 5120 μg/mL, and 10240 μg/mL) and PEG350-BPEI (1024 μg/mL, 5120 μg/mL, and 10240 μg/mL) were applied to the top of the established biofilms. The low volume (100 μL) of treatment delivered 0.17, 0.85, and 1.71 μmoles of 600 Da BPEI to the biofilm surface, respectively. Likewise, applying 100 μL of the varying concentrations of PEG350-BPEI to the top of the biofilms provided 0.11, 0.54, and 1.08 μmoles of the compound. The treated biofilms were transferred to Eppendorf tubes containing Tris-HCl buffer and the biofilms were dispersed into planktonic form by sonication. The ability of 600 Da BPEI and PEG350-BPEI to kill the *E. coli* cells was quantified by spreading aliquots on TSA plates and counting the colony forming units (Fig. 26A and 26B). As expected, treatment with Tris-HCl buffer showed no effect on biofilm eradication. Log reduction values (LRVs) against all the strains were determined using the difference in CFU/mL between Tris-HCl buffer and different concentrations of BPEI or PEG350-BPEI treatments (Fig. 26C and 26D).

The data in Fig. 26 demonstrate that 1.706 μmoles of 600 Da BPEI can kill the CRE *E. coli* cells within their biofilms. This biofilm eradication is more pronounced in *E. coli* ATCC 2340 (KPC positive) than *E. coli* ATCC 2452 (NDM-1 positive) at this concentration. The 600 Da BPEI derivative PEG350-BPEI has similar efficacy against *E. coli* ATCC 2452 even though the

concentration is lower (1.08 µmoles vs. 1.71 µmoles). A similar trend was observed for killing the cells in biofilms of *E. coli* ATCC 25922. However, PEGylation of 600 Da BPEI reduced the eradication activity of 600 Da BPEI against *E. coli* ATCC 2340. The opposite trend was found for 600 Da BPEI and PEG350-BPEI at 0.85 and 0.54 µmoles, respectively, against the two CRE biofilms. These 3-8 LRVs are impressive and indicate that PEG350-BPEI can eradicate biofilms of *E. coli* strains that are NDM-positive and KPC-positive.

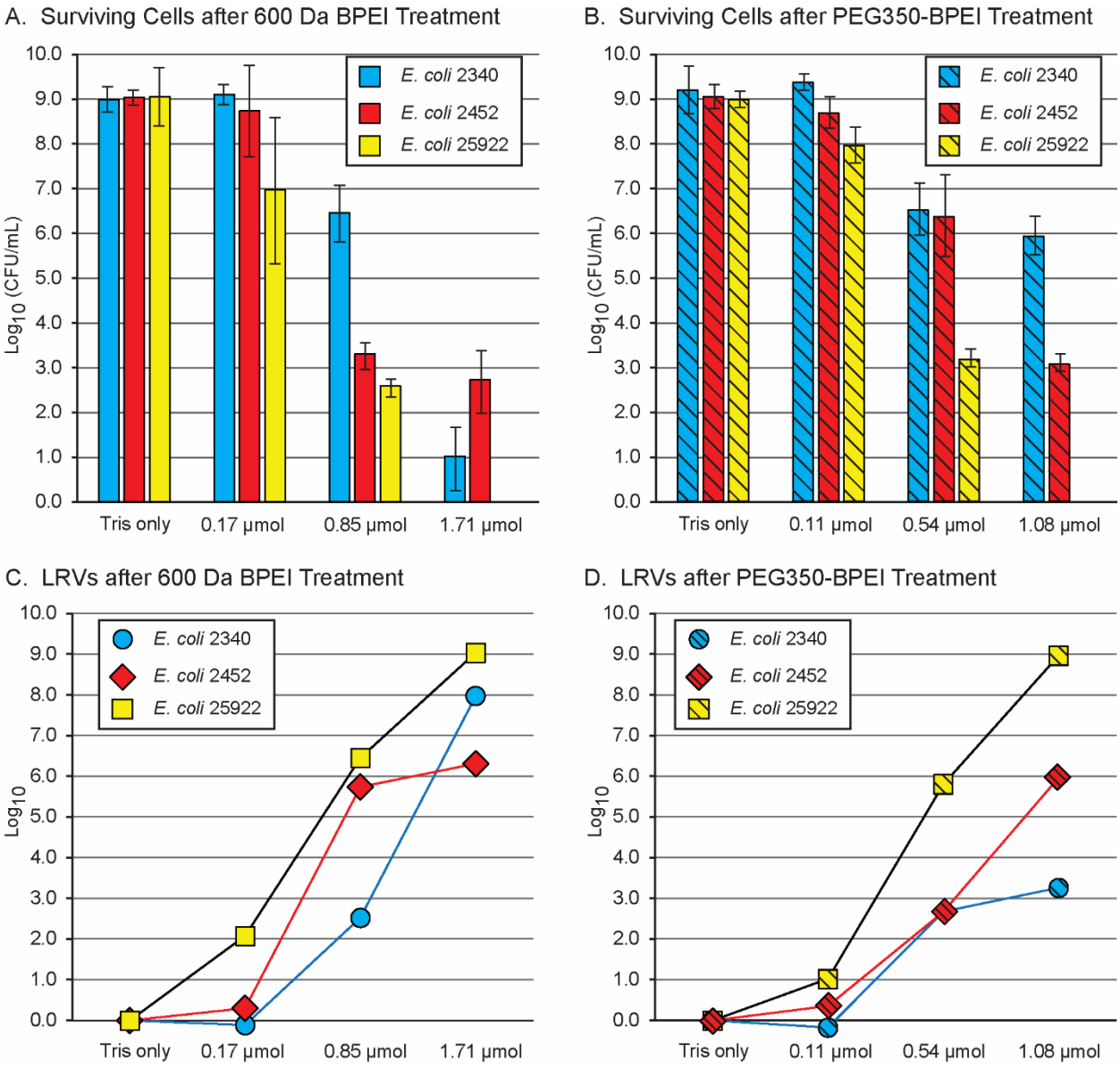

Figure 26. Biofilm eradication was determined by measuring the number of viable cells after treatment with 600 Da BPEI (A) and PEG350-BPEI (B). The reduction in colony forming units is shown with the log-reduction values in panels (C) and (D). Higher treatment concentrations resulted in greater eradication of biofilms formed by *E. coli* ATCC 2340 (NDM+), *E. coli* ATCC 2452 (KPC+), and *E. coli* ATCC 25922. Error bars denote standard deviation. Two technical replicates and three independent experiments were accomplished for each strain.

The results in Fig. 26 suggest that eradication of *E. coli* 2452 (NDM-1 present) biofilms is less efficient than biofilms formed by KPC-positive *E. coli*. One possibility is that the NDM-1 strain deposits a greater amount of biomass than the KPC strain, as suggested by the biofilm dispersion assay data in Fig. 26. A larger amount of biomass would bind a greater fraction of the 600 Da BPEI or PEG350-BPEI molecules, leaving a smaller fraction available to eradicate the planktonic cells and thus showing a lower biofilm eradication property.

Inverted Confocal Laser Scanning Microscopy

It is apparent that BPEI can kill CRE pathogens even when encased in a biofilm EPS matrix. To visualize the effect of 600 Da BPEI on the morphology of the CRE *E. coli* species, the bacteria were imaged using inverted confocal laser scanning microscopy. The cells were visualized using fluorescent dyes that localized to the cellular membrane or cytoplasm. However, planning these studies required the use of sub-lethal concentrations of 600 Da BPEI to induce antimicrobial stress on the bacterial cell population without killing the bacterial cell. The antimicrobial activity of BPEI against *E. coli* BAA-2340 (expresses KPC) and *E. coli* BAA-2452 (expresses NDM-1) was confirmed by monitoring bacterial growth behavior from 1 to 24 hours. As shown in Fig. 27, initial growth of both *E. coli* BAA-2340 and BAA-2452 was delayed in a dose-dependent manner. The MIC of BPEI for both *E. coli* strains was found to be 1024 μg/mL. However, 256 μg/mL of 600

Da BPEI was found to be sublethal against *E. coli* ATCC ATCC 2340 and ATCC 2452; and thus 256 µg/mL was used to treat the cells for the fluorescence microscopy studies.

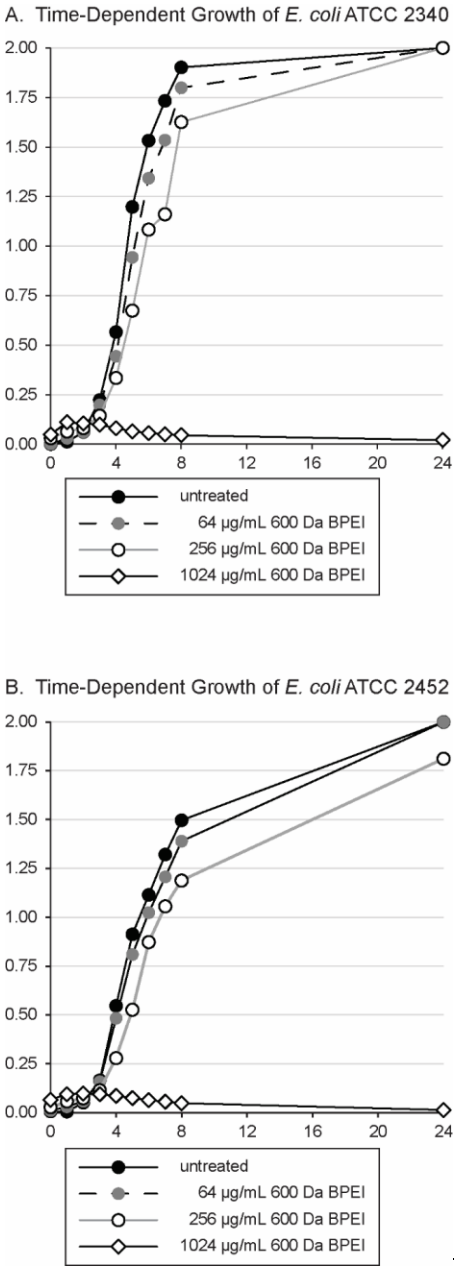

Figure 27. Time-dependent growth curve of (A) *E. coli* BAA-2340 that expresses KPC and (B) *E. coli* BAA-2452 that expresses NDM-1 in MHB liquid medium in the presence of BPEI with different concentrations. Y-axis shows bacterial growth absorbance at 600 nm (OD 600) measurement. The growth curves confirm antimicrobial activity of BPEI.

The growth inhibition data in Fig. 27 confirm that 256 μg/mL 600 Da BPEI is sublethal towards *E. coli* ATCC 2340 and *E. coli* ATCC 2452, and this concentration was used to prepare samples for CLSM imaging. Fig. 28 shows the optical cross sections of untreated and BPEI-treated *E. coli* ATCC 2340 cells. Staining cellular membranes with Nile red fluorescent dye reveals the localization of the division septum. As shown in Fig. 28A-C, the untreated *E. coli* 2340 cells have expected cell shape and size. Cell division septa are visible. However, for cells treated with BPEI (Fig. 28D-F), the bacteria are elongated. For some of the cells, there appears to be partially formed septa or the septum is missing. The incomplete formation of septa resulted in the dividing cells remaining attached to each other and unable to separate. As a result, large cells with irregular septum are established. Using a DNA-binding stain, DAPI, as a fluorescent marker for depicting the localization of the cytoplasm of the cells, the nucleic acid is shown to distribute throughout the cell (Fig. 28E). Similar effects are observed with *E. coli* ATCC 2452 (Fig. 29), however there appears to a greater extent of changes in cellular morphology. Together, these data suggests that low concentration of 600 Da BPEI alters the formation of septum divisome components and the restriction in the middle of the cells, a phenomenon which eventually prevents the bacterial cells from dividing properly.

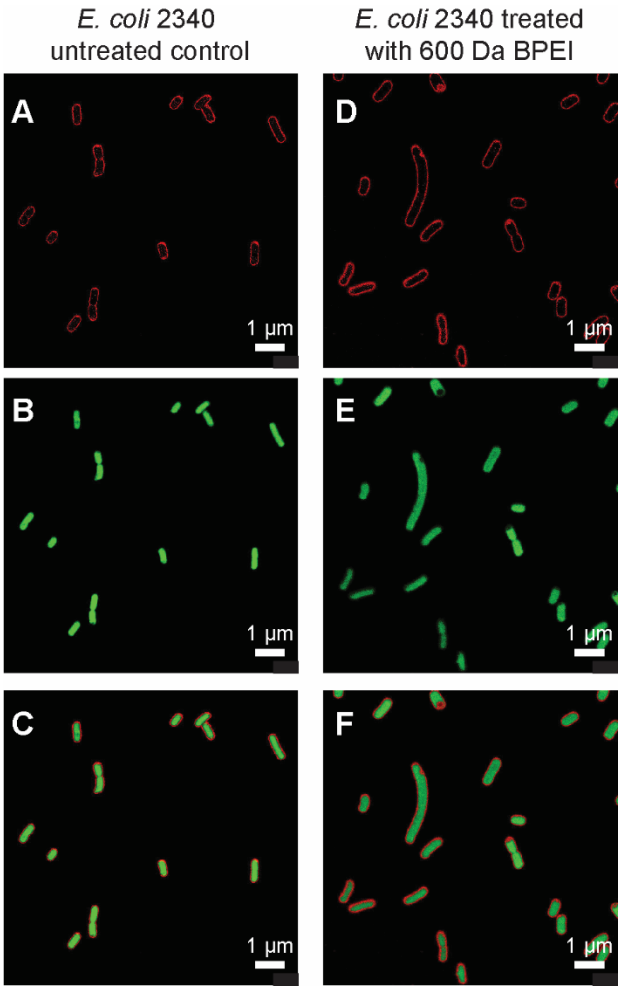

Figure 28. Optical sections of BPEI binding to *E. coli* 2340. Glutaraldehyde-fixed BPEI-treated CRE *E. coli* cells, stained with (A) membrane binding dye-Nile red, (B) DNA-binding dye DAPI, and (C) merge. Untreated *E. coli* 2340 cells were stained with the same dyes and imaged as control: (D) Nile red (E) DAPI, (F) merge. Scale bar = 1 µm.

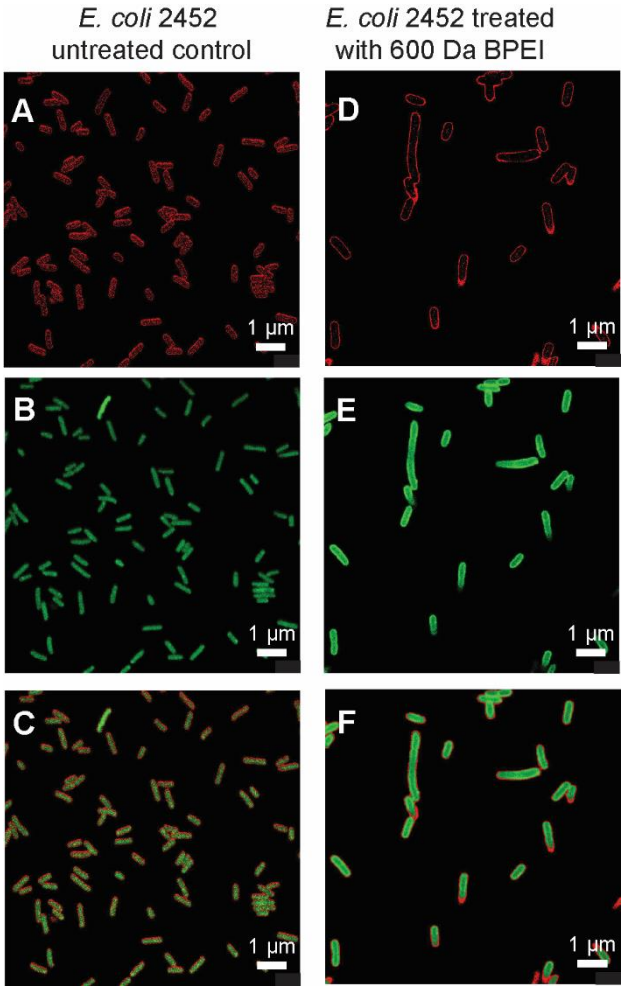

Figure 29. Optical sections of BPEI binding to *E. coli* 2452. Glutaraldehyde-fixed BPEI-treated CRE *E. coli* cells, stained with (A) membrane binding dye-Nile red, (B) DNA-binding dye DAPI, and (C) merge. Untreated *E. coli* 2340 cells were stained with the same dyes and imaged as control: (D) Nile red (E) DAPI, (F) merge. Scale bar = 1 µm.

Currently, it remains unclear whether there is a link between the biofilm formation capacity and drug resistance [214]. Dumaru *et al*. reported that about 63% of the *Enterobacteriaceae* isolates they studied were positive for biofilm-production [215]. There was a strong association between biofilm-positivity, multi-drug resistance properties, and the production of carbapenemase enzymes. While strong biofilm-producers are reported among carbapenem susceptible isolates, the majority of CRE strains also form strong biofilms [216]. In a study by Yaita *et al*., the microtiter biofilm assay data for 10 CRE strains indicated a high activity of biofilm formation for the isolates [205]. In our study,

biofilm formation for CRE *E. coli* bacteria was more robust for *E. coli* BAA-2452 expressing the metallo-β-lactamase NDM-1 than for *E. coli* BAA-2340 expressing *Klebsiella Pneumoniae* carbapenemase. Gallant *et al.,* suggests that there is a possible inverse relationship between the ability to form biofilm and the production of beta-lactamases. This might be attributed to the low adhesive potential of these bacteria [217]. On the other hand, it seems that a significant correlation exists between carbapenem resistance and biofilm formation for *E. coli* BAA-2452. Our observations are in line with previous reports that observed biofilm formation increases under low nutrient conditions [212, 218-220]. Regardless, the results of our investigation show biofilm disruption manner occurs for *E. coli* 2340 and *E. coli* 2452. Inverted laser scanning confocal microscopy images illustrate that BPEI disrupts the normal replication cycle of the CRE bacteria by developing elongated filaments, irregular cell divisions, and this is subjective to distortions in both size and shape of the cells after exposure to sublethal concentration of BPEI. Based on the imaging results in this study, we suggest that 600 Da BPEI interferes with cell division of the CRE *E. coli* species by preventing septum restriction that disrupts cell division. Additional studies are required to obtain a more complete understanding of the effect of 600 Da BPEI on bacterial cell division and components of the divisome.

Conclusion

The 2020-2025 National Action Plan for Combating Antibiotic Resistant Bacteria [221] calls for infection prevention through new strategies with innovative products and decolonizing agents to slow the emergence and spread of antibiotic resistance genes and antibiotic-resistant pathogens. There are many options to kill CRE pathogens in the planktonic state [200, 222-224] [208, 209] [110], such as polymyxins, colistin, aminoglycosides, fosfomycin, and tigecycline [192, 225]. Combination therapy takes advantage of synergy amongst antimicrobial compounds [192]. However, the high concentrations of antimicrobial agents needed against CRE biofilms [204] are accompanied by cytotoxicity issues and drug side effects [206, 207]. Biofilms are considered a primary driver in the pathology of wound infections [214]. Sequestration of bacteria within the matrix of extracellular polymeric substance [204] allows CRE bacteria to be in close proximity with each other. Not only does this hinder the penetration of antibiotics and provides bacteria with a protection mechanism against additional insults such as nutrient starvation and dehydration, [226] planktonic bacteria are periodically released from the biofilms into the environment which propagates the infection [227]. Furthermore, the close packing of bacterial cells in the biofilm increases the acquisition rate of new resistant determinants [58, 196-198, 228-230]. This leads to the development of multi-drug resistant CRE [227]. In response to the National Action Plan and reduced drug efficacy against biofilms, PEG-BPEI could be developed as a new agent to counteract CRE biofilms We previously demonstrated that 600 Da branched polyethylenimine (BPEI) and its less toxic PEGylated derivative (PEG350-BPEI) are able to render the CRE strains *K. pneumoniae* ATCC BAA-2146 and *E. coli* ATCC BAA-2452 more susceptible to the carbapenem antibiotics meropenem and imipenem by reducing the MIC to values below the resistance breakpoints [110]. These benefits are augmented by the antibiofilm activity of 600 Da BPEI and PEG350-BPEI against CRE strains *E. coli* BAA-2452,

and *E. coli* BAA-2340. The impact of using 600 Da BPEI against CRE *E. coli* biofilms expands on the ability of 600 Da BPEI and PEG350-BPEI to disrupt biofilms and antibiotic resistance in *Pseudomonas aeruginosa* and *Staphylococci* [111, 211]. As a result, new technological pipelines are opened to address drug-resistant pathogens and biofilm formation that place a significant burden on the health care system. [230, 231]

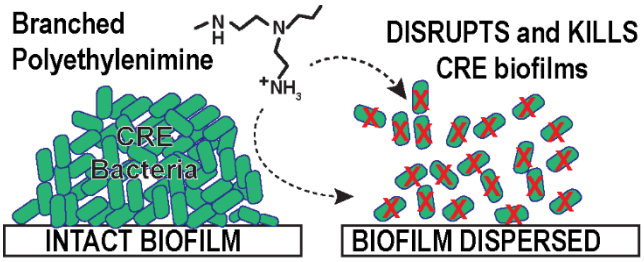

Figure 30. Graphical summary shows 600 Da BPEI disrupts and kills CRE biofilms.

Final Thoughts

In summary, I explained the role of microbial PAMPs in developing dysregulated inflammation in chronic wounds and I emphasized the need for developing innovative products specifically designed for treating non-healing chronic wounds in chapter 1. Then, I detailed how BPEI and PEG-BPEI which are developed technologies by our lab can mitigate TNF-α cytokine production caused by *S. aureus* LTA and PGN and whole cell *S. aureus* bacteria in human macrophage cells. Chapters 3 continued investigating the anti-inflammatory properties of BPEI against Gram-negative bacterial and fungal PAMPs. Lastly, in chapter 4 I described how BPEI and PEG-BPEI are effective against CRE biofilms and their planktonic cells. Overall, both 600 Da BPEI and PEG-BPEI have demonstrated the ability to eradicate biofilms and overcome resistance mechanisms in multiple strains of multi-drug resistant *P. aeruginosa*, methicillin-resistant *Staphylococcus aureus,* and methicillin-resistant *S. epidermidis*. Additionally, these compounds have shown effectiveness against resistance mechanisms in life-threatening *E. coli* and *K. pneumoniae* from CRE family. We envision 600 Da BPEI and its PEGylated derivative as topical agents for acute and chronic wounds because we propose that the potentiator molecules are multi-functional agents that can address bacterial infection and biofilms, reduce inflammation, and successfully speed up wound healing. BPEI and PEG-BPEI exhibit lower cytotoxicity effects on human cells, show minimal interactions with other proteins in serum, and are not susceptible to degradation by proteases in our body due to their non-peptide structural characteristics. Current graduate and undergraduate students in the Rice Lab are working toward a further understanding of the mechanisms of resistance to 600-Da BPEI across various pathogens, designing drug delivery devices as well as mouse studies on wound healing.

Abbreviations

PAMP: Pathogen Associated Molecular Pattern

DAMP: Damage Associated Molecular Pattern

PRR: Pattern Recognition Receptor

TLR: Toll-like Receptor

NOD: Nucleotide-binding Oligomerization Domain

MMPs: Matrix Metalloproteinases

iNOS: Inducible Nitric Oxide Synthase

TGF-β: Transforming Growth Factor Beta

TNF-α: Tumor Necrosis Factor Alpha

IFN-γ: Interferon Gamma

IL: Interleukin

LPS: Lipopolysaccharide

LTA: Lipoteichoic Acid

WTA: Wall Teichoic Acids

PGN: Peptidoglycan

LAM: Lipoarabinomannan

HMGB1: High-Mobility Group Box Protein 1

HSPs: Heat Shock Proteins

mtDNA: Mitochondrial DNA

CLRs: C-Type Lectin Receptors

RLRs: RIG-I-Like Receptors

NLRs: NOD-like receptors

IFNs: Interferons

ROS: Oxygen Species

NK: Natural Killer

DCs: Dendritic Cells

ER: Endoplasmic Reticulum

MAPK: Mitogen-Activated Protein Kinase

MYD88: Myeloid Differentiation Primary Response 88

IRAK: IL-1R-Associated Protein Kinases

TRAF6: TNF Receptor-Associated Factor 6

ERK: Extracellular Signal-Regulated Kinase

NF-kB: Nuclear Factor Kappa-B

AP-1: Activator Protein 1

IRF3: Interferon Regulatory Factor 3

ECM: Extracellular Matrix

FDA: the US Food and Drug Administration

CDC: the Centers for Disease Control and Prevention

DDD: the Division of Dermatology and Dentistry

BPEI: Branched Polyethylenimines

PEG: Polyethylene Glycol

CRE: Carbapenem Resistant *Enterobacteriaceae*

KPC*: Klebsiella Pneumoniae* Carbapenemase

NDM: New Delhi Metallo-β-Lactamase

MRSA: Methicillin Resistant *Staphylococcus aureus*

MRSE: Methicillin Resistant *Staphylococcus epidermidis*

MDR: Multi Drug Resistant

MD2: Myeloid Differentiation Factor 2

CD14: Cluster of Differentiation 14

LBP: LPS-Binding Protein

NO: Nitric Oxide

HKSA: Heat-Killed *S. aureus*

HKPA: Heat-Killed *P. aeruginosa* Bacteria

NMR: Nuclear Magnetic Resonance

ELISA: Enzyme-Linked Immunosorbent Assay

HRP: Horse Radish Peroxidase

MIC: Minimum Inhibitory Concentrations

CAMHB: Cation-Adjusted Mueller–Hinton Broth

LB: Luria–Bertani

CFU: Colony Forming Units

CV: Crystal Violet

OD: Optical Density

PBS: Phosphate-Buffer Saline

GA: Glutaraldehyde

LRV: Log Reduction Values

References

(1) van Loon, K.; Voor in ‘t holt, A. F.; Vos, M. C. A systematic review and meta-analyses of the clinical epidemiology of carbapenem-resistant Enterobacteriaceae. *Antimicrobial Agents and chemotherapy* **2018**, *62* (1), e01730-01717.

(2) Liu, T.; Zhang, L.; Joo, D.; Sun, S.-C. NF-κB signaling in inflammation. *Signal transduction and targeted therapy* **2017**, *2* (1), 1-9.

(3) Lawrence, T. The nuclear factor NF-kappaB pathway in inflammation. Cold Spring Harb Perspect Biol. 2009; 1 (6): a001651. Epub 2010/05/12. doi: 10.1101/cshperspect. a001651. PubMed PMID: 20457564.

(4) Zhang, H.; Sun, S.-C. NF-κB in inflammation and renal diseases. *Cell & bioscience* **2015**, *5* (1), 1-12.

(5) Saleh, H. A.; Yousef, M. H.; Abdelnaser, A. The anti-inflammatory properties of phytochemicals and their effects on epigenetic mechanisms involved in TLR4/NF-κB-mediated inflammation. *Frontiers in immunology* **2021**, *12*, 606069.

(6) Zhang, T.; Ma, C.; Zhang, Z.; Zhang, H.; Hu, H. NF-κB signaling in inflammation and cancer. *MedComm* **2021**, *2* (4), 618-653.

(7) El-Zayat, S. R.; Sibaii, H.; Mannaa, F. A. Toll-like receptors activation, signaling, and targeting: an overview. *Bulletin of the National Research Centre* **2019**, *43* (1), 1-12.

(8) Hoebe, K.; Du, X.; Georgel, P.; Janssen, E.; Tabeta, K.; Kim, S.; Goode, J.; Lin, P.; Mann, N.; Mudd, S. Identification of Lps2 as a key transducer of MyD88-independent TIR signalling. *Nature* **2003**, *424* (6950), 743-748.

(9) Piccinini, A.; Midwood, K. DAMPening inflammation by modulating TLR signalling. *Mediators of inflammation* **2010**, *2010*.

(10) Murad, S. Toll-like receptor 4 in inflammation and angiogenesis: a double-edged sword. *Frontiers in immunology* **2014**, *5*, 313.

(11) Takeuchi, O.; Akira, S. Pattern recognition receptors and inflammation. *Cell* **2010**, *140* (6), 805-820.

(12) Cao, X. Self-regulation and cross-regulation of pattern-recognition receptor signalling in health and disease. *Nature Reviews Immunology* **2016**, *16* (1), 35-50.

(13) Kumar, H.; Kawai, T.; Akira, S. Pathogen recognition by the innate immune system. *International reviews of immunology* **2011**, *30* (1), 16-34.

(14) Akira, S.; Uematsu, S.; Takeuchi, O. Pathogen recognition and innate immunity. *Cell* **2006**, *124* (4), 783-801.

(15) Escamilla-Tilch, M.; Filio-Rodríguez, G.; García-Rocha, R.; Mancilla-Herrera, I.; Mitchison, N. A.; Ruiz-Pacheco, J. A.; Sánchez-García, F. J.; Sandoval-Borrego, D.; Vázquez-Sánchez, E. A. The interplay between pathogen-associated and danger-associated molecular patterns: an inflammatory code in cancer? *Immunology and cell biology* **2013**, *91* (10), 601-610.

(16) Medzhitov, R. The spectrum of inflammatory responses. *Science* **2021**, *374* (6571), 1070-1075.

(17) Tosi, M. F. Innate immune responses to infection. *Journal of Allergy and Clinical Immunology* **2005**, *116* (2), 241-249.

(18) Cohen, J. The immunopathogenesis of sepsis. *Nature* **2002**, *420* (6917), 885-891.

(19) Beutler, B.; Cerami, A. The biology of cachectin/TNF--a primary mediator of the host response. *Annual review of immunology* **1989**, *7* (1), 625-655.

(20) Delneste, Y.; Beauvillain, C.; Jeannin, P. Innate immunity: structure and function of TLRs. *Medecine Sciences: M/S* **2007**, *23* (1), 67-73.

(21) Singh, K.; Kant, S.; Singh, V. K.; Agrawal, N. K.; Gupta, S. K.; Singh, K. Toll-like receptor 4 polymorphisms and their haplotypes modulate the risk of developing diabetic retinopathy in type 2 diabetes patients. *Molecular vision* **2014**, *20*, 704.

(22) Gao, W.; Xiong, Y.; Li, Q.; Yang, H. Inhibition of toll-like receptor signaling as a promising therapy for inflammatory diseases: a journey from molecular to nano therapeutics. *Frontiers in physiology* **2017**, *8*, 508.

(23) Kagan, J. C. Signaling organelles of the innate immune system. *Cell* **2012**, *151* (6), 1168-1178.

(24) Burns, K.; Janssens, S.; Brissoni, B.; Olivos, N.; Beyaert, R.; Tschopp, J. r. Inhibition of interleukin 1 receptor/Toll-like receptor signaling through the alternatively spliced, short form of MyD88 is due to its failure to recruit IRAK-4. *The Journal of experimental medicine* **2003**, *197* (2), 263-268.
(25) Yamamoto, M.; Sato, S.; Mori, K.; Hoshino, K.; Takeuchi, O.; Takeda, K.; Akira, S. Cutting edge: a novel Toll/IL-1 receptor domain-containing adapter that preferentially activates the IFN-β promoter in the Toll-like receptor signaling. *The Journal of Immunology* **2002**, *169* (12), 6668-6672.
(26) Kawai, T.; Akira, S. Toll-like receptors and their crosstalk with other innate receptors in infection and immunity. *Immunity* **2011**, *34* (5), 637-650.
(27) Lu, Y.-C.; Yeh, W.-C.; Ohashi, P. S. LPS/TLR4 signal transduction pathway. *Cytokine* **2008**, *42* (2), 145-151.
(28) Gohda, J.; Matsumura, T.; Inoue, J.-i. Cutting edge: TNFR-associated factor (TRAF) 6 is essential for MyD88-dependent pathway but not Toll/IL-1 receptor domain-containing adaptor-inducing IFN-β (TRIF)-dependent pathway in TLR signaling. *The Journal of Immunology* **2004**, *173* (5), 2913-2917.
(29) Sato, S.; Sanjo, H.; Takeda, K.; Ninomiya-Tsuji, J.; Yamamoto, M.; Kawai, T.; Matsumoto, K.; Takeuchi, O.; Akira, S. Essential function for the kinase TAK1 in innate and adaptive immune responses. *Nature immunology* **2005**, *6* (11), 1087-1095.
(30) Gay, N. J.; Symmons, M. F.; Gangloff, M.; Bryant, C. E. Assembly and localization of Toll-like receptor signalling complexes. *Nature Reviews Immunology* **2014**, *14* (8), 546-558.
(31) Moresco, E. M. Y.; LaVine, D.; Beutler, B. Toll-like receptors. *Current Biology* **2011**, *21* (13), R488-R493.
(32) Zhao, G.-N.; Jiang, D.-S.; Li, H. Interferon regulatory factors: at the crossroads of immunity, metabolism, and disease. *Biochimica et Biophysica Acta (BBA)-Molecular Basis of Disease* **2015**, *1852* (2), 365-378.
(33) Li, X.; Jiang, S.; Tapping, R. I. Toll-like receptor signaling in cell proliferation and survival. *Cytokine* **2010**, *49* (1), 1-9.
(34) Ganz, T. Defensins: antimicrobial peptides of innate immunity. *Nature reviews immunology* **2003**, *3* (9), 710-720.
(35) Palaniyar, N.; Nadesalingam, J.; Reid, K. B. Pulmonary innate immune proteins and receptors that interact with gram-positive bacterial ligands. *Immunobiology* **2002**, *205* (4-5), 575-594.
(36) SC, B. S. L. Functions of NF-kappaB 1 and NF-kappaB2 in immune cell biology. *Bioehem J* **2004**, *382*, 393-409.
(37) Dong, C. TH17 cells in development: an updated view of their molecular identity and genetic programming. *Nature Reviews Immunology* **2008**, *8* (5), 337-348.
(38) Teng, M. W.; Bowman, E. P.; McElwee, J. J.; Smyth, M. J.; Casanova, J.-L.; Cooper, A. M.; Cua, D. J. IL-12 and IL-23 cytokines: from discovery to targeted therapies for immune-mediated inflammatory diseases. *Nature medicine* **2015**, *21* (7), 719-729.
(39) Wei, F.; Chang, Y.; Wei, W. The role of BAFF in the progression of rheumatoid arthritis. *Cytokine* **2015**, *76* (2), 537-544.
(40) Schroder, K.; Tschopp, J. The inflammasomes. *cell* **2010**, *140* (6), 821-832.
(41) de Zoete, M.; Palm, N.; Zhu, S.; Flavell, R. Inflammasomes. Cold Spring Harb Perspect Biol 6: a016287. 2014.
(42) Subramanian, S.; Tus, K.; Li, Q.-Z.; Wang, A.; Tian, X.-H.; Zhou, J.; Liang, C.; Bartov, G.; McDaniel, L. D.; Zhou, X. J. A Tlr7 translocation accelerates systemic autoimmunity in murine lupus. *Proceedings of the National Academy of Sciences* **2006**, *103* (26), 9970-9975.
(43) Huang, Q.-Q.; Pope, R. M. The role of toll-like receptors in rheumatoid arthritis. *Current rheumatology reports* **2009**, *11* (5), 357.
(44) So, E. Y.; Ouchi, T. The application of Toll like receptors for cancer therapy. *International journal of biological sciences* **2010**, *6* (7), 675.
(45) Tsujimoto, H.; Ono, S.; Efron, P. A.; Scumpia, P. O.; Moldawer, L. L.; Mochizuki, H. Role of Toll-like receptors in the development of sepsis. *Shock* **2008**, *29* (3), 315-321.

(46) Zhang, Y.-w.; Thompson, R.; Zhang, H.; Xu, H. APP processing in Alzheimer's disease. *Molecular brain* **2011**, *4*, 1-13.
(47) Jialal, I.; Kaur, H.; Devaraj, S. Toll-like receptor status in obesity and metabolic syndrome: a translational perspective. *The Journal of Clinical Endocrinology & Metabolism* **2014**, *99* (1), 39-48.
(48) Guo, H.; Callaway, J. B.; Ting, J. P. Inflammasomes: mechanism of action, role in disease, and therapeutics. *Nature medicine* **2015**, *21* (7), 677-687.
(49) Oeckinghaus, A.; Ghosh, S. The NF-κB family of transcription factors and its regulation. *Cold Spring Harbor perspectives in biology* **2009**, *1* (4), a000034.
(50) Karin, M. NF-κB as a critical link between inflammation and cancer. *Cold Spring Harbor perspectives in biology* **2009**, *1* (5), a000141.
(51) DiDonato, J. A.; Mercurio, F.; Karin, M. NF-κB and the link between inflammation and cancer. *Immunological reviews* **2012**, *246* (1), 379-400.
(52) Eming, S. A.; Krieg, T.; Davidson, J. M. Inflammation in wound repair: molecular and cellular mechanisms. *Journal of Investigative Dermatology* **2007**, *127* (3), 514-525.
(53) Schilrreff, P.; Alexiev, U. Chronic inflammation in non-healing skin wounds and promising natural bioactive compounds treatment. *International journal of molecular sciences* **2022**, *23* (9), 4928.
(54) Wang, J. Neutrophils in tissue injury and repair. *Cell and tissue research* **2018**, *371*, 531-539.
(55) Szpaderska, A. M.; Egozi, E. I.; Gamelli, R. L.; DiPietro, L. A. The effect of thrombocytopenia on dermal wound healing. *Journal of Investigative Dermatology* **2003**, *120* (6), 1130-1137.
(56) Cañedo-Dorantes, L.; Cañedo-Ayala, M. Skin acute wound healing: a comprehensive review. *International journal of inflammation* **2019**, *2019*.
(57) Loots, M. A.; Lamme, E. N.; Zeegelaar, J.; Mekkes, J. R.; Bos, J. D.; Middelkoop, E. Differences in cellular infiltrate and extracellular matrix of chronic diabetic and venous ulcers versus acute wounds. *Journal of Investigative Dermatology* **1998**, *111* (5), 850-857.
(58) Bowler, P. G. Antibiotic resistance and biofilm tolerance: a combined threat in the treatment of chronic infections. *J Wound Care* **2018**, *27* (5), 273-277. DOI: 10.12968/jowc.2018.27.5.273.
(59) Zhao, R.; Liang, H.; Clarke, E.; Jackson, C.; Xue, M. Inflammation in chronic wounds. *International journal of molecular sciences* **2016**, *17* (12), 2085.
(60) Mustoe, T. Understanding chronic wounds: a unifying hypothesis on their pathogenesis and implications for therapy. *The American Journal of Surgery* **2004**, *187* (5), S65-S70.
(61) Versey, Z.; da Cruz Nizer, W. S.; Russell, E.; Zigic, S.; DeZeeuw, K. G.; Marek, J. E.; Overhage, J.; Cassol, E. Biofilm-innate immune interface: contribution to chronic wound formation. *Frontiers in immunology* **2021**, *12*, 648554.
(62) Cardona, A. F.; Wilson, S. E. Skin and soft-tissue infections: a critical review and the role of telavancin in their treatment. *Clinical Infectious Diseases* **2015**, *61* (suppl_2), S69-S78.
(63) Tomic-Canic, M.; Burgess, J. L.; O'Neill, K. E.; Strbo, N.; Pastar, I. Skin microbiota and its interplay with wound healing. *American journal of clinical dermatology* **2020**, *21* (Suppl 1), 36-43.
(64) Percival, S. L.; Thomas, J. G.; Williams, D. W. Biofilms and bacterial imbalances in chronic wounds: anti-Koch. *International wound journal* **2010**, *7* (3), 169-175.
(65) Heydarian, N.; Wouters, C. L.; Neel, A.; Ferrell, M.; Panlilio, H.; Haight, T.; Gu, T.; Rice, C. V. Eradicating Biofilms of Carbapenem-Resistant Enterobacteriaceae by Simultaneously Dispersing the Biomass and Killing Planktonic Bacteria with PEGylated Branched Polyethyleneimine. *ChemMedChem* **2023**, *18* (3), e202200428.
(66) Wu, Y.-K.; Cheng, N.-C.; Cheng, C.-M. Biofilms in chronic wounds: pathogenesis and diagnosis. *Trends in biotechnology* **2019**, *37* (5), 505-517.
(67) Wolcott, R. D.; Rhoads, D. D.; Dowd, S. E. Biofilms and chronic wound inflammation. *Journal of wound care* **2008**, *17* (8), 333-341.
(68) Burmølle, M.; Thomsen, T. R.; Fazli, M.; Dige, I.; Christensen, L.; Homøe, P.; Tvede, M.; Nyvad, B.; Tolker-Nielsen, T.; Givskov, M. Biofilms in chronic infections–a matter of opportunity–monospecies biofilms in multispecies infections. *FEMS Immunology & Medical Microbiology* **2010**, *59* (3), 324-336.
(69) Bjarnsholt, T. The role of bacterial biofilms in chronic infections. *Apmis* **2013**, *121*, 1-58.

(70) Bakshani, C. R.; Morales-Garcia, A. L.; Althaus, M.; Wilcox, M. D.; Pearson, J. P.; Bythell, J. C.; Burgess, J. G. Evolutionary conservation of the antimicrobial function of mucus: a first defence against infection. *npj Biofilms and Microbiomes* **2018**, *4* (1), 14.
(71) Sauer, K. The genomics and proteomics of biofilm formation. *Genome biology* **2003**, *4* (6), 1-5.
(72) Raziyeva, K.; Kim, Y.; Zharkinbekov, Z.; Kassymbek, K.; Jimi, S.; Saparov, A. Immunology of acute and chronic wound healing. *Biomolecules* **2021**, *11* (5), 700.
(73) Jones, R. E.; Foster, D. S.; Longaker, M. T. Management of chronic wounds—2018. *Jama* **2018**, *320* (14), 1481-1482.
(74) Sen, C. K. Human wounds and its burden: an updated compendium of estimates. Mary Ann Liebert, Inc., publishers 140 Huguenot Street, 3rd Floor New …: 2019; Vol. 8, pp 39-48.
(75) Matoori, S. Breakthrough Technologies in Diagnosis and Therapy of Chronic Wounds. ACS Publications: 2023.
(76) Verma, K. D.; Lewis, F.; Mejia, M.; Chalasani, M.; Marcus, K. A. Food and Drug Administration perspective: Advancing product development for non-healing chronic wounds. *Wound Repair and Regeneration* **2022**, *30* (3), 299-302.
(77) Whittam, A. J.; Maan, Z. N.; Duscher, D.; Wong, V. W.; Barrera, J. A.; Januszyk, M.; Gurtner, G. C. Challenges and opportunities in drug delivery for wound healing. *Advances in wound care* **2016**, *5* (2), 79-88.
(78) Saghazadeh, S.; Rinoldi, C.; Schot, M.; Kashaf, S. S.; Sharifi, F.; Jalilian, E.; Nuutila, K.; Giatsidis, G.; Mostafalu, P.; Derakhshandeh, H. Drug delivery systems and materials for wound healing applications. *Advanced drug delivery reviews* **2018**, *127*, 138-166.
(79) Werdin, F.; Tenenhaus, M.; Rennekampff, H.-O. Chronic wound care. *The Lancet* **2008**, *372* (9653), 1860-1862.
(80) Rahmani, S.; Mooney, D. J. Tissue-Engineered Wound Dressings for Diabetic Foot Ulcers. *The Diabetic Foot: Medical and Surgical Management* **2018**, 247-256.
(81) Matoori, S.; Veves, A.; Mooney, D. J. Advanced bandages for diabetic wound healing. *Science translational medicine* **2021**, *13* (585), eabe4839.
(82) Dai, C.; Shih, S.; Khachemoune, A. Skin substitutes for acute and chronic wound healing: an updated review. *Journal of Dermatological Treatment* **2020**, *31* (6), 639-648.
(83) Martinson, M.; Martinson, N. A comparative analysis of skin substitutes used in the management of diabetic foot ulcers. *Journal of wound care* **2016**, *25* (Sup10), S8-S17.
(84) Snyder, D.; Sullivan, N.; Margolis, D.; Schoelles, K. Skin substitutes for treating chronic wounds. **2020**.
(85) Eaglstein, W. H.; Kirsner, R. S.; Robson, M. C. Food and Drug Administration (FDA) drug approval end points for chronic cutaneous ulcer studies. *Wound repair and regeneration* **2012**, *20* (6), 793-796.
(86) Darwin, E.; Tomic-Canic, M. Healing chronic wounds: current challenges and potential solutions. *Current dermatology reports* **2018**, *7*, 296-302.
(87) Rodrigues, M.; Kosaric, N.; Bonham, C. A.; Gurtner, G. C. Wound healing: a cellular perspective. *Physiological reviews* **2019**, *99* (1), 665-706.
(88) Maderal, A. D.; Vivas, A. C.; Eaglstein, W. H.; Kirsner, R. S. The FDA and designing clinical trials for chronic cutaneous ulcers. In *Seminars in cell & developmental biology*, 2012; Elsevier: Vol. 23, pp 993-999.
(89) Falanga, V.; Isseroff, R. R.; Soulika, A. M.; Romanelli, M.; Margolis, D.; Kapp, S.; Granick, M.; Harding, K. Chronic wounds. *Nature Reviews Disease Primers* **2022**, *8* (1), 50.
(90) Niemiec, S. M.; Louiselle, A. E.; Liechty, K. W.; Zgheib, C. Role of microRNAs in pressure ulcer immune response, pathogenesis, and treatment. *International journal of molecular sciences* **2020**, *22* (1), 64.
(91) Raffetto, J. D.; Ligi, D.; Maniscalco, R.; Khalil, R. A.; Mannello, F. Why venous leg ulcers have difficulty healing: overview on pathophysiology, clinical consequences, and treatment. *Journal of clinical medicine* **2020**, *10* (1), 29.

(92) Strbo, N.; Yin, N.; Stojadinovic, O. Innate and adaptive immune responses in wound epithelialization. *Advances in wound care* **2014**, *3* (7), 492-501.
(93) He, L.; He, T.; Farrar, S.; Ji, L.; Liu, T.; Ma, X. Antioxidants maintain cellular redox homeostasis by elimination of reactive oxygen species. *Cellular Physiology and Biochemistry* **2017**, *44* (2), 532-553.
(94) Fischer, D.; Bieber, T.; Li, Y.; Elsässer, H.-P.; Kissel, T. A novel non-viral vector for DNA delivery based on low molecular weight, branched polyethylenimine: effect of molecular weight on transfection efficiency and cytotoxicity. *Pharmaceutical research* **1999**, *16*, 1273-1279.
(95) Jäger, M.; Schubert, S.; Ochrimenko, S.; Fischer, D.; Schubert, U. S. Branched and linear poly (ethylene imine)-based conjugates: synthetic modification, characterization, and application. *Chemical Society Reviews* **2012**, *41* (13), 4755-4767.
(96) Boussif, O.; Lezoualc'h, F.; Zanta, M. A.; Mergny, M. D.; Scherman, D.; Demeneix, B.; Behr, J.-P. A versatile vector for gene and oligonucleotide transfer into cells in culture and in vivo: polyethylenimine. *Proceedings of the National Academy of Sciences* **1995**, *92* (16), 7297-7301.
(97) Kirk, N.; Cowan, D. Optimising the recovery of recombinant thermostable proteins expressed in mesophilic hosts. *Journal of biotechnology* **1995**, *42* (2), 177-184.
(98) Milburn, P.; Bonnerjea, J.; Hoare, M.; Dunnill, P. Selective flocculation of nucleic acids, lipids, and colloidal particles from a yeast cell homogenate by polyethyleneimine, and its scale-up. *Enzyme and microbial technology* **1990**, *12* (7), 527-532.
(99) Vancha, A. R.; Govindaraju, S.; Parsa, K. V.; Jasti, M.; González-García, M.; Ballestero, R. P. Use of polyethyleneimine polymer in cell culture as attachment factor and lipofection enhancer. *BMC biotechnology* **2004**, *4*, 1-12.
(100) Foxley, M. A.; Friedline, A. W.; Jensen, J. M.; Nimmo, S. L.; Scull, E. M.; King, J. B.; Strange, S.; Xiao, M. T.; Smith, B. E.; Thomas III, K. J. Efficacy of ampicillin against methicillin-resistant Staphylococcus aureus restored through synergy with branched poly (ethylenimine). *The Journal of antibiotics* **2016**, *69* (12), 871-878.
(101) Foxley, M. A.; Wright, S. N.; Lam, A. K.; Friedline, A. W.; Strange, S. J.; Xiao, M. T.; Moen, E. L.; Rice, C. V. Targeting wall teichoic acid in situ with branched polyethylenimine potentiates β-lactam efficacy against MRSA. *ACS medicinal chemistry letters* **2017**, *8* (10), 1083-1088.
(102) Lam, A. K.; Hill, M. A.; Moen, E. L.; Pusavat, J.; Wouters, C. L.; Rice, C. V. Cationic Branched Polyethylenimine (BPEI) Disables Antibiotic Resistance in Methicillin-Resistant Staphylococcus epidermidis (MRSE). *ChemMedChem* **2018**, *13* (20), 2240-2248.
(103) Hill, M. A.; Lam, A. K.; Reed, P.; Harney, M. C.; Wilson, B. A.; Moen, E. L.; Wright, S. N.; Pinho, M. G.; Rice, C. V. BPEI-induced delocalization of PBP4 potentiates β-lactams against MRSA. *Biochemistry* **2019**, *58* (36), 3813-3822.
(104) Lam, A. K.; Panlilio, H.; Pusavat, J.; Wouters, C. L.; Moen, E. L.; Brennan, R. E.; Rice, C. V. Expanding the Spectrum of Antibiotics Capable of Killing Multidrug-Resistant Staphylococcus aureus and Pseudomonas aeruginosa. *ChemMedChem* **2020**, *15* (15), 1421-1428.
(105) Lam, A. K.; Panlilio, H.; Pusavat, J.; Wouters, C. L.; Moen, E. L.; Neel, A. J.; Rice, C. V. Low-molecular-weight branched polyethylenimine potentiates ampicillin against MRSA biofilms. *ACS Medicinal Chemistry Letters* **2020**, *11* (4), 473-478.
(106) Lam, A. K.; Panlilio, H.; Pusavat, J.; Wouters, C. L.; Moen, E. L.; Rice, C. V. Overcoming multidrug resistance and biofilms of Pseudomonas aeruginosa with a single dual-function potentiator of β-lactams. *ACS infectious diseases* **2020**, *6* (5), 1085-1097.
(107) Moen, E. L.; Lam, A. K.; Pusavat, J.; Wouters, C. L.; Panlilio, H.; Heydarian, N.; Peng, Z.; Lan, Y.; Rice, C. V. Dimerization of 600 Da branched polyethylenimine improves β-lactam antibiotic potentiation against antibiotic-resistant Staphylococcus epidermidis and Pseudomonas aeruginosa. *Chemical Biology & Drug Design* **2023**, *101* (3), 489-499.
(108) Wouters, C. L.; Heydarian, N.; Pusavat, J.; Panlilio, H.; Lam, A. K.; Moen, E. L.; Brennan, R. E.; Rice, C. V. Breaking membrane barriers to neutralize E. coli and K. pneumoniae virulence with PEGylated branched polyethylenimine. *Biochimica et Biophysica Acta (BBA)-Biomembranes* **2023**, 184172.

(109) Panlilio, H.; Neel, A.; Heydarian, N.; Best, W.; Atkins, I.; Boris, A.; Bui, M.; Dick, C.; Ferrell, M.; Gu, T. Antibiofilm Activity of PEGylated Branched Polyethylenimine. *ACS omega* **2022**, *7* (49), 44825-44835.
(110) Panlilio, H.; Lam, A. K.; Heydarian, N.; Haight, T.; Wouters, C. L.; Moen, E. L.; Rice, C. V. Dual-Function Potentiation by PEG-BPEI Restores Activity of Carbapenems and Penicillins against Carbapenem-Resistant Enterobacteriaceae. *ACS Infectious Diseases* **2021**, *7* (6), 1657-1665.
(111) Lam, A. K.; Moen, E. L.; Pusavat, J.; Wouters, C. L.; Panlilio, H.; Ferrell, M. J.; Houck, M. B.; Glatzhofer, D. T.; Rice, C. V. PEGylation of Polyethylenimine Lowers Acute Toxicity while Retaining Anti-Biofilm and β-Lactam Potentiation Properties against Antibiotic-Resistant Pathogens. *ACS omega* **2020**, *5* (40), 26262-26270.
(112) Saravanan, R.; Adav, S. S.; Choong, Y. K.; Van Der Plas, M. J.; Petrlova, J.; Kjellström, S.; Sze, S. K.; Schmidtchen, A. Proteolytic signatures define unique thrombin-derived peptides present in human wound fluid in vivo. *Scientific reports* **2017**, *7* (1), 13136.
(113) Kim, H. G.; Kim, N.-R.; Gim, M. G.; Lee, J. M.; Lee, S. Y.; Ko, M. Y.; Kim, J. Y.; Han, S. H.; Chung, D. K. Lipoteichoic acid isolated from Lactobacillus plantarum inhibits lipopolysaccharide-induced TNF-α production in THP-1 cells and endotoxin shock in mice. *The Journal of Immunology* **2008**, *180* (4), 2553-2561.
(114) Ahn, J. E.; Kim, H.; Chung, D. K. Lipoteichoic acid isolated from Lactobacillus plantarum maintains inflammatory homeostasis through regulation of Th1-and Th2-induced cytokines. **2019**.
(115) Prajitha, N.; Mohanan, P. V. Cellular and immunological response of THP-1 cells in response to lipopolysaccharides and lipoteichoic acid exposure. *Biomedical Research and Therapy* **2021**, *8* (9), 4562-4582.
(116) Kim, H. G.; Lee, S. Y.; Kim, N.-R.; Ko, M. Y.; Lee, J. M.; Yi, T.-H.; Chung, S. K.; Chung, D. K. Inhibitory effects of Lactobacillus plantarum lipoteichoic acid (LTA) on Staphylococcus aureus LTA-induced tumor necrosis factor-alpha production. *Journal of microbiology and biotechnology* **2008**, *18* (6), 1191-1196.
(117) Ginsburg, I. Role of lipoteichoic acid in infection and inflammation. *The Lancet infectious diseases* **2002**, *2* (3), 171-179.
(118) van Dalen, R.; Rumpret, M.; Fuchsberger, F. F.; van Teijlingen, N. H.; Hanske, J.; Rademacher, C.; Geijtenbeek, T. B.; van Strijp, J. A.; Weidenmaier, C.; Peschel, A. Wall teichoic acid is a pathogen-associated molecular pattern of Staphylococcus aureus that is recognized by langerin (CD207) on skin Langerhans cells.
(119) Pidwill, G. R.; Gibson, J. F.; Cole, J.; Renshaw, S. A.; Foster, S. J. The role of macrophages in Staphylococcus aureus infection. *Frontiers in immunology* **2021**, *11*, 3506.
(120) Xie, X.; Wang, L.; Gong, F.; Xia, C.; Chen, J.; Song, Y.; Shen, A.; Song, J. Intracellular Staphylococcus aureus-induced NF-κB activation and proinflammatory responses of P815 cells are mediated by NOD2. *Journal of Huazhong University of Science and Technology [Medical Sciences]* **2012**, *32*, 317-323.
(121) Zeng, R.-Z.; Kim, H. G.; Kim, N. R.; Gim, M. G.; Ko, M. Y.; Lee, S. Y.; Kim, C. M.; Chung, D. K. Differential gene expression profiles in human THP-1 monocytes treated with Lactobacillus plantarum or Staphylococcus aureus lipoteichoic acid. *Journal of the Korean Society for Applied Biological Chemistry* **2011**, *54* (5), 763-770.
(122) Jang, J.; Kim, W.; Kim, K.; Chung, S.-I.; Shim, Y. J.; Kim, S.-M.; Yoon, Y. Lipoteichoic acid upregulates NF-κB and proinflammatory cytokines by modulating β-catenin in bronchial epithelial cells. *Molecular Medicine Reports* **2015**, *12* (3), 4720-4726.
(123) Villéger, R.; Saad, N.; Grenier, K.; Falourd, X.; Foucat, L.; Urdaci, M. C.; Bressollier, P.; Ouk, T.-S. Characterization of lipoteichoic acid structures from three probiotic Bacillus strains: involvement of D-alanine in their biological activity. *Antonie Van Leeuwenhoek* **2014**, *106*, 693-706.
(124) Parolia, A.; Gee, L. S.; Porto, I.; Mohan, M. Role of cytokines, endotoxins (LPS), and lipoteichoic acid (LTA) in endodontic infection. *J Dent Oral Disord Ther* **2014**, *2* (4), 1-5.

(125) Kang, S.-S.; Sim, J.-R.; Yun, C.-H.; Han, S. H. Lipoteichoic acids as a major virulence factor causing inflammatory responses via Toll-like receptor 2. *Archives of pharmacal research* **2016**, *39*, 1519-1529.
(126) Jung, B.-J.; Kim, H.; Chung, D.-K. Differential immunostimulatory effects of lipoteichoic acids isolated from four strains of Lactiplantibacillus plantarum. *Applied Sciences* **2022**, *12* (3), 954.
(127) Schwandner, R.; Dziarski, R.; Wesche, H.; Rothe, M.; Kirschning, C. J. Peptidoglycan-and lipoteichoic acid-induced cell activation is mediated by toll-like receptor 2. *Journal of Biological Chemistry* **1999**, *274* (25), 17406-17409.
(128) Lebeer, S.; Claes, I. J.; Vanderleyden, J. Anti-inflammatory potential of probiotics: lipoteichoic acid makes a difference. *Trends in microbiology* **2012**, *20* (1), 5-10.
(129) Alan, A.; Alan, E.; Arslan, K.; Daldaban, F.; Aksel, E. G.; Çınar, M. U.; Akyüz, B. LPS-and LTA-induced expression of TLR4, MyD88, and TNF-α in lymph nodes of the Akkaraman and Romanov lambs. *Microscopy and Microanalysis* **2022**, *28* (6), 2078-2092.
(130) Kapetanovic, R.; Parlato, M.; Fitting, C.; Quesniaux, V.; Cavaillon, J.-M.; Adib-Conquy, M. Mechanisms of TNF induction by heat-killed Staphylococcus aureus differ upon the origin of mononuclear phagocytes. *American Journal of Physiology-Cell Physiology* **2011**, *300* (4), C850-C859.
(131) Schröder, N. W.; Morath, S.; Alexander, C.; Hamann, L.; Hartung, T.; Zähringer, U.; Göbel, U. B.; Weber, J. R.; Schumann, R. R. Lipoteichoic acid (LTA) of Streptococcus pneumoniaeand Staphylococcus aureus activates immune cells via Toll-like receptor (TLR)-2, lipopolysaccharide-binding protein (LBP), and CD14, whereas TLR-4 and MD-2 are not involved. *Journal of biological chemistry* **2003**, *278* (18), 15587-15594.
(132) Wang, Y.; Pawar, S.; Dutta, O.; Wang, K.; Rivera, A.; Xue, C. Macrophage mediated immunomodulation during cryptococcus pulmonary infection. *Frontiers in Cellular and Infection Microbiology* **2022**, 310.
(133) Leemans, J. C.; Heikens, M.; van Kessel, K. P.; Florquin, S.; van der Poll, T. Lipoteichoic acid and peptidoglycan from Staphylococcus aureus synergistically induce neutrophil influx into the lungs of mice. *Clinical and Vaccine Immunology* **2003**, *10* (5), 950-953.
(134) Carr, E. A. Systemic inflammatory response syndrome. In *Robinson's Current Therapy in Equine Medicine*, Elsevier, 2015; pp 741-745.
(135) Cen, X.; Liu, S.; Cheng, K. The role of toll-like receptor in inflammation and tumor immunity. *Frontiers in pharmacology* **2018**, *9*, 878.
(136) Midwood, K.; Piccinini, A.; Sacre, S. Targeting Toll-like receptors in autoimmunity. *Current drug targets* **2009**, *10* (11), 1139-1155.
(137) Ginsburg, I. The biochemistry of bacteriolysis: paradoxes, facts and myths. *Microbiological sciences* **1988**, *5* (5), 137-142.
(138) Periti, P.; Mazzei, T. Antibiotic-induced release of bacterial cell wall components in the pathogenesis of sepsis and septic shock: a review. *Journal of chemotherapy* **1998**, *10* (6), 427-448.
(139) Kumar, S. S.; Hira, K.; Begum Ahil, S.; Kulkarni, O. P.; Araya, H.; Fujimoto, Y. New synthetic coumarinolignans as attenuators of pro-inflammatory cytokines in LPS-induced sepsis and carrageenan-induced paw oedema models. *Inflammopharmacology* **2020**, *28*, 1365-1373.
(140) Brown, S.; Santa Maria Jr, J. P.; Walker, S. Wall teichoic acids of gram-positive bacteria. *Annual review of microbiology* **2013**, *67*, 313-336.
(141) Teissié, J.; Zerbib, D. Eradication of Bacteria Via Electropulsation. 2018.
(142) Plette, A. C.; van Riemsdijk, W. H.; Benedetti, M. F.; van der Wal, A. pH dependent charging behavior of isolated cell walls of a gram-positive soil bacterium. *Journal of Colloid and Interface Science* **1995**, *173* (2), 354-363.
(143) Rippon, M. G.; Westgate, S.; Rogers, A. A. Implications of endotoxins in wound healing: a narrative review. *Journal of Wound Care* **2022**, *31* (5), 380-392.
(144) Ovington, L. Bacterial toxins and wound healing. *Ostomy/wound management* **2003**, *49* (7A Suppl), 8-12.

(145) Ayoub Moubareck, C. Polymyxins and bacterial membranes: a review of antibacterial activity and mechanisms of resistance. *Membranes* **2020**, *10* (8), 181.
(146) Dijkmans, A. C.; Wilms, E. B.; Kamerling, I. M.; Birkhoff, W.; Ortiz-Zacarías, N. V.; Van Nieuwkoop, C.; Verbrugh, H. A.; Touw, D. J. Colistin: revival of an old polymyxin antibiotic. *Therapeutic drug monitoring* **2015**, *37* (4), 419-427.
(147) Zavascki, A. P.; Nation, R. L. Nephrotoxicity of polymyxins: is there any difference between colistimethate and polymyxin B? *Antimicrobial agents and chemotherapy* **2017**, *61* (3), e02319-02316.
(148) Shokouhi, S.; Sahraei, Z. A review on colistin nephrotoxicity. *European Journal of Clinical Pharmacology* **2015**, *71* (7), 801-810.
(149) Lim, T.-P.; Hee, D. K.-H.; Lee, W.; Teo, J. Q.-M.; Cai, Y.; Chia, S. Y.-H.; Leaw, J. Y.-K.; Lee, S. J.-Y.; Lee, L. S.-U.; Kwa, A. L. Physicochemical Stability Study of Polymyxin B in Various Infusion Solutions for Administration to Critically Ill Patients. *Annals of Pharmacotherapy* **2016**, *50* (9), 790-792.
(150) Wang, D.; Liu, Y.; Zhao, Y.-R.; Zhou, J.-L. Low dose of lipopolysaccharide pretreatment can alleviate the inflammatory response in wound infection mouse model. *Chinese Journal of Traumatology* **2016**, *19* (04), 193-198.
(151) Koff, J. L.; Shao, M. X.; Kim, S.; Ueki, I. F.; Nadel, J. A. Pseudomonas lipopolysaccharide accelerates wound repair via activation of a novel epithelial cell signaling cascade. *The Journal of Immunology* **2006**, *177* (12), 8693-8700.
(152) Yang, H.; Hu, C.; Li, F.; Liang, L.; Liu, L. Effect of lipopolysaccharide on the biological characteristics of human skin fibroblasts and hypertrophic scar tissue formation. *IUBMB life* **2013**, *65* (6), 526-532.
(153) Crompton, R.; Williams, H.; Ansell, D.; Campbell, L.; Holden, K.; Cruickshank, S.; Hardman, M. J. Oestrogen promotes healing in a bacterial LPS model of delayed cutaneous wound repair. *Laboratory Investigation* **2016**, *96* (4), 439-449.
(154) Velnar, T.; Bailey, T.; Smrkolj, V. The wound healing process: an overview of the cellular and molecular mechanisms. *Journal of international medical research* **2009**, *37* (5), 1528-1542.
(155) Dalton, T.; Dowd, S. E.; Wolcott, R. D.; Sun, Y.; Watters, C.; Griswold, J. A.; Rumbaugh, K. P. An in vivo polymicrobial biofilm wound infection model to study interspecies interactions. *PloS one* **2011**, *6* (11), e27317.
(156) Rhoads, D. D.; Wolcott, R. D.; Sun, Y.; Dowd, S. E. Comparison of culture and molecular identification of bacteria in chronic wounds. *International journal of molecular sciences* **2012**, *13* (3), 2535-2550.
(157) Percival, S. L.; McCarty, S. M.; Lipsky, B. Biofilms and wounds: an overview of the evidence. *Advances in wound care* **2015**, *4* (7), 373-381.
(158) Ge, Y.; Wang, Q. Current research on fungi in chronic wounds. *Frontiers in Molecular Biosciences* **2023**, *9*, 1057766.
(159) Larouche, J.; Sheoran, S.; Maruyama, K.; Martino, M. M. Immune regulation of skin wound healing: mechanisms and novel therapeutic targets. *Advances in wound care* **2018**, *7* (7), 209-231.
(160) Kalan, L.; Loesche, M.; Hodkinson, B. P.; Heilmann, K.; Ruthel, G.; Gardner, S. E.; Grice, E. A. Redefining the chronic-wound microbiome: fungal communities are prevalent, dynamic, and associated with delayed healing. *MBio* **2016**, *7* (5), e01058-01016.
(161) Haalboom, M. Chronic wounds: innovations in diagnostics and therapeutics. *Current medicinal chemistry* **2018**, *25* (41), 5772-5781.
(162) Nosrati, H.; Aramideh Khouy, R.; Nosrati, A.; Khodaei, M.; Banitalebi-Dehkordi, M.; Ashrafi-Dehkordi, K.; Sanami, S.; Alizadeh, Z. Nanocomposite scaffolds for accelerating chronic wound healing by enhancing angiogenesis. *Journal of Nanobiotechnology* **2021**, *19* (1), 1-21.
(163) Molteni, M.; Gemma, S.; Rossetti, C. The role of toll-like receptor 4 in infectious and noninfectious inflammation. *Mediators of inflammation* **2016**, *2016*.
(164) Huang, S.; Miao, R.; Zhou, Z.; Wang, T.; Liu, J.; Liu, G.; Chen, Y. E.; Xin, H.-B.; Zhang, J.; Fu, M. MCPIP1 negatively regulates toll-like receptor 4 signaling and protects mice from LPS-induced septic shock. *Cellular signalling* **2013**, *25* (5), 1228-1234.

(165) Lakhani, S. A.; Bogue, C. W. Toll-like receptor signaling in sepsis. *Current opinion in pediatrics* **2003**, *15* (3), 278-282.
(166) Chu, S.; Zhu, X.; You, N.; Zhang, W.; Zheng, F.; Cai, B.; Zhou, T.; Wang, Y.; Sun, Q.; Yang, Z. The fab fragment of a human anti-Siglec-9 monoclonal antibody suppresses LPS-induced inflammatory responses in human macrophages. *Frontiers in Immunology* **2016**, *7*, 649.
(167) Pradhan, A.; Avelar, G. M.; Bain, J. M.; Childers, D.; Pelletier, C.; Larcombe, D. E.; Shekhova, E.; Netea, M. G.; Brown, G. D.; Erwig, L. Non-canonical signalling mediates changes in fungal cell wall PAMPs that drive immune evasion. *Nature communications* **2019**, *10* (1), 5315.
(168) Taghavi, M.; Khosravi, A.; Mortaz, E.; Nikaein, D.; Athari, S. S. Role of pathogen-associated molecular patterns (PAMPS) in immune responses to fungal infections. *European journal of pharmacology* **2017**, *808*, 8-13.
(169) Kuzmich, N. N.; Sivak, K. V.; Chubarev, V. N.; Porozov, Y. B.; Savateeva-Lyubimova, T. N.; Peri, F. TLR4 signaling pathway modulators as potential therapeutics in inflammation and sepsis. *Vaccines* **2017**, *5* (4), 34.
(170) Patrick, S. Bacteroides. In *Molecular medical microbiology*, Elsevier, 2015; pp 917-944.
(171) Pålsson-McDermott, E. M.; O'Neill, L. A. Signal transduction by the lipopolysaccharide receptor, Toll-like receptor-4. *Immunology* **2004**, *113* (2), 153-162.
(172) Park, B. S.; Song, D. H.; Kim, H. M.; Choi, B.-S.; Lee, H.; Lee, J.-O. The structural basis of lipopolysaccharide recognition by the TLR4–MD-2 complex. *Nature* **2009**, *458* (7242), 1191-1195.
(173) Park, B. S.; Lee, J.-O. Recognition of lipopolysaccharide pattern by TLR4 complexes. *Experimental & molecular medicine* **2013**, *45* (12), e66-e66.
(174) Kalle, M.; Papareddy, P.; Kasetty, G.; Mörgelin, M.; van der Plas, M. J.; Rydengård, V.; Malmsten, M.; Albiger, B.; Schmidtchen, A. Host defense peptides of thrombin modulate inflammation and coagulation in endotoxin-mediated shock and Pseudomonas aeruginosa sepsis. *PloS one* **2012**, *7* (12), e51313.
(175) Briard, B.; Fontaine, T.; Kanneganti, T.-D.; Gow, N. A.; Papon, N. Fungal cell wall components modulate our immune system. *The Cell Surface* **2021**, *7*, 100067.
(176) Hatinguais, R.; Willment, J. A.; Brown, G. D. PAMPs of the fungal cell wall and mammalian PRRs. *The Fungal Cell Wall: An Armour and a Weapon for Human Fungal Pathogens* **2020**, 187-223.
(177) Kanno, E.; Kawakami, K.; Tanno, H.; Suzuki, A.; Sato, N.; Masaki, A.; Imamura, A.; Takagi, N.; Miura, T.; Yamamoto, H. Contribution of CARD 9-mediated signalling to wound healing in skin. *Experimental Dermatology* **2017**, *26* (11), 1097-1104.
(178) Jiang, D. Advances in animal models for bone and joint diseases. In *Joint and Bone*, Elsevier, 2023; pp 141-168.
(179) Frasnelli, M. E.; Tarussio, D.; Chobaz-Péclat, V.; Busso, N.; So, A. TLR2 modulates inflammation in zymosan-induced arthritis in mice. *Arthritis Res Ther* **2005**, *7* (2), 1-10.
(180) Sato, M.; Sano, H.; Iwaki, D.; Kudo, K.; Konishi, M.; Takahashi, H.; Takahashi, T.; Imaizumi, H.; Asai, Y.; Kuroki, Y. Direct binding of Toll-like receptor 2 to zymosan, and zymosan-induced NF-κB activation and TNF-α secretion are down-regulated by lung collectin surfactant protein A. *The Journal of Immunology* **2003**, *171* (1), 417-425.
(181) Venkatachalam, G.; Arumugam, S.; Doble, M. Synthesis, characterization, and biological activity of aminated zymosan. *ACS omega* **2020**, *5* (26), 15973-15982.
(182) Ostrop, J.; Lang, R. Contact, collaboration, and conflict: signal integration of Syk-coupled C-type lectin receptors. *The Journal of Immunology* **2017**, *198* (4), 1403-1414.
(183) Ozinsky, A.; Underhill, D. M.; Fontenot, J. D.; Hajjar, A. M.; Smith, K. D.; Wilson, C. B.; Schroeder, L.; Aderem, A. The repertoire for pattern recognition of pathogens by the innate immune system is defined by cooperation between toll-like receptors. *Proceedings of the National Academy of Sciences* **2000**, *97* (25), 13766-13771.
(184) Gantner, B. N.; Simmons, R. M.; Canavera, S. J.; Akira, S.; Underhill, D. M. Collaborative induction of inflammatory responses by dectin-1 and Toll-like receptor 2. *The Journal of experimental medicine* **2003**, *197* (9), 1107-1117.

(185) Farhana, A.; Khan, Y. S. Biochemistry, lipopolysaccharide. In *StatPearls [Internet]*, StatPearls Publishing, 2021.
(186) Maldonado, R. F.; Sá-Correia, I.; Valvano, M. A. Lipopolysaccharide modification in Gram-negative bacteria during chronic infection. *FEMS microbiology reviews* **2016**, *40* (4), 480-493.
(187) Bertani, B.; Ruiz, N. Function and biogenesis of lipopolysaccharides. *EcoSal Plus* **2018**, *8* (1).
(188) Gauthier, A. E.; Rotjan, R. D.; Kagan, J. C. Lipopolysaccharide detection by the innate immune system may be an uncommon defence strategy used in nature. *Open Biology* **2022**, *12* (10), 220146.
(189) Kaur, R.; Sharma, M.; Ji, D.; Xu, M.; Agyei, D. Structural features, modification, and functionalities of beta-glucan. *Fibers* **2019**, *8* (1), 1.
(190) Legentil, L.; Paris, F.; Ballet, C.; Trouvelot, S.; Daire, X.; Vetvicka, V.; Ferrières, V. Molecular interactions of β-(1→ 3)-glucans with their receptors. *Molecules* **2015**, *20* (6), 9745-9766.
(191) Li, R.; Zeng, Z.; Fu, G.; Wan, Y.; Liu, C.; McClements, D. J. Formation and characterization of tannic acid/beta-glucan complexes: Influence of pH, ionic strength, and temperature. *Food Research International* **2019**, *120*, 748-755.
(192) Sheu, C.-C.; Chang, Y.-T.; Lin, S.-Y.; Chen, Y.-H.; Hsueh, P.-R. Infections caused by carbapenem-resistant Enterobacteriaceae: an update on therapeutic options. *Frontiers in microbiology* **2019**, *10*, 80.
(193) Livorsi, D. J.; Chorazy, M. L.; Schweizer, M. L.; Balkenende, E. C.; Blevins, A. E.; Nair, R.; Samore, M. H.; Nelson, R. E.; Khader, K.; Perencevich, E. N. A systematic review of the epidemiology of carbapenem-resistant Enterobacteriaceae in the United States. *Antimicrobial Resistance & Infection Control* **2018**, *7* (1), 1-9.
(194) Vardakas, K. Z.; Tansarli, G. S.; Rafailidis, P. I.; Falagas, M. E. Carbapenems versus alternative antibiotics for the treatment of bacteraemia due to Enterobacteriaceae producing extended-spectrum β-lactamases: a systematic review and meta-analysis. *Journal of antimicrobial chemotherapy* **2012**, *67* (12), 2793-2803.
(195) Falagas, M. E.; Lourida, P.; Poulikakos, P.; Rafailidis, P. I.; Tansarli, G. S. Antibiotic treatment of infections due to carbapenem-resistant Enterobacteriaceae: systematic evaluation of the available evidence. *Antimicrobial agents and chemotherapy* **2014**, *58* (2), 654-663.
(196) Conlan, S.; Thomas, P. J.; Deming, C.; Park, M.; Lau, A. F.; Dekker, J. P.; Snitkin, E. S.; Clark, T. A.; Luong, K.; Song, Y.; et al. Single-molecule sequencing to track plasmid diversity of hospital-associated carbapenemase-producing Enterobacteriaceae. *Sci Transl Med* **2014**, *6* (254), 254ra126. DOI: 10.1126/scitranslmed.3009845.
(197) Potter, R. F.; D'Souza, A. W.; Dantas, G. The rapid spread of carbapenem-resistant Enterobacteriaceae. *Drug Resist Updat* **2016**, *29*, 30-46. DOI: 10.1016/j.drup.2016.09.002.
(198) Chavda, K. D.; Chen, L.; Jacobs, M. R.; Bonomo, R. A.; Kreiswirth, B. N. Molecular Diversity and Plasmid Analysis of KPC-Producing Escherichia coli. *Antimicrob Agents Chemother* **2016**, *60* (7), 4073-4081. DOI: 10.1128/AAC.00452-16.
(199) Nagulapalli Venkata, K. C.; Ellebrecht, M.; Tripathi, S. K. Efforts towards the inhibitor design for New Delhi metallo-beta-lactamase (NDM-1). *Eur J Med Chem* **2021**, *225*, 113747. DOI: 10.1016/j.ejmech.2021.113747.
(200) Linciano, P.; Cendron, L.; Gianquinto, E.; Spyrakis, F.; Tondi, D. Ten Years with New Delhi Metallo-beta-lactamase-1 (NDM-1): From Structural Insights to Inhibitor Design. *ACS Infect Dis* **2019**, *5* (1), 9-34. DOI: 10.1021/acsinfecdis.8b00247.
(201) Tzeng, A.; Tzeng, T. H.; Vasdev, S.; Korth, K.; Healey, T.; Parvizi, J.; Saleh, K. J. Treating periprosthetic joint infections as biofilms: key diagnosis and management strategies. *Diagnostic microbiology and infectious disease* **2015**, *81* (3), 192-200.
(202) Stoodley, P.; Brooks, J.; Peters, C. W.; Jiang, N.; Delury, C. P.; Laycock, P. A.; Aiken, S. S.; Dusane, D. H. Prevention and Killing Efficacy of Carbapenem Resistant Enterobacteriaceae (CRE) and Vancomycin Resistant Enterococci (VRE) Biofilms by Antibiotic-Loaded Calcium Sulfate Beads. *Materials* **2020**, *13* (15), 3258.

(203) Howlin, R.; Brayford, M.; Webb, J.; Cooper, J.; Aiken, S.; Stoodley, P. Antibiotic-loaded synthetic calcium sulfate beads for prevention of bacterial colonization and biofilm formation in periprosthetic infections. *Antimicrobial agents and chemotherapy* **2015**, *59* (1), 111-120.
(204) Rajni, E.; Rajpurohit, V.; Rathore, P. K.; Shikhar, D.; Khatri, P. Biofilm formation by carbapenem-resistant Enterobacteriaceae strains isolated from surveillance cultures in Intensive Care Unit patients: A significant problem. *Journal of Health Research and Reviews* **2018**, *5* (3), 147.
(205) Yaita, K.; Gotoh, K.; Nakano, R.; Iwahashi, J.; Sakai, Y.; Horita, R.; Yano, H.; Watanabe, H. Biofilm-forming by carbapenem resistant enterobacteriaceae may contribute to the blood stream infection. *International journal of molecular sciences* **2019**, *20* (23), 5954.
(206) Di Domenico, E. G.; Cavallo, I.; Sivori, F.; Marchesi, F.; Prignano, G.; Pimpinelli, F.; Sperduti, I.; Pelagalli, L.; Di Salvo, F.; Celesti, I. Biofilm Production by Carbapenem-Resistant Klebsiella pneumoniae significantly increases the risk of death in oncological patients. *Frontiers in cellular and infection microbiology* **2020**, *10*.
(207) Cubero, M.; Marti, S.; Domínguez, M. Á.; González-Díaz, A.; Berbel, D.; Ardanuy, C. Hypervirulent Klebsiella pneumoniae serotype K1 clinical isolates form robust biofilms at the air-liquid interface. *PLoS One* **2019**, *14* (9), e0222628.
(208) Control, C. f. D.; Prevention. Antibiotic resistance threats in the United States, 2019. Atlanta, GA: US Department of Health and Human Services, CDC; 2019. 2019.
(209) Logan, L. K.; Weinstein, R. A. The epidemiology of carbapenem-resistant Enterobacteriaceae: the impact and evolution of a global menace. *The Journal of infectious diseases* **2017**, *215* (suppl_1), S28-S36.
(210) Satlin, M. J.; Chen, L.; Patel, G.; Gomez-Simmonds, A.; Weston, G.; Kim, A. C.; Seo, S. K.; Rosenthal, M. E.; Sperber, S. J.; Jenkins, S. G. Multicenter clinical and molecular epidemiological analysis of bacteremia due to carbapenem-resistant Enterobacteriaceae (CRE) in the CRE epicenter of the United States. *Antimicrobial agents and chemotherapy* **2017**, *61* (4), e02349-02316.
(211) Lam, A. K.; Wouters, C. L.; Moen, E. L.; Pusavat, J.; Rice, C. V. Antibiofilm synergy of β-lactams and branched polyethylenimine against methicillin-resistant Staphylococcus epidermidis. *Biomacromolecules* **2019**, *20* (10), 3778-3785.
(212) Naves, P.; Del Prado, G.; Huelves, L.; Gracia, M.; Ruiz, V.; Blanco, J.; Rodríguez-Cerrato, V.; Ponte, M.; Soriano, F. Measurement of biofilm formation by clinical isolates of Escherichia coli is method-dependent. *Journal of applied microbiology* **2008**, *105* (2), 585-590.
(213) Merritt, J. H.; Kadouri, D. E.; O'Toole, G. A. Growing and analyzing static biofilms. *Current protocols in microbiology* **2011**, *22* (1), 1B. 1.1-1B. 1.18.
(214) Gajdács, M.; Kárpáti, K.; Nagy, Á. L.; Gugolya, M.; Stájer, A.; Burián, K. Association between biofilm-production and antibiotic resistance in Escherichia coli isolates: A laboratory-based case study and a literature review. *Acta Microbiologica et Immunologica Hungarica* **2021**, *68* (4), 217-226.
(215) Dumaru, R.; Baral, R.; Shrestha, L. B. Study of biofilm formation and antibiotic resistance pattern of gram-negative Bacilli among the clinical isolates at BPKIHS, Dharan. *Bmc Research Notes* **2019**, *12* (1), 1-6. DOI: ARTN 38

10.1186/s13104-019-4084-8.
(216) Rahdar, H. A.; Malekabad, E. S.; Dadashi, A. R.; Takei, E.; Keikha, M.; Kazemian, H.; Karami-Zarandi, M. Correlation between biofilm formation and carbapenem resistance among clinical isolates of Klebsiella pneumoniae. *Ethiopian Journal of Health Sciences* **2019**, *29* (6), 745-750. DOI: 10.4314/ejhs.v29i6.11.
(217) Gallant, C. V.; Daniels, C.; Leung, J. M.; Ghosh, A. S.; Young, K. D.; Kotra, L. P.; Burrows, L. L. Common beta-lactamases inhibit bacterial biofilm formation. *Mol Microbiol* **2005**, *58* (4), 1012-1024. DOI: 10.1111/j.1365-2958.2005.04892.x.
(218) Yang, H. H.; Vinopal, R. T.; Grasso, D.; Smets, B. F. High diversity among environmental Escherichia coli isolates from a bovine feedlot. *Applied and Environmental Microbiology* **2004**, *70* (3), 1528-1536. DOI: 10.1128/Aem.70.3.1528-1536.2004.

(219) Skyberg, J. A.; Siek, K. E.; Doetkott, C.; Nolan, L. K. Biofilm formation by avian Escherichia coli in relation to media, source and phylogeny. *J Appl Microbiol* **2007**, *102* (2), 548-554. DOI: 10.1111/j.1365-2672.2006.03076.x.
(220) Reisner, A.; Krogfelt, K. A.; Klein, B. M.; Zechner, E. L.; Molin, S. In vitro biofilm formation of commensal and pathogenic Escherichia coli strains: impact of environmental and genetic factors. *J Bacteriol* **2006**, *188* (10), 3572-3581. DOI: 10.1128/JB.188.10.3572-3581.2006.
(221) *National Action Plan for Combating Antibiotic-Resistant Bacteria (CARB), 2020-2025 from the Federal Task Force on Combating Antibiotic-Resistant Bacteria*. 2020. https://aspe.hhs.gov/system/files/pdf/264126/CARB-National-Action-Plan-2020-2025.pdf (accessed.
(222) Tamma, P. D.; Aitken, S. L.; Bonomo, R. A.; Mathers, A. J.; van Duin, D.; Clancy, C. J. Infectious Diseases Society of America Guidance on the Treatment of Extended-Spectrum beta-lactamase Producing Enterobacterales (ESBL-E), Carbapenem-Resistant Enterobacterales (CRE), and Pseudomonas aeruginosa with Difficult-to-Treat Resistance (DTR-P. aeruginosa). *Clin Infect Dis* **2021**, *72* (7), 1109-1116. DOI: 10.1093/cid/ciab295.
(223) Paterson, D. L.; Isler, B.; Stewart, A. New treatment options for multiresistant gram negatives. *Current opinion in infectious diseases* **2020**, *33* (2), 214-223.
(224) Bush, K. Game Changers: New beta-Lactamase Inhibitor Combinations Targeting Antibiotic Resistance in Gram-Negative Bacteria. *ACS Infect Dis* **2018**, *4* (2), 84-87. DOI: 10.1021/acsinfecdis.7b00243.
(225) Fuchs, F.; Becerra-Aparicio, F.; Xanthopoulou, K.; Seifert, H.; Higgins, P. G. In vitro activity of nitroxoline against carbapenem-resistant Acinetobacter baumannii isolated from the urinary tract. *J Antimicrob Chemother* **2022**. DOI: 10.1093/jac/dkac123.
(226) Fux, C. A.; Costerton, J. W.; Stewart, P. S.; Stoodley, P. Survival strategies of infectious biofilms. *Trends Microbiol* **2005**, *13* (1), 34-40. DOI: 10.1016/j.tim.2004.11.010.
(227) Vickery, K.; Deva, A.; Jacombs, A.; Allan, J.; Valente, P.; Gosbell, I. B. Presence of biofilm containing viable multiresistant organisms despite terminal cleaning on clinical surfaces in an intensive care unit. *Journal of Hospital Infection* **2012**, *80* (1), 52-55.
(228) Henig, O.; Cober, E.; Richter, S. S.; Perez, F.; Salata, R. A.; Kalayjian, R. C.; Watkins, R. R.; Marshall, S.; Rudin, S. D.; Domitrovic, T. N.; et al. A Prospective Observational Study of the Epidemiology, Management, and Outcomes of Skin and Soft Tissue Infections Due to Carbapenem-Resistant Enterobacteriaceae. *Open Forum Infect Dis* **2017**, *4* (3), ofx157. DOI: 10.1093/ofid/ofx157.
(229) Gjodsbol, K.; Christensen, J. J.; Karlsmark, T.; Jorgensen, B.; Klein, B. M.; Krogfelt, K. A. Multiple bacterial species reside in chronic wounds: a longitudinal study. *Int Wound J* **2006**, *3* (3), 225-231. DOI: 10.1111/j.1742-481X.2006.00159.x.
(230) Swarna, S.; Gomathi, S. Biofilm Production in Carbapenem Resistant Isolates from Chronic Wound Infections. *International Journal of Medical Research & Health Sciences* **2017**, *6* (2), 61-67.
(231) Wang, L.; Tong, X.; Huang, J.; Zhang, L.; Wang, D.; Wu, M.; Liu, T.; Fan, H. Triple Versus Double Therapy for the Treatment of Severe Infections Caused by Carbapenem-Resistant Enterobacteriaceae: A Systematic Review and Meta-Analysis. *Front Pharmacol* **2019**, *10*, 1673. DOI: 10.3389/fphar.2019.01673.